Factorization connecting continuum & lattice TMDs

Markus A. Ebert,[a] **Stella T. Schindler,**[b] **Iain W. Stewart**[b] **and Yong Zhao**[c]

[a] *Max Planck Institut für Physik,*
Föhringer Ring 6, 80805 Munich, Germany

[b] *Center for Theoretical Physics, Massachusetts Institute of Technology,*
Cambridge, MA 02139, U.S.A.

[c] *Physics Division, Argonne National Laboratory,*
Lemont, IL 60439, U.S.A.

E-mail: ebert@mpp.mpg.de, stellas@mit.edu, iains@mit.edu,
yong.zhao@anl.gov

ABSTRACT: Transverse-momentum-dependent parton distribution functions (TMDs) can be studied from first principles by a perturbative matching onto lattice-calculable quantities: so-called lattice TMDs, which are a class of equal-time correlators that includes quasi-TMDs and TMDs in the Lorentz-invariant approach. We introduce a general correlator that includes as special cases these two Lattice TMDs and continuum TMDs, like the Collins scheme. Then, to facilitate the derivation of a factorization relation between lattice and continuum TMDs, we construct a new scheme, the Large Rapidity (LR) scheme, intermediate between the Collins and quasi-TMDs. The LR and Collins schemes differ only by an order of limits, and can be matched onto one another by a multiplicative kernel. We show that this same matching also holds between quasi and Collins TMDs, which enables us to prove a factorization relation between these quantities to all orders in α_s. Our results imply that there is no mixing between various quark flavors or gluons when matching Collins and quasi TMDs, making the lattice calculation of individual flavors and gluon TMDs easier than anticipated. We cross-check these results explicitly at one loop and discuss implications for other physical-to-lattice scheme factorizations.

Contents

1 Introduction

Nuclear and particle physicists have striven to ascertain the full three-dimensional structure of hadrons for decades, through a combination of experimental measurements and their theoretical description via parton distribution functions (PDFs). The study of PDFs in the longitudinal momentum direction has reached a high level of maturity within many frameworks, such as global fitting efforts [1–8], lattice QCD calculations using moments [9–11], quasi-distributions in large-momentum effective theory (LaMET) [12–14], and various other techniques [15–22]. A major thrust of current research is to extend this progress to transverse-momentum-dependent PDFs (TMDs). In principle, TMDs can be extracted from experiments using global fits [23, 24], but due to limited data these extractions have not yet yielded the same precision as PDFs. However, ongoing and planned experiments such as the Electron-Ion Collider [25, 26] will have enhanced capabilities to probe TMDs, and it is important to complement them with theoretical insight.

TMDs are intrinsically nonperturbative at small transverse momenta and so lattice QCD provides the only practical method for their first-principles calculation. Unfortunately, TMDs are defined along nonlocal lightlike or close-to-lightlike Wilson line paths, which depend explicitly on a real-valued time variable and thus lie outside the reach of current lattice techniques due to a sign problem, the speculated non-deterministic non-polynomial hard issue of numerically averaging over complex weights in a Euclidean path integral. To circumvent this obstacle, one can construct equal-time correlators that are calculable on the lattice, which we collectively dub "Lattice TMDs". We can then extract information from lattice calculations by relating a lattice TMD to a physical continuum TMD (that appear in cross sections) through a so-called factorization formula, which forms the focus of this paper.

There exist several approaches for defining continuum and lattice TMDs. The first lattice TMD studies used the Lorentz-invariant approach of refs. [27–32], which we refer to as the Musch-Hägler-Engelhardt-Negele-Schäfer (MHENS) scheme. This approach defines TMDs which are calculated with lattice QCD using spacelike Wilson line paths, and then uses Lorentz invariance to relate them to the path considered for the continuum TMD definitions, which is spacelike but close to the light-cone. This method has so far primarily been used to calculate ratios of physical TMD moments. Later on, LaMET motivated the study of quasi-TMDs [33–42], which are Euclidean distributions defined using boosted hadron matrix elements of somewhat different spacelike Wilson line paths. Since the quasi-TMD obeys the Collins-Soper evolution [33], one can extract the nonperturbative Collins-Soper (CS) evolution of TMDs using ratios of quasi-TMDs at different hadron momenta [35], and first lattice results were obtained in refs. [43–48]. Methods to calculate the so-called soft function have also been proposed [38] and implemented on the lattice [46, 47].

To relate lattice TMDs and physical continuum TMDs one should derive a factorization formula that demonstrates that these TMDs agree in the infrared, and perhaps differ in the ultraviolet by perturbative matching coefficients [33, 34, 36, 39, 41, 49]. In this work, we set up a unified notational framework for lattice and continuum TMDs and derive the factorization formula between the physical Collins TMD and quasi-TMD to all orders in α_s, for both quark and gluon TMDs. Up until now, no lattice-to-continuum factorization

formlula has been proven, but a matching between the quasi-TMD and Collins-TMD for the non-singlet quark case has been verified at one-loop order.[1] In our analysis here we also fully account for lattice renormalization, soft function subtractions, and finite Wilson line lengths; items that are important to account for in analyses for lattice-QCD-friendly TMDs.

1.1 Statement of factorization

Factorization formulae that relate the non-singlet quark quasi-TMD and physical TMD have been proposed in refs. [35, 36, 38, 39]. The objects we are interested in here include both a naive quasi-TMD $\tilde{f}_{\rm ns}^{\rm naive}$ that can be directly calculated with lattice QCD, but whose infrared structure differs from the physical TMD, and a proper quasi-TMD $\tilde{f}_{\rm ns}$ whose infrared structure agrees. The factorization theorem for both of these quasi-TMDs can be expressed as

$$\tilde{f}_{\rm ns}^{\rm (naive)}(x, \vec{b}_T, \mu, x\tilde{P}^z) = C_{\rm ns}(x\tilde{P}^z, \mu) g_S^q(b_T, \mu) \exp\left[\frac{1}{2}\gamma_\zeta^q(b_T, \mu) \ln \frac{(2x\tilde{P}^z)^2}{\zeta}\right] f_{\rm ns}(x, \vec{b}_T, \mu, \zeta)$$

$$\times \left\{1 + \mathcal{O}\left[\frac{1}{(x\tilde{P}^z b_T)^2}, \frac{\Lambda_{\rm QCD}^2}{(x\tilde{P}^z)^2}\right]\right\}. \tag{1.1}$$

Here ns $= u - d$ for non-singlet flavor, and $C_{\rm ns}$ is a perturbative matching coefficient which does not depend on spin [40, 49]. In eq. (1.1) x is the fraction of the hadron's longitudinal momentum carried by the parton, $\vec{b}_T$ with $b_T = |\vec{b}_T|$ is the Fourier conjugate of parton transverse momentum, and μ is the $\overline{\rm MS}$ renormalization scale. The quasi-TMD depends on the hadron momentum $\tilde{P}^z$, while the TMD depends on the CS scale ζ; also, γ_ζ^q is the anomalous dimension for ζ-evolution, which is often referred to as the CS kernel [50–52]. Since we are interested in nonperturbative $b_T \sim \Lambda_{\rm QCD}^{-1}$, for the proper quasi-TMD $\tilde{f}_{\rm ns}$ we must have $g_S^q = 1$, while for the naive quasi-TMD $\tilde{f}_{\rm ns}^{\rm naive}$ the function $g_S^q(b_T, \mu)$ is nonperturbative and arises from using a *naive* quasi-soft function $\tilde{S}_{\rm naive}^R$, but can be calculated from the reduced soft function with the methods proposed in ref. [39]. The definition of the proper quasi-TMD we use here is not the same as earlier literature, see section 2.3.1 for more details. This factorization is valid at large but finite $\tilde{P}^z$, with power corrections suppressed by the parton momentum $x\tilde{P}^z$ as shown in eq. (1.1).

In this work, we prove eq. (1.1) at all orders in α_s and generalize it to the quasi-TMDs of all partons i, including light quark flavors (u, d, s) and gluons. Specifically, for the TMDs for hadron h we find

$$\tilde{f}_{i/h}^{[s]}(x, \vec{b}_T, \mu, \tilde{\zeta}, x\tilde{P}^z) = C_i(x\tilde{P}^z, \mu) \exp\left[\frac{1}{2}\gamma_\zeta^i(\mu, b_T) \ln \frac{\tilde{\zeta}}{\zeta}\right] f_{i/h}^{[s]}(x, \vec{b}_T, \mu, \zeta)$$

$$\times \left\{1 + \mathcal{O}\left[\frac{1}{(x\tilde{P}^z b_T)^2}, \frac{\Lambda_{\rm QCD}^2}{(x\tilde{P}^z)^2}\right]\right\}, \tag{1.2}$$

---

[1]In ref. [39] arguments for the factorization based on an analysis of leading regions were suggested. The presentation of such an analysis will be an important complement to the proof given here. We note that the collinear, soft and hard leading regions, respectively correspond to the collinear beam function, soft factor and the perturbative matching coefficient considered here. Ref. [49] analyzes factorization for lattice-friendly correlators. The transverse distribution that they study there is not the same as the quasi-TMD in refs. [33, 34, 36, 39, 41] and this work.

where $[s]$ denotes the choice of spin-polarization for the hadronic state and operator, and C_i and γ_ζ^i depend only on the choice of fundamental or adjoint color representations, so $C_i = C_q$ and $\gamma_\zeta^i = \gamma_\zeta^q$ for all quarks, and $C_i = C_g$ and $\gamma_\zeta^i = \gamma_\zeta^g$ for gluons. The quasi-TMD in eq. (1.2) differs from eq. (1.1) by the soft factor,

$$\tilde{f}_{i/h}^{[s]}\left(x, \vec{b}_T, \mu, \tilde{\zeta}, x\tilde{P}^z\right) = \tilde{f}_{i/h}^{[s]\text{naive}}(x, \vec{b}_T, \mu, x\tilde{P}^z)\sqrt{\frac{\tilde{S}_{\text{naive}}^R(b_T, \mu)}{S_C^R(b_T, \mu, 2y_n, 2y_B)}}\,, \qquad (1.3)$$

where $S_C^R(b_T, \mu, 2y_n, 2y_B)$ is the soft function in the Collins scheme [53], $R = q, g$ for quarks in the fundamental or gluons in the adjoint representation, and y_n and y_B are two different rapidities (see section 2.2.1). Notably, the quasi-TMD depends on a new variable $\tilde{\zeta} = x^2 m_h^2 e^{2(y_{\tilde{P}} + y_B - y_n)}$ with hadron mass m_h and rapidity $y_{\tilde{P}}$, which is equivalent to a CS scale. Comparing eqs. (1.1)–(1.3), we also show that g_S^q can be calculated as a ratio of soft functions, in agreement with the definition of the reduced soft function in ref. [39].

Two key results of this work are that eq. (1.2) holds for both quark and gluon quasi-TMDs, and there is no mixing between the quark and gluon channels or quarks of different flavors. This differs from the case of the factorizations of quark and gluon longitudinal quasi-PDFs [54]. The matching coefficient C_i takes different values for the two different cases $i = q, g$, but is independent of quark flavor and spin.

1.2 Strategy for proving factorization

We begin by developing a unified notational framework that is applicable to both lattice and continuum TMDs. This framework brings to the forefront the common underlying structural features of different TMD schemes, allowing one to more easily construct factorization formulae relating them to one another. We can write every lattice and continuum TMD as the product of a proton matrix element (beam function), vacuum matrix element (soft factor), and appropriate renormalization factors. In the cases studied in the literature, we show that the beam function can be expressed as the Fourier transform of a generic, common correlator Ω. Each scheme manifests as a special case of the correlator, encoded by a choice of Ω's arguments and of the order in which we take parameter limits needed for proper TMD regularization and renormalization. More details are provided later, and we summarize the choices needed for various schemes in tables 1 and 2.

Having a unified notational framework is useful for constructing relationships between continuum TMD schemes that can be connected to physical observables, with schemes that can be computed on the lattice. From the structure of the correlator Ω, we observe that the Collins and quasi-TMDs are closely related. To relate these schemes we begin by constructing a new TMD scheme that is intermediate between the quasi and Collins TMDs: the Large-Rapidity (LR) scheme. The LR scheme uses the same ingredients as the Collins scheme, but performs UV renormalization at large but finite Wilson line rapidities. Using Lorentz invariance, we show that the quasi- and LR scheme TMDs are equivalent, up to terms suppressed at large proton rapidity. We then show that we can relate the LR and Collins TMDs simply by a perturbative matching kernel, which is flavor-diagonal and spin-independent for both quarks and gluons. Combining the quasi-to-LR and LR-to-Collins
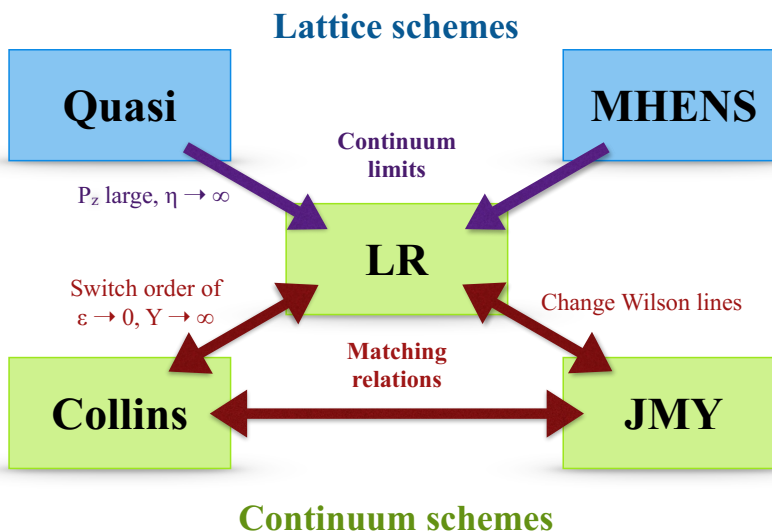
Figure 1. An overview of schemes and their relationships, including the LR scheme introduced in this work. See section 3 for details.

relations leads to eq. (1.2). We summarize relationships between a number of common TMD schemes in figure 1.

This proof is a beautiful application of the fundamental principle underlying LaMET [12–14]: partons encode the internal degrees of freedom of a highly energetic hadron, with the hadron momentum limit $P^z \to \infty$ taken prior to UV renormalization. In contrast, on the lattice one must carry out UV renormalization prior to the large-momentum limit. This different order of limits in an asymptotically free theory like QCD induces a nontrivial matching kernel between a parton observable and its corresponding lattice construction.

Peculiarly, in TMDs this noncommutativity of orders of limits appears naturally, since at intermediate steps of the calculation one must regulate so-called rapidity divergences [50, 53, 55–64], usually by choosing to deviate from lightcone kinematics or by introducing an additional regulator on the lightcone. These divergences cancel when combining the hadronic and soft matrix elements, allowing one to take the lightcone limit (or infinite rapidity-regulator limit), but also forcing one to decide whether to take this limit before or after UV renormalization. Many schemes for constructing TMDs take the lightcone limit first, e.g. the Collins scheme [53]; others, such as the Ji-Ma-Yuan (JMY) scheme, do the opposite [56]. Once again, exchanging these orders of limits is a UV effect, and thus induces a nontrivial matching relation between Collins and JMY TMDs.

This paper is structured as follows: section 2 introduces our new notational framework for defining TMDs. We then provide an overview of the definitions of common physical and lattice TMD schemes. Section 3 presents the proof of the factorization statement in eq. (1.2). We then discuss the physical implications of this proof, in particular the lack of flavor mixing in the matching and utility for calculating ratios of TMDs. We also confirm the momentum evolution RGE equation for the hard matching coefficient, and give a complete solution for it with next-to-leading-logarithmic resummation. From our proof, we also gain intuition for factorization relations between other lattice and continuum TMD schemes, in

particular for the MHENS and Collins schemes which differ due to the presence of Wilson line cusp angles in the former that are not in the latter, and by the need for different soft factors in these two TMDs. We make concluding remarks and outline future directions in section 4. In the appendices, we verify our quasi-to-Collins factorization results analytically at one-loop order, present a one-loop comparison of the continuum JMY and Collins TMDs, and also discuss Wilson line self-energies.

2 Definition of TMDs

Let us consider the process of hard hadron-hadron scattering:

$$h_1(P_1) + h_2(P_2) \to L(q) + X \,, \tag{2.1}$$

where $h_{1,2}$ are colliding hadrons with momenta $P_{1,2}$, L is a detected color-singlet final state with momentum q^μ (such as $L = Z/\gamma^*$, which decays to leptons), and X denotes additional final-state particles. Let L have invariant mass Q, rapidity Y, and transverse momentum $\vec{q}_T$ with $q_T = |\vec{q}_T|$. For $q_T \ll Q$, we can factorize the cross-section of eq. (2.1) as [50–53]

$$\frac{\mathrm{d}\sigma}{\mathrm{d}Q^2 \mathrm{d}Y \mathrm{d}^2\vec{q}_T} = \sigma_0 \sum_{i,j} H_{ij}(Q,\dots) \int \frac{\mathrm{d}^2\vec{b}_T}{(2\pi)^2} e^{\mathrm{i}\vec{q}_T \cdot \vec{b}_T} f_{i/h_1}(x_1, \vec{b}_T, \dots) f_{j/h_2}(x_2, \vec{b}_T, \dots) \,. \tag{2.2}$$

Here, σ_0 is the Born cross-section; the sum runs over all parton flavors i, j contributing to the Born process $ij \to L$; H_{ij} is the hard function, which encodes virtual corrections to the Born process; and $f_{i/h}$ are the TMDs, functions which describe the dynamics of partonic quarks and gluons inside the parent hadron h. A struck hadron carries a fraction $x_{1,2} = Qe^{\pm Y}/E_{\mathrm{cm}}$ of its parent hadron's longitudinal momentum, with $E_{\mathrm{cm}} = \sqrt{(P_1 + P_2)^2}$ the center-of-mass energy of the incoming hadrons. The ellipses in eq. (2.1) denote additional parameters related to UV and rapidity renormalization, whose precise forms are scheme dependent. Note that we suppress indices related to spin-dependent processes and contributions.

The literature is rife with schemes for defining TMDs, each of which has different strengths for different types of calculations. This section reviews schemes relevant for lattice studies; in particular, we only discuss schemes based on off-lightcone Wilson lines. Schemes with intrinsically lightlike Wilson lines [58, 60, 62–65] are not accessible on a Euclidean lattice, but many are equivalent to the Collins scheme once limits needed to obtain TMD PDFs are taken; see refs. [36, 66] for an overview. Because each scheme in the literature employs its own conventions and notation, in section 2.1 we begin by introducing new unified TMD Lorentz-invariant correlators for which all schemes follow as special cases. Then, we provide definitions of physical and lattice schemes in sections 2.2 and 2.3, respectively.

2.1 Unified TMD notation

A TMD $f_{i/h}$ generally contains two pieces: a hadronic matrix element (called the beam function or unsubtracted TMD), which encodes partonic radiation associated with the initial hadrons; as well as a vacuum matrix element (the soft function). These matrix
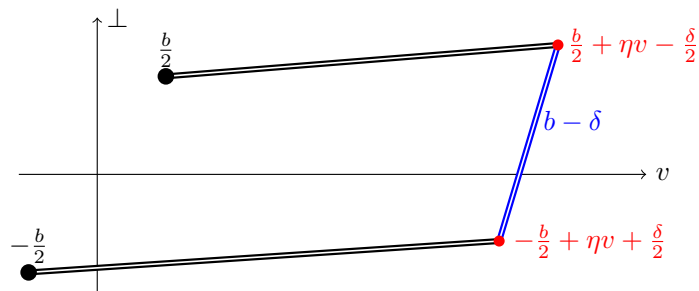
Figure 2. Generic staple-shaped Wilson line defined in eq. (2.4). Black double-lines extend along ηv, and the blue segment along $b - \delta$ closes the staple. For certain choices of δ, red points can be cusps. Edges may extend along the conjugate direction P, which is not shown.

elements involve open and closed staple-shaped Wilson lines, for which we develop a generic notation. Let us first define a Wilson line along a path γ in color representation R as:

$$W^R[\gamma] = P \exp\left[\mathrm{i}g \int_\gamma \mathrm{d}x^\mu \mathcal{A}_\mu^a(x) \, T_R^a \right], \tag{2.3}$$

where $R = q$ in the fundamental and $R = g$ in the adjoint representation. It is useful to define a general class of Wilson lines using the three-sided staple shape shown in figure 2,

$$W_{\sqcup}^R(b, \eta v, \delta) = W^R\left[\frac{b}{2} \;\rightarrow\; \frac{b}{2} + \eta v - \frac{\delta}{2} \;\rightarrow\; -\frac{b}{2} + \eta v + \frac{\delta}{2} \;\rightarrow\; -\frac{b}{2} \right], \tag{2.4}$$

where b^μ is the separation of the quark or gluon fields in the beam function, v^μ is a dimensionless vector, and $\eta v \pm \delta/2$ are the paths of Wilson lines attached to the fields. Different choices of b, v, and δ constitute different, equally valid ways of defining a TMD. Continuum and lattice TMDs are distinguished by the length parameter, η, which may be infinite or finite. The length of the staple is relevant for its renormalization properties; here we have

$$L_{\text{staple}} = |\eta v - \delta/2| + |\eta v + \delta/2| + |b - \delta|, \tag{2.5}$$

where the length of a four-vector is given by $|X| = \sqrt{|X^2|}$. At the red points in figure 2, the staple has cusp angles $\gamma_\pm$, which can be computed from

$$\cosh\gamma_\pm = \frac{(\eta v \pm \delta/2) \cdot (b - \delta)}{|\eta v \pm \delta/2||b - \delta|}, \tag{2.6}$$

where for space-like separations $\gamma_\pm \in [-\mathrm{i}\pi, \mathrm{i}\pi]$.[2] Generic quark and gluon beam function correlators take the form

$$\Omega_{q_i/h}^{[\Gamma]}[b, P, \epsilon, \eta v, \delta] = \left\langle h(P) \Big| \bar{q}_i\left(\frac{b}{2}\right) \frac{\Gamma}{2} W_{\sqcup}^q(b, \eta v, \delta) q_i\left(-\frac{b}{2}\right) \Big| h(P) \right\rangle,$$

$$\Omega_{g/h}^{\mu\nu\rho\sigma}[b, P, \epsilon, \eta v, \delta] = \left\langle h(P) \Big| G^{\mu\nu}\left(\frac{b}{2}\right) W_{\sqcup}^g(b, \eta v, \delta) G^{\rho\sigma}\left(-\frac{b}{2}\right) \Big| h(P) \right\rangle. \tag{2.7}$$

---

[2]Note that we develop our generic TMD framework with a *three*-sided staple. Adding more than three sides will induce extra Wilson line cusps, that create additional complications for renormalization.
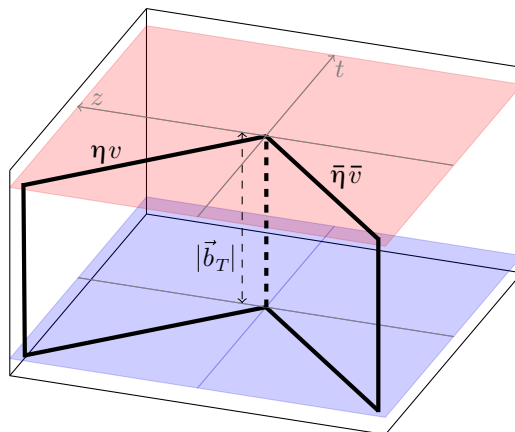
Figure 3. Wilson line structure of the soft function, eq. (2.8) for $\eta, \bar{\eta} < 0$. Figure adapted from ref. [63].

In eq. (2.7), $q_i(x)$ is a quark field of flavor i, and $G^{\mu\nu}(x)$ is the gluon field strength tensor. The quark and gluon fields are spatially separated by b, which is Fourier-conjugate to the momentum of the struck parton. In the quark correlator, Γ denotes a generic Dirac structure, while for the gluon correlator μ, ν, ρ, and σ are Lorentz indices. See refs. [40, 67] for decompositions of different choices of Γ into independent spin structures for quark TMDs, and refs. [68, 69] for the decomposition for gluon TMDs. In both cases, h denotes the struck hadron with momentum P, ϵ is the UV regulator, and ηv and δ characterize the longitudinal and transverse segments of the Wilson line, which we illustrate in figure 2.

We define the generic soft vacuum matrix element as

$$S^R(b, \epsilon, \eta v, \bar{\eta}\bar{v}) = \frac{1}{d_R}\Big\langle 0\Big|\text{Tr}\Big[S_{\gg}^R(b, \eta v, \bar{\eta}\bar{v})\Big]\Big|0\Big\rangle, \tag{2.8}$$

where the trace is over color. The color averaging factor d_R takes values $d_q = N_c$ and $d_g = N_c^2 - 1$. The soft Wilson line is given by

$$S_{\gg}^R(b, \eta v, \bar{\eta}\bar{v}) = W^R\Big[\frac{b}{2} \to \frac{b}{2} + \bar{\eta}\bar{v} \to -\frac{b}{2} + \bar{\eta}\bar{v} \to -\frac{b}{2}$$
$$\to -\frac{b}{2} + \eta v \to \frac{b}{2} + \eta v \to \frac{b}{2}\Big], \tag{2.9}$$

as shown in figure 3. $S_{\gg}$ consists of two beam function staples glued together at the points $\pm b/2$; the long sides of the staples run along the $\bar{\eta}\bar{v}$ and ηv directions. The dependence on two conjugate directions arises from the appearance of two TMDs in the physical cross section in eq. (2.2). The length of the soft function path is $L_{\gg} = 2|\bar{\eta}\bar{v}| + 2|\eta v| + 2|b|$.

We define the transverse direction with respect to the plane spanned by P and v, taking $P_\perp = v_\perp = 0$. Formally, this can be expressed as $b_\perp^\mu = g_\perp^{\mu\nu}b_\nu$ with

$$g_\perp^{\mu\nu} = g^{\mu\nu} - \frac{1}{1 + \hat{\zeta}^2}\left[\frac{v^\mu v^\nu}{v^2} + \frac{P^\mu P^\nu}{P^2} + \frac{\hat{\zeta}^2}{P \cdot v}\big(P^\mu v^\nu + v^\mu P^\nu\big)\right], \quad \hat{\zeta} = \frac{v \cdot P}{\sqrt{|v^2|P^2}}. \tag{2.10}$$

We always take v and P to span the same plane as v and $\bar{v}$. It follows that $v_\perp = \bar{v}_\perp = 0$.

Our unified notation facilitates the comparison of different TMD schemes, particularly when we examine their Lorentz invariants. In the most generic case, the beam function correlator in eq. (2.7) is specified by four independent vectors: b^μ, P^μ, ηv^μ, and δ^μ. From these vectors we can construct ten independent Lorentz invariants, which we choose to be

$$
\begin{aligned}
&P^2\,, \quad b^2\,, \quad \eta^2 v^2\,, \quad P\cdot b\,, \quad \frac{P\cdot(\eta v)}{\sqrt{P^2|(\eta v)^2|}}\,, \quad \frac{b\cdot(\eta v)}{\sqrt{|b^2(\eta v)^2|}}\,, \\
&\frac{\delta^2}{b^2}\,, \quad \frac{b\cdot\delta}{b^2}\,, \quad \frac{P\cdot\delta}{P\cdot b}\,, \quad \frac{\delta\cdot(\eta v)}{b\cdot(\eta v)}\,.
\end{aligned}
\tag{2.11}
$$

None of the TMD schemes we study in this paper contains a vector δ^μ that is linearly independent of b^μ, P^μ, and ηv^μ; thus, these schemes have six independent Lorentz invariants. However, the quasi and MHENS TMDs do not follow from the same correlator defined with six invariants, since they fix δ^μ in different ways, as we will see below. Hence, even if the first six invariants in eq. (2.11) are fixed to be the same, the two approaches have different values for the last four invariants, and thus the quasi- and MHENS TMDs belong to distinct schemes.

2.2 Continuum TMD schemes

In this section, we provide an overview of physical TMD schemes, which are defined on a continuous spacetime and have infinitely long Wilson lines, with $|\eta| = |\bar{\eta}| = \infty$.

Lightcone coordinate conventions. It is convenient to work in a frame where the hadron momenta $P_{1,2}$ in eq. (2.1) are close to the lightlike unit vectors

$$
n_a^\mu = \frac{1}{\sqrt{2}}(1,0,0,1)\,, \qquad n_b^\mu = \frac{1}{\sqrt{2}}(1,0,0,-1)\,,
\tag{2.12}
$$

which obey $n_a^2 = n_b^2 = 0$ and $n_a \cdot n_b = 1$. We define the lightcone decomposition of an arbitrary four-vector p^μ as

$$
p^\mu = (p^+, p^-, p_\perp) = p^+ n_a^\mu + p^- n_b^\mu + p_\perp^\mu\,,
\tag{2.13}
$$

where $p^\pm = (p^0 \pm p^z)/\sqrt{2}$ and $p_\perp^\mu = (0, p_x, p_y, 0) = (0, \vec{p}_T, 0)$. Here $p_\perp^\mu$ is a Minkowski vector, and $\vec{p}_T$ is the corresponding transverse Euclidean vector with magnitude $p_T \equiv (\vec{p}_T^{\,2})^{1/2} = (-p_\perp^2)^{1/2}$. In lightcone coordinates, the incoming hadrons in eq. (2.1) have momenta

$$
P_1^\mu = P_1^+ (1, e^{-2y_1}, 0_\perp)\,, \qquad P_2^\mu = P_2^- (e^{+2y_2}, 1, 0_\perp)\,,
\tag{2.14}
$$

where $y_{1,2}$ are the hadron rapidities.

2.2.1 Collins scheme

In the Collins TMD scheme [53], the factorization formula in eq. (2.1) takes the form

$$
\frac{d\sigma}{dQ^2 dY d^2\vec{q}_T} = \sigma_0 \sum_{i,j} H_{ij}(Q,\mu) \int \frac{d^2\vec{b}_T}{(2\pi)^2} e^{i\vec{q}_T \cdot \vec{b}_T} f_{i/h_1}(x_1, \vec{b}_T, \mu, \zeta_1) f_{j/h_2}(x_2, \vec{b}_T, \mu, \zeta_2)\,,
\tag{2.15}
$$

where μ is the renormalization scale, and the CS scales [50, 51] are

$$\zeta_1 = 2(x_1 P_1^+)^2 e^{-2y_n} , \qquad \zeta_2 = 2(x_2 P_2^-)^2 e^{+2y_n} . \qquad (2.16)$$

Here, y_n is an arbitrary scheme-dependent parameter that cancels in eq. (2.15). In particular, we have that $\zeta_1 \zeta_2 = (2x_1 x_2 P_1^- P_2^+)^2 = Q^2$.

The Collins scheme is characterized by spacelike Wilson lines with directions

$$\begin{aligned} n_A^\mu(y_A) &\equiv n_a^\mu - e^{-2y_A} n_b^\mu = (1, -e^{-2y_A}, 0_\perp) , \\ n_B^\mu(y_B) &\equiv n_b^\mu - e^{2y_B} n_a^\mu \ = (-e^{2y_B}, 1, 0_\perp) , \end{aligned} \qquad (2.17)$$

parametrized by the rapidities y_A and y_B. The Collins TMD for a hadron h moving along n_a with rapidity y_P is

$$f_{i/h}^C(x, \vec{b}_T, \mu, \zeta) = \lim_{\epsilon \to 0} Z_{\mathrm{uv}}^R(\epsilon, \mu, \zeta) \lim_{y_B \to -\infty} \frac{B_{i/h}^C(x, \vec{b}_T, \epsilon, y_P - y_B)}{\sqrt{S_C^R(b_T, \epsilon, 2y_n, 2y_B)}} , \qquad (2.18)$$

where $B_{i/h}^C$ is the beam function and S_C^R is the soft function. Z_{uv}^R absorbs ϵ-poles that result from working in $d = 4 - 2\epsilon$ dimensions to regulate UV divergences. Z_{uv}^R and S_C^R depend on the color representation R of the parton i (fundamental $R = q$ for quarks and adjoint $R = g$ for gluons) but are independent of parton flavor. We emphasize that in eq. (2.18) the lightcone limit $y_B \to -\infty$ is taken *before* UV renormalization.

The Collins beam and soft functions for quarks and gluons are defined as

$$\begin{aligned} B_{q_i/h}^C(x, \vec{b}_T, \epsilon, y_P - y_B) &= \int \frac{\mathrm{d}b^-}{2\pi} e^{-ib^-(xP^+)} \Omega_{q_i/h}^{[\gamma^+]}[b, P, \epsilon, -\infty n_B(y_B), b^- n_b] , \\ B_{g/h}^{C\rho\sigma}(x, \vec{b}_T, \epsilon, y_P - y_B) &= \int \frac{\mathrm{d}b^-}{2\pi} \frac{e^{-ib^-(xP^+)}}{xP^+} \Omega_{g/h}^{-\rho-\sigma}[b, P, \epsilon, -\infty n_B(y_B), b^- n_b] , \\ S_C^R(b_T, \epsilon, y_A, y_B) &= S^R[b_\perp, \epsilon, -\infty n_A(y_A), -\infty n_B(y_B)] , \end{aligned} \qquad (2.19)$$

where $\Omega_{i/h}$ and S^R are the correlators in eqs. (2.7) and (2.8). The beam function path is

$$b = (0, b^-, b_\perp) , \qquad \delta = (0, b^-, 0) , \qquad v = n_B(y_B) \quad \text{with} \quad |\eta| \to \infty . \qquad (2.20)$$

This implies that $b - \delta = b_\perp$, and hence the Wilson line's tranverse segment is perpendicular to its longitudinal segments. This transverse segment is important in singular gauges [70]. Note that the transverse segment is often not specified in the literature: in nonsingular gauges such as Feynman gauge, a Wilson line at lightcone infinity does not make contributions, and its self-energy cancels against the corresponding piece in the soft function [53]. The longitudinal Wilson line segments extend along $\eta v \pm \frac{\delta}{2} = (\eta e^{2y_B}, \eta \pm \frac{\delta}{2}, 0_\perp)$ and thus only depend on the rapidity y_B in the limit $|\eta| \to \infty$. The limit $\eta \to -\infty$ taken in eq. (2.19) applies to Drell-Yan kinematics, whereas SIDIS kinematics uses $\eta \to \infty$.

Finally, we remark that due to taking the lightcone limit prior to UV renormalization, the Collins scheme is equivalent to schemes defined with rapidity regulators on the lightcone [58, 60, 62–65] that are often employed in higher-order perturbative calculations and higher-order resummed phenomenological analyses, see e.g. ref. [66] for a discussion. Such equivalence can be derived from the TMD factorization formula eq. (2.2), where the Feynman diagrams and leading-power contributions are identical for off-the-light-cone and lightcone schemes [66].

2.2.2 Ji-Ma-Yuan (JMY) scheme

The JMY scheme [56] was introduced for the semi-inclusive deep-inelastic scattering (SIDIS) process, $e^- p \to e^- h X$. The factorization theorem eq. (2.2) for Drell-Yan-like processes takes the form

$$\frac{\mathrm{d}\sigma}{\mathrm{d}Q^2 \mathrm{d}Y \mathrm{d}^2 \vec{q}_T} = \sigma_0 \sum_{i,j} H_{ij}(Q,\mu,\rho) \tag{2.21}$$
$$\times \int \frac{\mathrm{d}^2 \vec{b}_T}{(2\pi)^2} e^{\mathrm{i}\vec{q}_T \cdot \vec{b}_T} f_{i/h_1}^{\mathrm{JMY}}(x_1, \vec{b}_T, \mu, x_1 \zeta_v, \rho) \, f_{j/h_2}^{\mathrm{JMY}}(x_2, \vec{b}_T, \mu, x_2 \zeta_{\tilde{v}}, \rho) \,.$$

This scheme is characterized by timelike Wilson lines with directions

$$v^\mu = v^+ n_a^\mu + v^- n_b^\mu = (v^+, v^-, 0_\perp) \,, \qquad v^- \gg v^+ > 0 \,,$$
$$\tilde{v}^\mu = \tilde{v}^+ n_a^\mu + \tilde{v}^- n_b^\mu = (\tilde{v}^+, \tilde{v}^-, 0_\perp) \,, \qquad \tilde{v}^+ \gg \tilde{v}^- > 0 \,. \tag{2.22}$$

The definitions below always use these hierarchies, but not as strict limits; for simplicity we leave them implicit. The offshellness of Wilson lines is encoded in the parameters

$$\zeta_v^2 = \frac{(2P_1 \cdot v)^2}{v^2} = 2(P_1^+)^2 \frac{v^-}{v^+} \,, \quad \zeta_{\tilde{v}}^2 = \frac{(2P_2 \cdot \tilde{v})^2}{\tilde{v}^2} = 2(P_2^-)^2 \frac{\tilde{v}^+}{\tilde{v}^-} \,, \quad \rho^2 = \frac{4(v \cdot \tilde{v})^2}{v^2 \tilde{v}^2} = \frac{v^- \tilde{v}^+}{v^+ \tilde{v}^-} \,. \tag{2.23}$$

We define the JMY scheme TMD as

$$f_{i/h}^{\mathrm{JMY}}(x, \vec{b}_T, \mu, x\zeta_v, \rho) = \frac{B_{i/h}^{\mathrm{JMY}}(x, b_T, \mu, \zeta_v)}{\sqrt{S_{\mathrm{JMY}}^R(b_T, \mu, \rho)}} \,. \tag{2.24}$$

Here $B_{i/h}^{\mathrm{JMY}}$ and S_{JMY} are *renormalized* beam and soft functions. This is a crucial distinction from the Collins scheme, in which we first combine the beam and soft functions, then take the lightlike limit $\rho \to \infty$, and only thereafter carry out renormalization, cf. eq. (2.18).

For a hadron moving in the n_a direction, the JMY quark beam and soft functions are

$$B_{q_i/h}^{\mathrm{JMY}}(x, \vec{b}_T, \mu, \zeta_v) = \int \frac{\mathrm{d}b^-}{2\pi} e^{-\mathrm{i}b^-(xP^+)} \Omega_{q_i/h}^{[\gamma^+]}[b, P, \mu, -\infty v, b^- n_b] \,,$$
$$S_{\mathrm{JMY}}^R(b_T, \mu, \rho) = S^R[b_\perp, \mu, -\infty v, -\infty \tilde{v}] \,, \tag{2.25}$$

where $\Omega_{i/h}$ and S^R are the renormalized generic correlators in eqs. (2.7) and (2.8). Just as in the Collins scheme, we take $b^\mu = (0, b^-, b_\perp)$ and $\delta = (0, b^-, 0_\perp)$ (note that this is usually not specified in the literature). The JMY correlator differs from the Collins correlator in eq. (2.19) by the presence of timelike ($v^2 > 0$) rather than spacelike ($n_B^2 < 0$) Wilson lines. We can perturbatively match the JMY and Collins scheme TMDs, see appendix B.

JMY gluon TMDs are not explicitly defined in the literature; nonetheless, one can define them in an analogous manner to the quark TMDs through eq. (2.7).

2.2.3 Large Rapidity (LR) scheme

Finally, we introduce a new continuum TMD scheme, the LR scheme. The LR scheme uses the same beam and soft functions as the Collins scheme, but a different order of carrying out UV renormalization and approaching the lightcone. Specifically,

$$f_{i/h}^{\mathrm{LR}}(x, \vec{b}_T, \mu, \zeta, y_P - y_B) = \lim_{-y_B \gg 1} \lim_{\epsilon \to 0} Z_{\mathrm{uv}}^{\mathrm{LR}}(\epsilon, \mu, y_n - y_B) \frac{B_{i/h}^C(x, \vec{b}_T, \epsilon, y_P - y_B)}{\sqrt{S_C^R(b_T, \epsilon, 2y_n, 2y_B)}} \,, \quad (2.26)$$

where $\epsilon \to 0$ implements UV renormalization. The UV counterterm $Z_{\mathrm{uv}}^{\mathrm{LR}}$ does not depend on the rapidities in the beam function because the beam function does not involve nontrivial cusp angles, and the renormalization of its staple-shaped Wilson line and quark operators are rapidity-independent. It does however explicitly depend on the Wilson line rapidity difference $y_n - y_B$ through the renormalization of the soft function. In particular, the UV renormalization constant $Z_{\mathrm{uv}}^{\mathrm{LR}}$ is the product of those of the bare beam function and soft factor. As will be shown in section 3.1.2, the bare beam function at large, but finite, $(-y_B)$ is equal to the quasi-beam function in a hadron state with momentum given by $y_P - y_B$. Using the auxiliary field formalism of the Wilson lines, one can show [37, 71–73] that renormalization of the quasi-beam function is multiplicative in coordinate space and independent of the external hadron momentum. Therefore, $Z_{\mathrm{uv}}^{\mathrm{LR}}$ is independent of $y_P - y_B$, and only depends on $y_n - y_B$ due to the renormalization of the soft factor. This should be contrasted with the Collins scheme, where $Z_{\mathrm{uv}}^{\mathrm{C}}$ depends on $\zeta \propto e^{2(y_P - y_n)}$, cf. eq. (2.18).

We note that the renormalized LR scheme TMD depends on $y_P - y_B$; hence, the limit $-y_B \gg 1$ is to be understood as taking $(-y_B)$ large but finite instead of taking the limit $y_B \to -\infty$. The LR and Collins TMDs use the same $\zeta = (2x m_h e^{y_P - y_n})^2$ to encode y_n dependence. We can also view the LR scheme as the JMY scheme defined with spacelike instead of timelike Wilson lines. See section 3.1 for further elaboration on and derivation of LR scheme properties.

2.3 Lattice TMD matrix elements

Next, we provide a brief overview of TMD functions that are amenable to calculation using lattice QCD. Unlike the continuum schemes in section 2.2, lattice TMDs are defined using finite-length Wilson lines. We can obtain their matrix elements from paths involving equal-time spacelike Wilson lines.

2.3.1 Quasi-TMDs

Quasi-TMDs are objects that share the same infrared physics as TMDs, but have finite-length spacelike Wilson lines and are computable on the lattice [34, 36]. The general structure of a quasi-TMD looks quite similar to a TMD:

$$\begin{aligned} \tilde{f}_{i/h}^{[s]}(x, \vec{b}_T, \mu, \tilde{\zeta}, x\tilde{P}^z, \tilde{\eta}) = \lim_{a \to 0} & Z_{\mathrm{uv}}'(\mu, \tilde{\mu}, \tilde{\zeta}) \, Z_{\mathrm{uv}}(a, \tilde{\mu}, y_n - y_B) \\ & \times \tilde{B}_{i/h}^{[s]}(x, \vec{b}_T, a, \tilde{\eta}, x\tilde{P}^z) \, \tilde{\Delta}_S^R(b_T, a, \tilde{\eta}, y_n, y_B) \,, \end{aligned} \quad (2.27)$$

where $\tilde{B}_i$ is the quasi-beam function; $\tilde{\Delta}_S^R$ is the quasi-soft factor; $Z_{\mathrm{uv}}(a, \tilde{\mu}, \tilde{\zeta})$ implements a lattice renormalization with the corresponding scale $\tilde{\mu}$; $Z'_{\mathrm{uv}}(\mu, \tilde{\mu}, \tilde{\zeta})$ implements a conversion to the $\overline{\mathrm{MS}}$ scheme with the $\overline{\mathrm{MS}}$ scale μ; $\tilde{\eta}$ is the extent of the Wilson lines in the quasi-beam and soft functions; and the dependence on $\tilde{\zeta}$ and the rapidities $y_{n,B}$ of the Wilson lines is explained below. As $|\tilde{\eta}| \to \infty$, the leading term in $\tilde{f}_{i/h}$ becomes independent of $\tilde{\eta}$,

$$\tilde{f}_{i/h}(x, \vec{b}_T, \mu, \tilde{\zeta}, x\tilde{P}^z) \equiv \lim_{\tilde{\eta} \to \infty} \tilde{f}_{i/h}(x, \vec{b}_T, \mu, \tilde{\zeta}, x\tilde{P}^z, \tilde{\eta}), \qquad (2.28)$$

with corrections of $\mathcal{O}[b_T/\tilde{\eta}, 1/(\tilde{P}^z \tilde{\eta})]$.

The quasi-beam functions for quarks and gluons can be expressed using the generic correlator in eq. (2.7) as

$$\tilde{B}_{q_i/h}^{[\tilde{\Gamma}]}(x, \vec{b}_T, a, \tilde{\eta}, x\tilde{P}^z) = N_{\tilde{\Gamma}} \int \frac{\mathrm{d}\tilde{b}^z}{2\pi} e^{i\tilde{b}^z(x\tilde{P}^z)} \Omega_{q_i/h}^{[\tilde{\Gamma}]} \left[\tilde{b}, \tilde{P}, a, \tilde{\eta}\hat{z}, \tilde{b}^z \hat{z}\right],$$

$$\tilde{B}_{g/h}^{\alpha\rho\beta\sigma}(x, \vec{b}_T, a, \tilde{\eta}, x\tilde{P}^z) = N^{\alpha\rho\beta\sigma} \int \frac{\mathrm{d}\tilde{b}^z}{2\pi} \frac{e^{i\tilde{b}^z(x\tilde{P}^z)}}{x\tilde{P}^z} \Omega_{g/h}^{\alpha\rho\beta\sigma} \left[\tilde{b}, \tilde{P}, a, \tilde{\eta}\hat{z}, \tilde{b}^z \hat{z}\right]. \qquad (2.29)$$

Here, $\tilde{\Gamma}$ is a Dirac structure, α and β are generic Lorentz indices, ρ and σ are transverse indices, and $N_{\tilde{\Gamma}}$ and $N^{\alpha\rho\beta\sigma}$ are normalization factors. To enable calculations on the lattice, we use equal-time paths

$$\tilde{b} = (0, b_T^x, b_T^y, \tilde{b}^z), \qquad \tilde{\eta}v = \tilde{\eta}\hat{z} = (0, 0, 0, \tilde{\eta}), \qquad \delta = \tilde{b}^z \hat{z} = (0, 0, 0, \tilde{b}^z), \qquad (2.30)$$

as illustrated in figure 4. This choice of δ guarantees that the transverse Wilson line segment is perpendicular to the longitudinal segments and that the total length of the staple $\ell = 2\tilde{\eta} + b_T$ is independent of $\tilde{b}^z$. Therefore, the cusp angles in the quasi-beam function are always trivially $\pi/2$, so that the UV renormalization factor is independent of $\tilde{b}^z$ and can be pulled out of the Fourier integral in eq. (2.29) [37]. This is a key difference to the MHENS scheme discussed in section 2.3.2.

The construction of the quasi-beam function in eq. (2.29) is guided by the observation that by boosting the operator and taking $|\tilde{\eta}| \to \infty$, one recovers eq. (2.19). In contrast, the soft function depends on two almost-lightlike directions and thus cannot be obtained by boosting an equal-time operator [36]; several potential (quasi-)soft functions have been proposed [33, 34, 36] despite the fact that these proposals cannot recover eq. (2.19) under any Lorentz boost. Here, we construct the lattice soft function as a finite-length version of the Collins soft function in eq. (2.19),

$$\tilde{S}^R(b_T, a, \tilde{\eta}, y_A, y_B) = S^R \left[b_\perp, a, -\tilde{\eta}\frac{n_A(y_A)}{|n_A(y_A)|}, -\tilde{\eta}\frac{n_B(y_B)}{|n_B(y_B)|}\right]. \qquad (2.31)$$

Here the length of the soft function path is $L_\gg = 2(2\tilde{\eta} + b_T) = 2L_{\mathrm{staple}}$. The choice of the minus sign in the last two arguments, ηv and $\bar{\eta}\bar{v}$, allows Lorentz-invariant products obtained from these choices to be more easily related to continuum schemes.
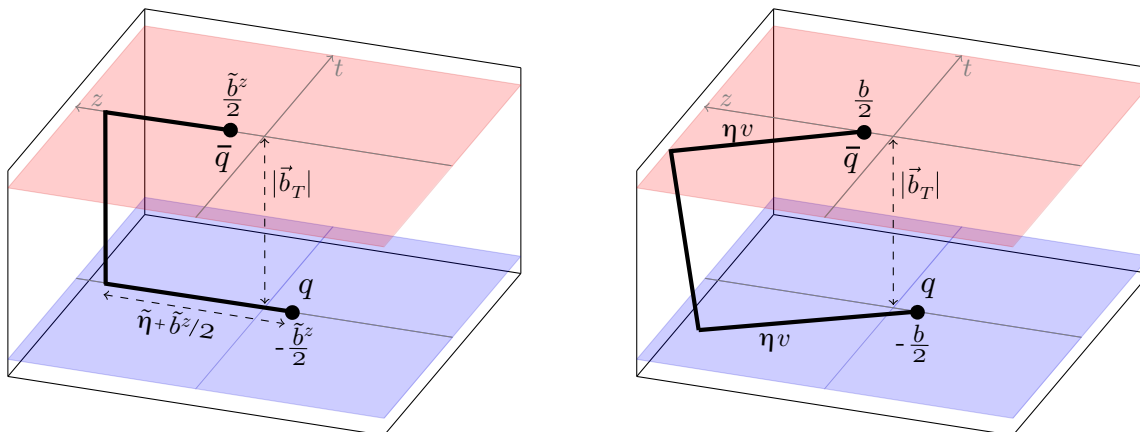
Figure 4. Wilson line structure of (left) the quasi-beam function in eq. (2.29), and (right) the MHENS scheme in eq. (2.39). Quasi-TMD staple legs extend along the z direction and are closed by a perpendicular segment, whereas MHENS staple legs extend along a generic spacelike direction v^μ and are closed by a segment with nontrivial cusp angle γ.

Combining eqs. (2.29) and (2.31) as required by eq. (2.27) gives

$$
\tilde{f}_{i/h}^{[\tilde{\Gamma}]}(x, \vec{b}_T, \mu, \tilde{\zeta}, x\tilde{P}^z) = \lim_{\substack{\tilde{\eta}\to\infty \\ a\to 0}} Z'_{\rm uv}(\mu, \tilde{\mu}) Z_{\rm uv}(a, \tilde{\mu}, y_n - y_B) \frac{\tilde{B}_{i/h}^{[\tilde{\Gamma}]}(x, \vec{b}_T, a, \tilde{\eta}, x\tilde{P}^z)}{\sqrt{\tilde{S}^R(b_T, a, \tilde{\eta}, 2y_n, 2y_B)}}
$$

$$
= \lim_{\tilde{\eta}\to\infty} \frac{\tilde{B}_{i/h}^{[\tilde{\Gamma}]}(x, \vec{b}_T, \mu, \tilde{\eta}, x\tilde{P}^z)}{\sqrt{\tilde{S}^R(b_T, \mu, \tilde{\eta}, 2y_n, 2y_B)}} \,. \tag{2.32}
$$

Here $\tilde{\zeta} = \left(x m_h e^{y_{\tilde{P}} + y_B - y_n}\right)^2 = (2x\tilde{P}^z e^{y_B - y_n})^2$, and the second equality holds for large $\tilde{P}^z$.

In practice, calculating (quasi-)TMD soft functions poses a significant challenge for the lattice. It is possible to construct the quasi-soft function indirectly through the spacelike meson form factor and quasi-wavefunction [38]; promising first results using this approach have been reported in refs. [46, 47].

Prior to this work, the literature has studied different proposals of the quasi-soft function which are constructed from equal-time Wilson lines [33–36, 38, 39]. The naive quasi-soft function features a rectangle-shaped Wilson loop along the z direction,

$$
\tilde{S}_{\rm naive}^R(b_T, a, \tilde{\eta}) \equiv S^R\big[b_\perp, a, \tilde{\eta}\hat{z}, -\tilde{\eta}\hat{z}\big] \,, \tag{2.33}
$$

whose renormalized continuum version with $\tilde{\eta} = \infty$ in the $\overline{\rm MS}$ scheme is denoted

$$
\tilde{S}_{\rm naive}^R(b_T, \mu) \equiv S^R\big[b_\perp, \mu, \infty\hat{z}, -\infty\hat{z}\big] \,. \tag{2.34}
$$

However, it has been shown at one-loop level [36] that $\tilde{S}_{\rm naive}^R(b_T, \mu)$ does not have the correct IR physics for the quasi-TMD to be perturbatively matchable to the Collins TMD. Although refs. [34, 36] proposed a bent quasi-soft function that works at one-loop order, it was argued that the factorization utilizing this function will break down at two loops [38].

Nevertheless, the naive quasi-soft function $\tilde{S}^R_{\rm naive}$ can still serve a useful purpose for lattice calculations, where it can be used to cancel linear power divergences proportional to $\tilde{\eta}$ and b_T. For this reason it is useful to define the naive quasi-TMD as

$$\tilde{f}^{[\tilde{\Gamma}]{\rm naive}}_{i/h}(x,\vec{b}_T,\mu,x\tilde{P}^z) = \lim_{\tilde{\eta}\to\infty} \frac{\tilde{B}^{[\tilde{\Gamma}]}_{i/h}(x,\vec{b}_T,\mu,\tilde{\eta},x\tilde{P}^z)}{\sqrt{\tilde{S}^R_{\rm naive}(b_T,\mu,\tilde{\eta})}}\,. \tag{2.35}$$

This can then be compared to the quasi-TMD $\tilde{f}_{i/h}$ defined with a quasi-soft function $\tilde{S}^R$ that yields the correct infrared structure. Since the η-dependence cancels exactly between the quasi beam and soft functions, we have

$$\lim_{\tilde{\eta}\to\infty} \frac{\tilde{S}^R_{\rm naive}(b_T,\mu,\tilde{\eta})}{\tilde{S}^R(b_T,\mu,\tilde{\eta},2y_n,2y_B)} = \frac{\tilde{S}^R_{\rm naive}(b_T,\mu)}{S^R_C(b_T,\mu,2y_n,2y_B)}\,, \tag{2.36}$$

which leads to the relationship between $\tilde{f}^{\rm naive}_i$ and $\tilde{f}_i$ in eq. (1.3). A further discussion of the equivalence in eq. (2.36) is provided in section 3.1.2.

Moreover, at large rapidity the Collins soft function behaves as [50–52]

$$\lim_{-y_B\gg 1} S^R_C(b_T,\mu,2y_n,2y_B) = S_I(b_T,\mu)\, e^{2(y_n-y_B)\gamma^q_\zeta(b_T,\mu)}\,, \tag{2.37}$$

where $S_I(b_T,\mu)$ is a rapidity-independent component of the soft function. Although the entire S^R_C exponentiates due to the non-Abelian exponentiation theorem for Wilson line operators [74, 75], the important aspect of eq. (2.37) is the particular dependence on rapidity. Using eq. (2.37), the multiplicative factor relating $\tilde{f}^{\rm naive}_i$ and $\tilde{f}_i$ can be simplified as

$$\lim_{y_B\to-\infty} \sqrt{\frac{\tilde{S}^R_{\rm naive}(b_T,\mu)}{S^R_C(b_T,\mu,2y_n,2y_B)}} = \sqrt{\frac{\tilde{S}^R_{\rm naive}(b_T,\mu)}{S_I(b_T,\mu)}} e^{-(y_n-y_B)\gamma^q_\zeta(b_T,\mu)}$$

$$\equiv [g^q_S(b_T,\mu)]^{-1} \exp\left[-\frac{1}{2}\gamma^q_\zeta(b_T,\mu)\ln\frac{(2x\tilde{P}^z)^2}{\zeta}\right]\,, \tag{2.38}$$

Plugging eq. (2.38) into eq. (1.2) gives the original factorization formula eq. (1.1) proposed in refs. [35, 36, 38, 39]. We identify $g^q_S(b_T,\mu)$ as the same factor introduced in ref. [36], which is equivalent to the square root of the *reduced soft function* $S_r(b_T,\mu)$ in refs. [38, 39].

2.3.2 Musch-Hägler-Engelhardt-Negele-Schäfer (MHENS) scheme

TMDs were first studied on the lattice in refs. [27–32] using a Lorentz-invariant approach. We discuss this scheme as formulated in ref. [29], and name it after the authors as the MHENS scheme. The goal of this scheme is to calculate the beam function

$$B^{\rm MHENS\ [\Gamma]}_{q_i/h}(x,\vec{b}_T,P,a,\eta,v) = N_\Gamma \int \frac{{\rm d}b^-}{2\pi} e^{-ix(P\cdot b)} \Omega^{[\Gamma]}_{q_i/h}[b,P,a,\eta v,0]\Big|_{b^+=0} \tag{2.39}$$

using lattice QCD. Here, $\Omega^{[\Gamma]}_{q/h}$ is our usual correlator defined in eq. (2.7), supplemented with the special choice $\delta=0$ that reduces the number of Lorentz invariants in eq. (2.11) to

six. Note that the MHENS scheme is based on a Lorentz-invariant formulation of the TMD correlator in the $\delta = 0$ case. Their correlator Φ is related to our Ω by

$$\tilde{\Phi}_{\text{unsubtr.}}^{[\Gamma]}(b, P, a, \eta v) = \Omega_{q_i/h}^{[\Gamma]}[b, P, a, \eta v, 0] \,. \tag{2.40}$$

To make the connection between Minkowksi and Euclidean spaces for the correlator in eq. (2.39), ref. [29] decomposes it for generic choices of b, P and v as

$$\frac{1}{2}\Omega_{q_i/h}^{[\gamma^\mu]}[b, P, a, \eta v, 0] = P^\mu \tilde{A}_2\left(b^2, b \cdot P, \frac{v \cdot b}{v \cdot P}, \frac{v^2}{(v \cdot P)^2}, \eta v \cdot P\right)$$
$$+ \frac{P^2 v^\mu}{v \cdot P}\tilde{B}_1\left(b^2, b \cdot P, \frac{v \cdot b}{v \cdot P}, \frac{v^2}{(v \cdot P)^2}, \eta v \cdot P\right) + \dots, \tag{2.41}$$

where the ellipses stand for other spin-dependent and higher-twist structures. For the full parametrization and similar decompositions for all Γ, see ref. [29].

The scalar amplitudes $\tilde{A}_2$ and $\tilde{B}_1$ depend on all six Lorentz invariants, though we leave implicit dependence on the hadron mass $P^2 = m_h^2$. For the beam function in eq. (2.39), it remains to specify $b^+ = 0$ and $v_\perp = P_\perp = 0$, which in a Lorentz-invariant fashion reads [29]

$$\frac{v \cdot b}{v \cdot P} = \frac{b \cdot P}{P^2}R(\hat{\zeta}^2)\,, \quad R(\hat{\zeta}^2) = 1 - \sqrt{1 + \hat{\zeta}^{-2}}\,. \tag{2.42}$$

Thus, the third argument of $\tilde{A}_2$ and $\tilde{B}_1$ in eq. (2.41) is not independent of the other arguments, and on the lattice one is forced to choose b and v such that eq. (2.42) is fulfilled. The CS-like parameter $\hat{\zeta}$ entering eq. (2.42) is defined as

$$\hat{\zeta} = \frac{v \cdot P}{\sqrt{|v^2|P^2}}\,. \tag{2.43}$$

Parameterizing P and v by their rapidities shows that $\hat{\zeta}$ essentially is a rapidity difference,

$$P^\mu = \frac{m_h}{\sqrt{2}}(e^{y_P}, e^{-y_P}, 0_\perp)\,, \quad v^\mu \propto (e^{y_v}, -e^{-y_v}, 0_\perp) \quad \Rightarrow \quad \hat{\zeta} = \sinh(y_v - y_P)\,. \tag{2.44}$$

Note the minus sign for v^- is required for spacelike $v^2 < 0$; thus, y_v is not an actual rapidity. To connect to the continuum TMDs one considers the large rapidity limit, equivalent to $v \cdot P \to \infty$ with P^2 fixed, so $\hat{\zeta} \to \infty$.

Inserting eq. (2.42) into eq. (2.41) and specifying $\Gamma = \gamma^+$ as required for the unpolarized TMD, at leading twist we obtain

$$\frac{1}{2}\Omega_{q_i/h}^{[\gamma^+]}[b, P, a, \eta v, 0]\Big|_{b^+=0} = P^+ \tilde{A}_{2B}\left(b^2, b \cdot P, \frac{v \cdot b}{v \cdot P} = \frac{b \cdot P}{P^2}R(\hat{\zeta}^2), \frac{v^2}{(v \cdot P)^2}, \eta v \cdot P\right), \tag{2.45}$$

where $\tilde{A}_{2B} = \tilde{A}_2 + R(\hat{\zeta}^2)\tilde{B}_1$. Inserting this result into eq. (2.39), the unpolarized MHENS beam function is given by

$$\frac{1}{2}B_{q_i/h}^{\text{MHENS }[\gamma^+]}(x, \vec{b}_T, P, a, \eta v) = \int \frac{\mathrm{d}(b \cdot P)}{2\pi}e^{-\mathrm{i}x(P \cdot b)}\tilde{A}_{2B}\left(b^2, b \cdot P, \frac{b \cdot P}{P^2}R(\hat{\zeta}^2), \frac{v^2}{(v \cdot P)^2}, \eta v \cdot P\right). \tag{2.46}$$

One can obtain other leading-twist and spin-dependent beam functions in a similar fashion. Due to its Lorentz-invariant formulation, eq. (2.46) can be evaluated in any frame so long as eq. (2.42) is satisfied. This includes a frame where $b^0 = v^0 = 0$, as required on the lattice.

The above method has been applied to calculating the moments of TMDs. Since integrating over x sets $P \cdot b = 0$, the moments can be calculated in a frame where $b = (0, 0, b_\perp)$. In this case the beam functions $\Omega_{q/h}^{[\gamma^+]}$ agree between the MHENS and Collins schemes since we have $\delta = 0$ in both cases. We elaborate on this further in section 3.2.4.

To calculate the x-dependence, one must evaluate eq. (2.46) for generic $P \cdot b \neq 0$. In this case, the MHENS and Collins staples are shaped differently, and thus their beam functions are *not* equivalent. There are two key differences. First, the Collins staple is closed along $b - \delta = b_\perp$, and thus its tranverse and longitudinal Wilson line segments are perpendicular to one another. In contrast, the MHENS staple closes along $b - \delta = b$, which for $v \cdot b \neq 0$ induces a $(P \cdot b)$-dependent cusp angle according to eq. (2.42). Second, in the frame where $b^0 = 0$, the MHENS staple length is not b^z-independent, leading to nontrivial Wilson-line self-energies that depend on b^z or $P \cdot b$. Overall, this leads to a nontrivial Wilson line renormalization that depends on $P \cdot b$ which cannot be factored out of the Fourier integral. We demonstrate this at one-loop order in appendix C, and discuss the relation between the MHENS and Collins TMDs in depth in section 3.2.4.

3 Factorization between physical and lattice TMDs

This section proves the factorization between the quasi- and Collins TMDs, eq. (1.2). Our proof of factorization takes two steps, as depicted in figure 1: first connecting the quasi-TMD to the intermediate LR scheme, then connecting the LR and Collins schemes.

We begin with a bird's eye view of various TMD schemes and their relationships to one another. By using the general correlator Ω that we introduced in eq. (2.7), in table 1 we see that TMDs take on a similar form in all schemes. Key differences manifest in the order of limits taken to form the TMD, as well as the specific arguments of the beam function correlator Ω. Notably, we can express Ω in terms of Lorentz-invariant combinations of its arguments. Comparing the values that these Lorentz invariants take on in each scheme, as shown in table 2, provides a useful way of relating different schemes to one another. These tables are central to our proof, which we present in section 3.1. We discuss implications of our results in section 3.2.

3.1 Proof

We now present a proof of the quasi-to-Collins TMD factorization in detail for the unpolarized quark TMD case. The proof of factorization for other leading-twist TMDs follows naturally using the same framework, with only minor, straightforward modifications for gluon TMDs or other spin structures. We also remark that our proof employs dimensional regularization and the same UV regulator for the quasi and LR schemes.

We begin our proof in section 3.1.1 by considering the correlator Ω as a function of Lorentz invariants, and examining the values that these Lorentz invariants take on in various schemes. In section 3.1.2, we see that the quasi and LR scheme Lorentz invariants are

	TMD	Beam function	Soft function
Collins	$\lim\limits_{\epsilon \to 0} Z_{\rm UV}^R \lim\limits_{y_B \to -\infty} \dfrac{\Omega_{i/h}}{\sqrt{S^R}}$	$\Omega_{q/h}^{[\gamma^+]}\,[b, P, \epsilon, -\infty n_B(y_B), b^- n_b]$	$S^R\,[b_\perp, \epsilon, -\infty n_A(y_A), -\infty n_B(y_B)]$
LR	$\lim\limits_{-y_B \gg 1} \lim\limits_{\epsilon \to 0} Z_{\rm UV}^R \dfrac{\Omega_{i/h}}{\sqrt{S^R}}$	$\Omega_{q/h}^{[\gamma^+]}\,[b, P, \epsilon, -\infty n_B(y_B), b^- n_b]$	$S^R\,[b_\perp, \epsilon, -\infty n_A(y_A), -\infty n_B(y_B)]$
JMY	$\lim\limits_{\frac{v^-}{v^+} \gg 1} \lim\limits_{\epsilon \to 0} Z_{\rm UV}^R \dfrac{\Omega_{i/h}}{\sqrt{S^R}}$	$\Omega_{q/h}^{[\gamma^+]}\,[b, P, \mu, -\infty v, b^- n_b]$	$S^R\,[b_\perp, \mu, -\infty v, -\infty \tilde{v}]$
Quasi	$\lim\limits_{a \to 0} Z_{\rm UV} \dfrac{\Omega_{i/h}}{\sqrt{\tilde{S}^R}}$	$\Omega_{q/h}^{[\gamma^{0,z}]}\,[\tilde{b}, \tilde{P}, a, \tilde{\eta}\hat{z}, \tilde{b}^z\hat{z}]$	$S^R\left[b_\perp, a, -\tilde{\eta}\dfrac{n_A(y_A)}{|n_A(y_A)|}, -\tilde{\eta}\dfrac{n_A(y_A)}{|n_A(y_A)|}\right]$
MHENS		$\Omega_{q/h}^{[\Gamma]}\,[b, P, a, \eta v, 0]$	

Table 1. Overview of TMD schemes, as presented in section 2. The correlator Ω is a function of Lorentz invariants constructed from its arguments. See table 2 for a comparison of parameter values, Wilson line definitions, and Lorentz invariants in each scheme.

identical at large proton momenta by evaluating the quasi-TMD in a boosted frame. We thus can move from the quasi to the LR scheme through a large rapidity expansion. In section 3.1.3 we demonstrate that reversing the renormalization and lightcone limits to go from the LR to the Collins scheme gives rise to a perturbative matching coefficient. The combination of expansion and matching leads to the desired factorization relation.

3.1.1 Beam correlators as a function of Lorentz invariants

Let us begin by examining the structure of the quasi-TMD. In dimensional regularization, the quark quasi-beam function in eq. (2.29) reads

$$\tilde{B}_{q_i/h}^{[\tilde{\Gamma}]}(x, \vec{b}_T, \epsilon, \tilde{\eta}, x\tilde{P}^z) = N_{\tilde{\Gamma}} \int \frac{\mathrm{d}\tilde{b}^z}{2\pi} e^{\mathrm{i}\tilde{b}^z(x\tilde{P}^z)} \Omega_{q_i/h}^{[\tilde{\Gamma}]}\left[\tilde{b}, \tilde{P}, \epsilon, \tilde{\eta}\hat{z}, \tilde{b}^z\hat{z}\right]\,, \tag{3.1}$$

where $\tilde{b}^\mu = (0, \vec{b}_T, \tilde{b}^z)$. To study an unpolarized Collins TMD, we must set $\Gamma = \gamma^+$ in eq. (2.19). To compare this to the quasi-TMD, we must take $\tilde{\Gamma} = \gamma^0$ or γ^z, which require normalization factors

$$N_{\gamma^z} = 1\,, \qquad N_{\gamma^0} = \frac{\tilde{P}^z}{\tilde{P}^0} = \tanh(y_{\tilde{P}}) \stackrel{y_{\tilde{P}} \gg 1}{=} 1\,. \tag{3.2}$$

We can decompose the coordinate-space correlator with arbitrary b, P, v and δ into Lorentz-covariant structures as[3]

$$\Omega_{q_i/h}^{[\gamma^\mu]}[b, P, \epsilon, \tilde{\eta}v, \delta] = P^\mu \Omega_{q_i/h} + \frac{b^\mu}{-b^2}\Omega_{q_i/h}^b + \frac{v^\mu\sqrt{P^2}}{\sqrt{|v|^2}}\Omega_{q_i/h}^v + \frac{\delta^\mu}{-b^2}\Omega_{q_i/h}^\delta$$

$$= P^\mu \Omega_{q_i/h} + \text{higher twist}\,, \tag{3.3}$$

---

[3]For the full parameterization including spin-dependent terms, see e.g. ref. [29]. Note however that they work with the correlator Ω where $\delta = 0$. The more general analysis carried out with our Ω at $\delta \neq 0$ gives rise to additional terms.

	Collins / LR	JMY	Quasi	MHENS
b^μ	$(0,b^-,b_\perp)$	$(0,b^-,b_\perp)$	$(0,b_T^x,b_T^y,\tilde{b}^z)$	$(0,b_T^x,b_T^y,\tilde{b}^z)$
v^μ	$(-e^{2y_B},1,0_\perp)$	$(v^-e^{2y'_B},v^-,0_\perp)$	$(0,0,0,-1)$	$(0,v^x,v^y,v^z)$
δ^μ	$(0,b^-,0_\perp)$	$(0,b^-,0_\perp)$	$(0,0,0,\tilde{b}^z)$	$(0,0,0_\perp)$
P^μ	$\frac{m_h}{\sqrt{2}}(e^{y_P},e^{-y_P},0_\perp)$	$\frac{m_h}{\sqrt{2}}(e^{y_P},e^{-y_P},0_\perp)$	$m_h(\cosh y_{\tilde{P}},0,0,\sinh y_{\tilde{P}})$	$m_h\left(\cosh y_P,\frac{P^x}{m_h},\frac{P^y}{m_h},\sinh y_P\right)$
b^2	$-b_T^2$	$-b_T^2$	$-b_T^2-(\tilde{b}^z)^2$	$-b_T^2-(\tilde{b}^z)^2$
$(\eta v)^2$	$-2\eta^2 e^{2y_B}$	$2\eta^2(v^-)^2 e^{2y'_B}$	$-\tilde{\eta}^2$	$-\eta^2\vec{v}^2$
$P\cdot b$	$\frac{m_h}{\sqrt{2}}b^- e^{y_P}$	$\frac{m_h}{\sqrt{2}}b^- e^{y_P}$	$-m_h\tilde{b}^z\sinh y_{\tilde{P}}$	$m_h\sinh y_P\tilde{b}^z+P^x b_T^x+P^y b_T^y$
$\dfrac{b\cdot(\eta v)}{\sqrt{|(\eta v)^2 b^2|}}$	$-\dfrac{b^- e^{y_B}}{\sqrt{2}\,b_T}\operatorname{sgn}(\eta)$	$\dfrac{b^- e^{y'_B}}{\sqrt{2}\,b_T}\operatorname{sgn}(\eta)$	$\dfrac{\tilde{b}^z}{\sqrt{(\tilde{b}^z)^2+b_T^2}}\operatorname{sgn}(\eta)$	$\dfrac{b_T^x v^x+b_T^y v^y+\tilde{b}^z v^z}{\sqrt{v_T^2+(v^z)^2}\sqrt{b_T^2+(\tilde{b}^z)^2}}$
$\dfrac{P\cdot(\eta v)}{\sqrt{P^2|\eta v|^2}}$	$\sinh(y_P-y_B)\operatorname{sgn}(\eta)$	$\cosh(y_P-y'_B)\operatorname{sgn}(\eta)$	$\sinh y_{\tilde{P}}\operatorname{sgn}(\eta)$	$\dfrac{P^x v^x+P^y v^y+m_h v^z\sinh y_P}{\sqrt{v_T^2+(v^z)^2}\sqrt{m_h^2+P_x^2+P_y^2}}$
$\dfrac{\delta^2}{b^2}$	0	0	$\dfrac{(\tilde{b}^z)^2}{b_T^2+(\tilde{b}^z)^2}$	0
$\dfrac{b\cdot\delta}{b^2}$	0	0	$\dfrac{(\tilde{b}^z)^2}{b_T^2+(\tilde{b}^z)^2}$	0
$\dfrac{P\cdot\delta}{P\cdot b}$	1	1	1	0
$\dfrac{\delta\cdot(\eta v)}{b\cdot(\eta v)}$	1	1	1	0
P^2	m_h^2	m_h^2	m_h^2	m_h^2

Table 2. Overview of the Lorentz invariants entering the generic TMD correlator as specified by eq. (2.11). Note that the Collins and LR schemes use the same four-vectors.

where the dimensionless form factors Ω on the right-hand side are functions of the 10 Lorentz invariants in eq. (2.11), which we suppress for brevity. The prefactors share the same mass dimension and are finite as $\delta\to0$ or $b\cdot v/\sqrt{|v^2 b^2|}\to0$. In the second line, we neglect terms that are suppressed at large momentum P, which do not contribute at leading power.

Combining eqs. (3.1) and (3.3) and using $\tilde{P}_\perp=0$, we have

$$\tilde{B}_{q_i/h}^{[\tilde{\Gamma}]}(x,\vec{b}_T,\epsilon,\tilde{\eta},x\tilde{P}^z) = \int \frac{\mathrm{d}(\tilde{b}\cdot\tilde{P})}{2\pi}\, e^{-ix(\tilde{b}\cdot\tilde{P})}\, \Omega_{q_i/h}\left[\tilde{b},\tilde{P},\epsilon,\tilde{\eta}\hat{z},\tilde{b}^z\hat{z}\right]. \qquad (3.4)$$

Note that the integration measure, the Fourier phase, and $\Omega_{q_i/h}$ are Lorentz invariants. We can write the LR/Collins beam function similarly:

$$B_{q_i/h}^C(x,\vec{b}_T,\epsilon,y_P-y_B) = \int \frac{\mathrm{d}(b\cdot P)}{2\pi}\, e^{-ix(b\cdot P)}\, \Omega_{q_i/h}[b,P,\epsilon,-\infty n_B(y_B),b^- n_b]. \qquad (3.5)$$

The only differences between eqs. (3.4) and (3.5) lie in the beam function parametrization, as well as the gauge link's direction, length, and closure at infinity, as seen in table 2:

Quasi-TMD: $\quad \tilde{b}^\mu=(0,b_T^x,b_T^y,\tilde{b}^z),\quad \tilde{P}^\mu=\frac{m_h}{2}(e^{y_{\tilde{P}}},e^{-y_{\tilde{P}}},0_\perp),\quad \tilde{\eta}\hat{z}^\mu=(0,0,0,\tilde{\eta}),\quad (3.6)$

LR scheme: $\quad b^\mu=(0,b^-,b_\perp),\qquad P^\mu=\frac{m_h}{2}(e^{y_P},e^{-y_P},0_\perp),\quad \eta n_B^\mu=\eta(-e^{2y_B},1,0_\perp).$

Note that we distinguish quasi components by tildes. Both schemes have the same transverse components $b_\perp^\mu = (0, b_T^x, b_T^y, 0)$.

3.1.2 Relating LR and quasi-TMDs

As we saw in section 2.1, we can express the quasi-, LR, and Collins TMDs in terms of the same Lorentz-invariant function Ω in eq. (2.7), albeit with different parametrizations for its arguments. We can relate the LR and quasi-TMDs to one another by considering Lorentz-transforms of their arguments. Boosting the quasi-TMD four-vectors in eq. (3.6) by a rapidity y_B, we have

$$
\begin{aligned}
\tilde{b}^\mu &= (0, b_T^x, b_T^y, \tilde{b}^z) = \left(\frac{\tilde{b}^z}{\sqrt{2}}, -\frac{\tilde{b}^z}{\sqrt{2}}, b_\perp\right) && \xrightarrow{\text{boost}} && \left(\frac{\tilde{b}^z e^{y_B}}{\sqrt{2}}, -\frac{\tilde{b}^z e^{-y_B}}{\sqrt{2}}, b_\perp\right), \\
\tilde{P}^\mu &= \frac{m_h}{\sqrt{2}}(e^{y_{\tilde{P}}}, e^{-y_{\tilde{P}}}, 0_\perp) && \xrightarrow{\text{boost}} && \frac{m_h}{\sqrt{2}}(e^{y_{\tilde{P}}+y_B}, e^{-(y_{\tilde{P}}+y_B)}, 0_\perp), \\
\tilde{\eta}\hat{z} &= (0,0,0,1) = \frac{\tilde{\eta}}{\sqrt{2}}(1, -1, 0_\perp) && \xrightarrow{\text{boost}} && -\frac{\tilde{\eta}e^{-y_B}}{\sqrt{2}}(-e^{2y_B}, 1, 0_\perp), \\
\delta^\mu &= \tilde{b}^z \hat{z}^\mu = (0,0,0,\tilde{b}^z) = \frac{\tilde{b}^z}{\sqrt{2}}(1, -1, 0_\perp) && \xrightarrow{\text{boost}} && -\frac{\tilde{b}^z e^{-y_B}}{\sqrt{2}}(-e^{2y_B}, 1, 0_\perp), \quad (3.7)
\end{aligned}
$$

where we recall that δ encodes the geometry of the transverse Wilson line. We use lightcone coordinates to make the boost manifest. Comparing eq. (3.7) to eq. (3.6), we can match all but one component of the boosted-quasi and LR schemes if we take

$$
b^- \equiv -\frac{\tilde{b}^z e^{-y_B}}{\sqrt{2}}, \qquad y_P \equiv y_{\tilde{P}} + y_B, \qquad \eta \equiv -\frac{\tilde{\eta}e^{-y_B}}{\sqrt{2}}; \qquad (3.8)
$$

that is, except for $\tilde{b}^+$ of the boosted $\tilde{b}^\mu$. Fortunately, this does not hold us back: to make the correspondence we need to fix the parameters b^-, y_P, and η to their LR scheme values in eq. (3.8), whereas $\tilde{b}^+$ is a derived quantity. Additionally, in the large rapidity limit we can neglect $\tilde{b}^+$:

$$
\tilde{b}^+ \equiv \frac{\tilde{b}^z e^{y_B}}{\sqrt{2}} = -b^- e^{2y_B} \xrightarrow{y_B \to -\infty} 0. \qquad (3.9)
$$

In this limit, we also have that

$$
\tilde{b}^z = -\sqrt{2}b^- e^{y_B} \xrightarrow{y_B \to -\infty} 0, \qquad y_{\tilde{P}} = y_P - y_B \xrightarrow{y_B \to -\infty} \infty, \qquad (3.10)
$$

so at large $\tilde{P}^z$ and small $\tilde{b}^z$ relative to b_T, the quasi-correlator is equivalent to the LR correlator.

Note that we could have alternatively demonstrated the equivalence of the quasi- and LR/Collins Lorentz invariants by transforming $\tilde{b}^z$, y_P, and $\tilde{\eta}$ from the values in table 2 to those in eq. (3.8), and then applying the limit $y_B \to -\infty$. For example,

$$
\begin{aligned}
\tilde{P} \cdot \tilde{b} &= -m_h \tilde{b}^z \sinh y_{\tilde{P}} = m_h \sqrt{2} e^{y_B} b^- \sinh(y_P - y_B) && \xrightarrow{y_B \to -\infty} && \frac{m_h}{\sqrt{2}} b^- e^{y_P}, \\
\frac{\delta^2}{\tilde{b}^2} &= \frac{1}{1 + (b_T/\tilde{b}^z)^2} = \frac{1}{1 + \left(\frac{b_T e^{-y_B}}{\sqrt{2}b^-}\right)^2} && \xrightarrow{y_B \to -\infty} && 0. \qquad (3.11)
\end{aligned}
$$

By definition, the Lorentz invariants of a TMD remain unchanged by Lorentz boosts. If we expand the quasi-TMD invariants in the boosted frame at large $-y_B$ around those of the LR/Collins scheme, we can write a relationship between correlators:

$$\Omega_{q_i/h}\left[\tilde{b}, \tilde{P}, \epsilon, \tilde{\eta}\hat{z}, \tilde{b}^z\hat{z}\right]\Big|_{\text{quasi}} = \Omega_{q_i/h}\left[\tilde{b}, \tilde{P}, \epsilon, \tilde{\eta}\hat{z}, \tilde{b}^z\hat{z}\right]\Big|_{\text{boosted quasi}}, \tag{3.12}$$

$$\lim_{y_B \ll -1} \Omega_{q_i/h}\left[\tilde{b}, \tilde{P}, \epsilon, \tilde{\eta}\hat{z}, \tilde{b}^z\hat{z}\right]\Big|_{\text{boosted quasi}} = \lim_{y_B \ll -1} \Omega_{q_i/h}\left[b, P, \epsilon, \eta n_B(y_B), b^- n_b\right]\Big|_{\text{Collins/LR}}.$$

Making the parameterizations of b and P in both schemes explicit and shifting $y_{\tilde{P}} \to y_P - y_B$ (this is not a boost, but rather a change in the parametrization of the proton's momentum) we obtain

$$\lim_{y_B \ll -1} \Omega_{q_i/h}\left[\tilde{b}=(0,\vec{b}_T,-\sqrt{2}b^- e^{y_B}), \tilde{P}=\frac{m_h}{2}(e^{y_P-y_B}, e^{-(y_P-y_B)}, 0_\perp), \epsilon, \tilde{\eta}\hat{z}, \tilde{b}^z\hat{z}\right]$$

$$= \lim_{y_B \ll -1} \Omega_{q_i/h}\left[b=(0,b^-,b_\perp), P=\frac{m_h}{2}(e^{y_P}, e^{-y_P}, 0_\perp), \epsilon, -\frac{\tilde{\eta}e^{-y_B}}{\sqrt{2}}n_B(y_B), b^- n_b\right]. \tag{3.13}$$

Here, the first correlator yields the quasi-beam function at the shifted proton momentum, while the second correlator is that of the Collins/LR scheme at *finite* length

$$\eta = -\frac{\tilde{\eta}e^{-y_B}}{\sqrt{2}}. \tag{3.14}$$

Note that η and $\tilde{\eta}$ always have opposite signs, and that $\eta < 0$ corresponds to the TMD PDF for Drell-Yan, while $\eta > 0$ corresponds to the TMD PDF for SIDIS.

Next, we supplement eq. (3.13) with a soft subtraction and UV renormalization. On the lattice we cannot take the strict limit $y_B \to -\infty$, so we must keep y_B large but finite. The Collins scheme entails taking the lightcone limit of $B/\sqrt{S}$ prior to UV renormalization, but here we must renormalize at finite y_B. Up until this point, all statements we made hold for both the bare Collins and LR schemes, but for the remainder of this subsection, we only compare the renormalized quasi- and LR TMDs. Let us now write the renormalized quasi- and LR TMDs as

$$\tilde{f}_{q_i/h}(x, \vec{b}_T, \mu, \tilde{\zeta}, x\tilde{P}^z, \tilde{\eta})$$
$$= \int \frac{\mathrm{d}(\tilde{P}\cdot\tilde{b})}{2\pi} e^{-ix(\tilde{P}\cdot\tilde{b})} \lim_{\epsilon \to 0} Z^q_{\text{uv}}(\mu, \epsilon, y_n - y_B) \frac{\Omega_{q_i/h}\left[\tilde{b}, \tilde{P}, \epsilon, \tilde{\eta}\hat{z}, \tilde{b}^z\hat{z}\right]}{\sqrt{\tilde{S}^q(b_T, \epsilon, \tilde{\eta}, 2y_n, 2y_B)}}, \tag{3.15}$$

and

$$f^{\text{LR}}_{q_i/h}(x, \vec{b}_T, \mu, \zeta, y_P - y_B, \eta)$$
$$= \int \frac{\mathrm{d}(P\cdot b)}{2\pi} e^{-ix(P\cdot b)} \lim_{\epsilon \to 0} Z^q_{\text{uv}}(\mu, \epsilon, y_n - y_B) \frac{\Omega_{q_i/h}[b, P, \epsilon, \eta n_B(y_B), b^- n_b]}{\sqrt{S^q(b_T, \epsilon, \eta, 2y_n, 2y_B)}}. \tag{3.16}$$

Here we define the five argument S^q by

$$S^q(b_T, \epsilon, \eta, 2y_n, 2y_B) = \tilde{S}^q(b_T, \epsilon, \tilde{\eta}, 2y_n, 2y_B). \tag{3.17}$$

The parameter y_n governs the amount of soft radiation absorbed into the TMDs and gives rise to the CS scales

$$\tilde{\zeta} = 2(x\tilde{P}^+ e^{y_B-y_n})^2 = x^2 m_h^2 e^{2(y_{\tilde{P}}+y_B-y_n)}, \quad \zeta = 2(xP^+ e^{-y_n})^2 = x^2 m_h^2 e^{2(y_P-y_n)}. \quad (3.18)$$

In eq. (3.15), following standard notation for quasi-TMDs, we encode dependence on $y_P - y_B$ in $\tilde{P}^z = m_h \sinh(y_P - y_B)$, whereas in eq. (3.16) we state this dependence explicitly. The constraint of $y_{\tilde{P}} = y_P - y_B$ leads to $\zeta = \tilde{\zeta}$. For both TMDs, we use the finite-length soft function in eq. (2.31), repeated here for convenience:

$$\tilde{S}^R(b_T, \epsilon, \tilde{\eta}, y_A, y_B) = S^R\left[b_\perp, \epsilon, -\tilde{\eta}\frac{n_A(y_A)}{|n_A(y_A)|}, -\tilde{\eta}\frac{n_B(y_B)}{|n_B(y_B)|}\right]. \quad (3.19)$$

The geometric length of the soft function Wilson line is twice of that of the quasi-beam function, so that all linear divergences from Wilson line self-energies cancel in eq. (3.15).[4]

Since the hadronic matrix elements in eqs. (3.15) and (3.16) are related by a boost, we naturally also employ this soft function for the finite-length LR scheme.

Finally, we discuss the form of the UV counterterm Z^q, which is simply the ratio of the individual counterterms Z_{uv}^B and Z_{uv}^S for the beam and soft functions,

$$Z_{\mathrm{uv}}^q(\mu, \epsilon, y_n - y_B) = \frac{Z_{\mathrm{uv}}^B(\mu, \epsilon)}{\sqrt{Z_{\mathrm{uv}}^S(\mu, \epsilon, 2y_n - 2y_B)}}. \quad (3.20)$$

Here, we use that in the $\overline{\mathrm{MS}}$ scheme, the UV divergences of the quasi-beam and soft functions are multiplicative and $x\tilde{P}^z$-independent, according to the auxiliary field formalism [40, 73].

Using eq. (3.13), we can now relate the renormalized finite-length quasi-TMD and LR TMD defined in eqs. (3.15) and (3.16),

$$\lim_{y_B \ll -1} \tilde{f}_{q_i/h}(x, \vec{b}_T, \mu, \tilde{\eta}, \zeta, x\tilde{P}^z) = \lim_{y_B \ll -1} f_{q_i/h}^{\mathrm{LR}}\left(x, \vec{b}_T, \mu, -\frac{\tilde{\eta}}{\sqrt{2}}e^{-y_B}, \tilde{\zeta}, y_P - y_B\right). \quad (3.21)$$

Here, we have accounted for the change of Wilson line length in the LR scheme and used $\tilde{\zeta}$ as the common CS scale.

The final step is to take the limit $\tilde{\eta} \to \infty$ to relate this result to the continuum TMD. In the continuum TMD, this limit is taken prior to UV renormalization (or $\epsilon \to 0$), while on the lattice one is forced to extrapolate to infinite $\tilde{\eta}$ after renormalization. Thus, we must show that the limits $\tilde{\eta} \to \infty$ and $\epsilon \to 0$ commute. First, for $\tilde{\eta} \gg b_T \gg \tilde{b}^z$ the Wilson-line self-energy contributions cancel exactly in the ratio $\Omega/\sqrt{S}$, which is not affected by the order of the $\tilde{\eta} \to \infty$ and $\epsilon \to 0$ limits. The reason is that the staple geometry in the correlator Ω is one half of that of the quasi-soft function S, and the exchange of gluons between the two halves in S is exponentially suppressed due to the spacelike separation and

---

[4]Recall that in dimensional regularization considered here, these linear divergences appear as poles in $1/(d-3)$, and hence are absent in the $\overline{\mathrm{MS}}$ scheme where only poles in $1/(d-4)$ are subtracted. Hence, these linear divergences are set to zero for perturbative calculations in the $\overline{\mathrm{MS}}$ scheme, but it is important to take them into account for a definition amenable to lattice calculations.

large $\tilde{\eta}$. Second, after the subtraction of Wilson-line self-energy diagrams, the remaining diagrams will include the eikonal propagators

$$\frac{1 - e^{\pm i(n_B \cdot (k \pm i\varepsilon)\tilde{\eta}/|n_B|}}{n_B \cdot k \pm i\varepsilon}\,, \tag{3.22}$$

which have a singularity at $n_B \cdot k = 0$. Such a singularity can be regulated either with a finite $\tilde{\eta}$ and without the imaginary part $i\varepsilon$, or if we keep $i\varepsilon$ and throw away the second term in the numerator. For both regulators, the results are the same and independent of $\tilde{\eta}$ if one takes the $\tilde{\eta} \to \infty$ or $\varepsilon \to 0$ limit in the end, which we have also verified explicitly at one-loop order. Therefore, the $\tilde{\eta} \to \infty$ and $\epsilon \to 0$ limits also commute for these diagrams.

In summary, this commutativity leads to the equivalence of the quasi- and LR TMDs with infinite Wilson lines:

$$
\begin{aligned}
\tilde{f}_{q_i/h}&(x, \vec{b}_T, \mu, \tilde{\zeta}, x\tilde{P}^z) \\
&= \lim_{-y_B \gg 1} \int \frac{\mathrm{d}(\tilde{P}\cdot\tilde{b})}{2\pi} e^{-\mathrm{i}x(\tilde{P}\cdot\tilde{b})} \lim_{\epsilon \to 0} Z_{\mathrm{uv}}^q(\mu, \epsilon, y_n - y_B) \lim_{\tilde{\eta} \to \infty} \frac{\Omega_{q_i/h}\left[\tilde{b}, \tilde{P}, \epsilon, \tilde{\eta}\hat{z}, \tilde{b}^z \hat{z}\right]}{\sqrt{\tilde{S}^q(b_T, \epsilon, \tilde{\eta}, 2y_n, 2y_B)}} \\
&= \lim_{-y_B \gg 1} \int \frac{\mathrm{d}(P\cdot b)}{2\pi} e^{-\mathrm{i}x(P\cdot b)} \lim_{\epsilon \to 0} Z_{\mathrm{uv}}^q(\mu, \epsilon, y_n - y_B) \lim_{\eta \to -\infty} \frac{\Omega_{q_i/h}[b, P, \epsilon, \eta n_B(y_B), b^- n_b]}{\sqrt{S^q(b_T, \epsilon, \eta, 2y_n, 2y_B)}} \\
&= f_{q_i/h}^{\mathrm{LR}}(x, \vec{b}_T, \mu, \tilde{\zeta}, y_P - y_B)\,.
\end{aligned}
\tag{3.23}
$$

Here we used the commutativity of the $\epsilon \to 0$ and $\tilde{\eta} \to \infty$ limits in first step, used eq. (3.21) in the second step, and used that the $\eta \to -\infty$ limit naturally gives the continuum LR TMD defined in eq. (2.26) in the last step. Note that we could equally well have obtained the LR TMD with $\eta \to +\infty$ by choosing to consider the quasi TMD with the limit $\tilde{\eta} \to -\infty$. This choice of obtaining the limits $\eta \to \pm\infty$ is physically relevant for the time reversal odd TMD PDFs, namely the Sivers and Boer-Mulders functions, which are known to differ by an overall sign in Drell-Yan and SIDIS.

3.1.3 Matching LR and Collins TMDs

We now know that the quasi and LR schemes are equivalent in the large $\tilde{P}^z$, large rapidity, and $\tilde{\eta} \to \infty$ limits. The next step is to derive the relation between the LR and Collins schemes. According to eqs. (2.18) and (2.26), the only difference between these schemes is the order of their $\epsilon \to 0$ and $y_B \to -\infty$ limits. In the LR scheme, large $(-y_B)$ corresponds to a momentum scale

$$\zeta_{\mathrm{LR}} = 4x^2 m_h^2 \sinh^2(y_P - y_B)\,, \tag{3.24}$$

so the limit $y_B \to -\infty$ corresponds to $\zeta_{\mathrm{LR}} \to \infty$.

Due to asymptotic freedom in QCD, changing the order of limits $\epsilon \to 0$ and $\zeta_{\mathrm{LR}} \to \infty$ should only affect the UV region while leaving infrared (IR) physics intact. Using the LaMET formalism [12–14], behind which is the general principle for effective field theories (EFTs), we can relate the two different orders of limits with a factorization formula or

perturbative matching,[5] which takes the form

$$f_{q_i/h}(x,\vec{b}_T,\mu,\zeta) = C_q^{-1}\big(\sqrt{\zeta_{\mathrm{LR}}}/2,\mu\big)\, f_{q_i/h}^{\mathrm{LR}}(x,\vec{b}_T,\mu,\zeta,y_P-y_B) + \mathcal{O}(y_B^k e^{y_B})\,, \qquad (3.25)$$

where we have expanded at large $(-y_B)$ or in $\Lambda_{\mathrm{QCD}}^2/\zeta_{\mathrm{LR}}$. Here, y_B^k captures logarithms of ζ_{LR} where k is a positive integer. At large $(-y_B)$, the matching coefficient C cancels the overall y_B dependence in the renormalized beam and soft functions through its ζ_{LR} dependence. By dimensional analysis, C_q could depend on the logarithm of $\zeta_{\mathrm{LR}}/\mu^2$ or the rapidity difference $(y_n - y_B)$. However, according to eq. (2.37), the dependence on $(y_n - y_B)$ implies dependence on the CS kernel $\gamma_\zeta^q(b_T,\mu)$, which at $b_T \sim 1/\Lambda_{\mathrm{QCD}}$ is nonperturbative and hence infrared sensitive. Therefore, C_q can only depend on $\zeta_{\mathrm{LR}}/\mu^2$ and $\alpha_s(\mu)$, and so the factorization formula for the LR-TMD is

$$f_{q_i/h}^{\mathrm{LR}}(x,\vec{b}_T,\mu,\zeta,y_P-y_B) = C_q\big(\sqrt{\zeta_{\mathrm{LR}}}/2,\mu\big)\, f_{q_i/h}(x,\vec{b}_T,\mu,\zeta) + \mathcal{O}(y_B^k e^{y_B})\,, \qquad (3.26)$$

where ζ_{LR} is given by eq. (3.24). Combining this with the relation derived above in eqs. (1.3) and (2.38) for the quasi-TMD, with $\zeta_{\mathrm{LR}} = (2x\tilde{P}^z)^2$, we have

$$\tilde{f}_{q_i/h}(x,\vec{b}_T,\mu,\tilde{\zeta},x\tilde{P}^z) = C_q(x\tilde{P}^z,\mu) f_{q_i/h}(x,\vec{b}_T,\mu,\tilde{\zeta}) + \mathcal{O}(\tilde{y}_P^k e^{-\tilde{y}_P}) \qquad (3.27)$$

$$= C_q(x\tilde{P}^z,\mu)\exp\left[\frac{1}{2}\gamma_\zeta^q(\mu,b_T)\ln\frac{\tilde{\zeta}}{\zeta}\right] f_{q_i/h}(x,\vec{b}_T,\mu,\zeta) + \mathcal{O}(\tilde{y}_P^k e^{-\tilde{y}_P})\,.$$

where ζ can be of any value. All the steps in our analysis work equally well for gluons, simply replacing subscripts $q_i \to g$. Thus, this completes our proof of the factorization formula in eq. (1.2).

3.2 Implications

Next, we discuss implications of the factorization relation. In section 3.2.1, we show how the factorization implies that in the matching quarks and gluons do not mix, nor do different quark flavors. In section 3.2.2 we derive the momentum evolution of the quasi-beam function and hard matching coefficient. In section 3.2.3 we discuss using ratios of quasi-TMDs or quasi-beam functions to extract ratios of TMDs. In section 3.2.4 we examine implications of our analysis for the MHENS scheme, outlining the additional steps that need to be considered to derive a complete relation to the Collins scheme.

3.2.1 Absence of mixing

Our derivation of the factorization formula has not specified the quark flavor, and the result actually implies that mixings between quarks of different flavors or quarks and gluons do not exist. This lack of mixing is a generic feature for quasi-TMDs of all parton species.

The LR and Collins schemes differ only in the order of their $\epsilon \to 0$ and $y_B \to -\infty$ limits. When matching the schemes, mixing between quark and gluon channels could only occur if

---

[5]The impact of exchanging these limits has also been pointed out in the discussion of the Sudakov form factor in ref. [53], in particular eq. (10.97) therein. The EFT argument for the matching would also be reinforced by an order-by-order diagrammatical analysis [76] following ref. [39].

$y_B \to -\infty$ leads to a UV-divergent counterterm that contracts the flavor indices of the quark fields in the nonlocal bilinear operator. This cannot happen because these quark fields are always spacelike separated, and thus their exchange of intermediate particles in a Feynman diagram is exponentially suppressed and does not generate a new UV divergence. As a result, the $y_B \to -\infty$ limit can only change UV divergences locally at quark-Wilson line vertices and in Wilson line wavefunction renormalization, which leaves the parton flavor intact.

In contrast to the quasi-TMDs, the quark quasi-PDFs are defined from bilinear operators with a straight Wilson line along the z direction. In the infinite boost limit, the spacelike separated quarks will approach the light-cone, thus inducing a nonlocal UV divergence that contracts the quark flavor indices and allows mixing with the gluon quasi-PDF [54].

There is another perspective from which we can understand the lack of mixing. The LR and JMY schemes are related to each other by analytic continuation between space- and timelike Wilson lines. Thus, the JMY scheme should factorize similarly to eq. (3.26), as we check at one-loop order in appendix A.1. If there were quark-gluon or flavor mixing in the Collins-to-JMY matching, then such mixing would manifest in the TMD factorization formula for the Drell-Yan or SIDIS cross-section in either scheme; but it does not. Therefore, no mixing should occur in the Collins-to-JMY or Collins-to-LR matching.

Note that this factorization relation holds for quark and gluon quasi-TMDs with all spin-dependent structures [40, 49], so we can use it to compute the ratios of spin-dependent TMDs from the quasi-TMDs or quasi-beam functions, an approach that has been proposed and used in refs. [27–32]. In summary, all quark and gluon quasi-TMDs should satisfy the factorization relation in eq. (1.2). We cross-check our all-orders analysis above by explicit one-loop order calculations in appendix A.2.

3.2.2   Resummed result for the matching coefficient

From eq. (2.32) we can write $\ln \tilde{f}_{q_i/h} = \ln \lim_{\tilde{\eta} \gg b_T} \tilde{B}_{q_i/h}^{[\tilde{\Gamma}]} - \frac{1}{2} \ln \lim_{\tilde{\eta} \gg b_T} \tilde{S}^q$, and then using eq. (3.27) in the form $\ln \tilde{f}_{q_i/h} = \ln C_q + \ln f_{q_i/h}$ we can derive the momentum evolution equation of the quasi-beam function [33]:

$$\frac{\mathrm{d}}{\mathrm{d} \ln(2x\tilde{P}^z)} \ln \lim_{\tilde{\eta} \gg b_T} \tilde{B}_{q_i/h}^{[\tilde{\Gamma}]}(x, \vec{b}_T, \mu, \tilde{\eta}, x\tilde{P}^z) = \gamma_\zeta^q(b_T, \mu) + \gamma_C^q(2x\tilde{P}^z, \mu). \tag{3.28}$$

Here the limit $\tilde{\eta} \gg b_T$ should be understood as expanding in large $\tilde{\eta}$, where the quasi-beam function has a divergent dependence on $\tilde{\eta}$ which is however independent of $x\tilde{P}^z$, and hence drops out. In taking the $\ln(2x\tilde{P}^z)$ derivative we hold $y_B - y_n$ fixed, so there is no contribution from the $\tilde{S}^R$ term. We also used the large momentum formula $\tilde{\zeta} = 2(x\tilde{P}^+ e^{y_B - y_n})^2 \approx (2x\tilde{P}^z e^{y_B - y_n})^2$ to convert the $\ln \tilde{\zeta}$ derivative of $f_{q_i/h}$ to give $\mathrm{d} f_{q_i/h}/\mathrm{d} \ln(2x\tilde{P}^z) = \gamma_\zeta^q(b_T, \mu)$. The other anomalous dimension appearing in eq. (3.28) is

$$\gamma_C^q(2x\tilde{P}^z, \mu) = \frac{\mathrm{d}}{\mathrm{d} \ln(2x\tilde{P}^z)} \ln C_q(x\tilde{P}^z, \mu). \tag{3.29}$$

Since the quasi-beam function $\tilde{B}_{q_i/h}^{[\tilde{\Gamma}]}$ has a local UV counterterm $Z_{\mathrm{uv}}^B(\mu, \epsilon)$ according to the auxiliary field formalism, the sum of anomalous dimensions in eq. (3.28) must be μ

independent. The known perturbative structure of the CS kernel $\gamma_\zeta^q(b_T, \mu)$ then implies that

$$\frac{\mathrm{d}}{\mathrm{d}\ln\mu}\gamma_C^q(2x\tilde{P}^z, \mu) = -\frac{\mathrm{d}}{\mathrm{d}\ln\mu}\gamma_\zeta^q(b_T, \mu) = 2\Gamma_{\mathrm{cusp}}^q[\alpha_s(\mu)]\,. \tag{3.30}$$

It follows that γ_C^q can be written to all orders as [39]

$$\gamma_C^q(2x\tilde{P}^z, \mu) = 2\int_{2x\tilde{P}^z}^\mu \frac{\mathrm{d}\mu'}{\mu'}\,\Gamma_{\mathrm{cusp}}^q[\alpha_s(\mu')] + \gamma_C^q[\alpha_s(2x\tilde{P}^z)]\,. \tag{3.31}$$

Here, Γ_{cusp}^q and γ_C^q are the cusp and noncusp anomalous dimensions, whose series expansions are given by

$$\Gamma_{\mathrm{cusp}}^q[\alpha_s] = \sum_{n=0}^\infty \left(\frac{\alpha_s}{4\pi}\right)^{n+1}\Gamma_n^q\,, \qquad \gamma_C^q[\alpha_s] = \sum_{n=0}^\infty \left(\frac{\alpha_s}{4\pi}\right)^{n+1}\gamma_{C\,n}^q\,, \tag{3.32}$$

$$\text{with} \quad \Gamma_0^q = 4C_F\,, \qquad\qquad \Gamma_1^q = 4C_F\left[\left(\frac{67}{9} - \frac{\pi^2}{3}\right)C_A - \frac{20}{9}T_F n_f\right]\,, \ldots\,.$$

Here n_f is the number of light quark flavors and for QCD $C_F = 4/3$, $C_A = 3$, and $T_F = 1/2$. We also expand the QCD β-function, $\mathrm{d}\alpha_s(\mu)/\mathrm{d}\ln\mu = \beta[\alpha_s(\mu)]$ as

$$\beta[\alpha_s] = -2\alpha_s \sum_{n=0}^\infty \left(\frac{\alpha_s}{4\pi}\right)^{n+1}\beta_n\,, \tag{3.33}$$

$$\text{with} \quad \beta_0 = \frac{11}{3}C_A - \frac{4}{3}T_F n_f\,, \qquad \beta_1 = \frac{34}{3}C_A^2 - \left(\frac{20}{3}C_A + 4C_F\right)T_F n_f\,, \ldots\,.$$

Solving eq. (3.29) gives the general all-orders resummed result

$$C_q(x\tilde{P}^z, \mu) = C_q[\alpha_s(\mu)]\,\exp\left[\int_\mu^{2x\tilde{P}^z}\frac{\mathrm{d}\tau}{\tau}\,\gamma_C^q(\tau, \mu)\right] \tag{3.34}$$

$$= C_q[\alpha_s(\mu)]\exp\left[\int_{\alpha_s(\mu)}^{\alpha_s(2x\tilde{P}^z)}\frac{\mathrm{d}\alpha}{\beta[\alpha]}\left(\int_\alpha^{\alpha_s(\mu)}\frac{\mathrm{d}\alpha'}{\beta[\alpha']}2\Gamma_{\mathrm{cusp}}^q[\alpha'] + \gamma_C^q[\alpha]\right)\right]\,,$$

where the boundary condition is given by $C_q[\alpha_s(\mu)] = C_q(\mu/2, \mu)$. Explicit results at a given order can be obtained by substituting fixed order series for $\Gamma_{\mathrm{cusp}}[\alpha']$, $\gamma_C^q[\alpha]$, and $C_q[\alpha_s]$.

Using the known one-loop results [33, 35] we have

$$\gamma_C^q(2x\tilde{P}^z, \mu) = \frac{\alpha_s(\mu)C_F}{\pi}\left(-\ln\frac{(2x\tilde{P}^z)^2}{\mu^2} + 1\right) + \mathcal{O}(\alpha_s^2)\,, \tag{3.35}$$

$$C_q[\alpha_s] = 1 + \frac{\alpha_s C_F}{2\pi}\left(-2 + \frac{\pi^2}{12}\right) + \mathcal{O}(\alpha_s^2)\,,$$

which is consistent with $\Gamma_0^q = 4C_F$ and allows us to identify $\gamma_{C\,0}^q = 4C_F$. To obtain results for eq. (3.34) at next-to-leading-logarithmic (NLL) order for the double logarithmic series present in C_q, we can utilize $C_q[\alpha_s(\mu)] = 1$ together with the two-loop cusp anomalous

dimension, and one-loop regular anomalous dimension. Using the notation of ref. [77] for evolution kernels, the matching coefficient at NLL is then

$$C_q(x\tilde{P}^z, \mu)^{\mathrm{NLL}} = \exp\left[-2K_\Gamma^q(2x\tilde{P}^z, \mu) - K_\gamma^q(2x\tilde{P}^z, \mu)\right], \tag{3.36}$$

$$K_\Gamma^q(\mu_0, \mu) = -\frac{\Gamma_0^q}{4\beta_0^2}\left\{\frac{4\pi}{\alpha_s(\mu_0)}\left(1 - \frac{1}{r} - \ln r\right) + \left(\frac{\Gamma_1^q}{\Gamma_0^q} - \frac{\beta_1}{\beta_0}\right)(1 - r + \ln r) + \frac{\beta_1}{2\beta_0}\ln^2 r\right\},$$

$$K_\gamma^q(\mu_0, \mu) = -\frac{\gamma_{C0}^q}{2\beta_0}\ln r,$$

where $r = \alpha_s(\mu)/\alpha_s(\mu_0)$. Expanding we find agreement with an earlier $\mathcal{O}(\alpha_s^2)$ analysis for the terms we can predict at NLL, given by all the $\mathcal{O}(\alpha_s^2 \ln^j \frac{2x\tilde{P}^z}{\mu})$ terms with $j = 2, 3, 4$ in eqs. (25,26) of ref. [39]. Equation (3.36) can be expanded to higher orders in α_s, and then predicts the terms in $\ln C_q(x\tilde{P}^z, \mu)$ of the form $\alpha_s^j \ln^{j+1} \frac{2x\tilde{P}^z}{\mu}$ and $\alpha_s^j \ln^j \frac{2x\tilde{P}^z}{\mu}$ for any j.

Results for $C_q(x\tilde{P}^z, \mu)$ beyond NLL can be obtained from eq. (3.34) by substituting in higher order results for the anomalous dimensions and boundary condition. (Results for K_Γ^q and K_γ^q in terms of anomalous dimensions can be found in many places in the literature to order N³LL, see also ref. [78] for an exact solution.) An RGE equation in the form in eq. (3.28) will also hold for the $x\tilde{P}^z$ anomalous dimension for the gluon TMD, so a resummed formula for its matching coefficient $C_g(x\tilde{P}^z, \mu)$ is given by the above expressions with $q \to g$ and replacement by the gluon cusp and non-cusp anomalous dimensions.

3.2.3 Ratios of quasi-TMDs

The lack of mixing in the factorization formula eq. (1.2) for quasi-TMDs allows us to calculate ratios of TMDs of all flavor and spin structures more easily since there are cancellations between the numerator and denominators. This approach of studying ratios was pioneered in the Lorentz-invariant method of refs. [27, 28] using the MHENS scheme. This has been shown to have great utility for exploring ratios involving an integral over x and different spin and flavor choices [28–32]. We return to discuss the prospects for including renormalization and matching corrections in the MHENS scheme approach in section 3.2.4.

For quasi-TMDs the ability to more easily calculate ratios of spin dependent structure functions was observed for quark non-singlet distributions in refs. [40, 41], and occur due to the universality of the quasi-TMD to Collins-TMD matching coefficient. Our result in eq. (1.2) enable us to extend these observations to all orders in α_s, and include singlet quark distributions and gluon distributions. Since the quasi soft factor $\tilde{\Delta}^R$ in eq. (2.27) and the matching coefficients $C_{q,g}$ in eq. (1.2) only depend on the color representation, we can formulate ratios of quark or gluon quasi-TMDs where these components cancel, and thus immediately can be related to the analogous ratios for the quark and gluon TMDs in the Collins scheme. In particular we have

$$\frac{\tilde{f}_{q_i/h}^{[\tilde{\Gamma}_1]}(x, \vec{b}_T, \mu, \tilde{\zeta}, x\tilde{P}^z)}{\tilde{f}_{q_j/h'}^{[\tilde{\Gamma}_2]}(x, \vec{b}_T, \mu, \tilde{\zeta}, x\tilde{P}^z)} = \lim_{\tilde{\eta}\to\infty} \frac{\tilde{B}_{q_i/h}^{[\tilde{\Gamma}_1]}(x, \vec{b}_T, \mu, \tilde{\eta}, x\tilde{P}^z)}{\tilde{B}_{q_j/h'}^{[\tilde{\Gamma}_2]}(x, \vec{b}_T, \mu, \tilde{\eta}, x\tilde{P}^z)} = \frac{f_{q_i/h}^{[\Gamma_1]}(x, \vec{b}_T, \mu, \zeta)}{f_{q_j/h'}^{[\Gamma_2]}(x, \vec{b}_T, \mu, \zeta)}, \tag{3.37}$$

$$\frac{\tilde{f}_{g/h}^{[\tilde{\mu}_1\tilde{\nu}_1\tilde{\rho}_1\tilde{\sigma}_1]}(x, \vec{b}_T, \mu, \tilde{\zeta}, x\tilde{P}^z)}{\tilde{f}_{g/h'}^{[\tilde{\mu}_2\tilde{\nu}_2\tilde{\rho}_2\tilde{\sigma}_2]}(x, \vec{b}_T, \mu, \tilde{\zeta}, x\tilde{P}^z)} = \lim_{\tilde{\eta}\to\infty} \frac{\tilde{B}_{g/h}^{[\tilde{\mu}_1\tilde{\nu}_1\tilde{\rho}_1\tilde{\sigma}_1]}(x, \vec{b}_T, \mu, \tilde{\eta}, x\tilde{P}^z)}{\tilde{B}_{g/h'}^{[\tilde{\mu}_2\tilde{\nu}_2\tilde{\rho}_2\tilde{\sigma}_2]}(x, \vec{b}_T, \mu, \tilde{\eta}, x\tilde{P}^z)} = \frac{f_{g/h}^{[\mu_1\nu_1\rho_1\sigma_1]}(x, \vec{b}_T, \mu, \zeta)}{f_{g/h'}^{[\mu_2\nu_2\rho_2\sigma_2]}(x, \vec{b}_T, \mu, \zeta)}.$$

Here q_i and q_j can be different quark flavors, h and h' can be different hadrons, and the superscripts can be different spin structures with Dirac matrices Γ^1, Γ^2 for quark (quasi-)TMDs and Lorentz indices $\mu_k, \nu_k, \rho_k, \sigma_k$ with $k = 1, 2$ for gluon (quasi-)TMDs.

To calculate the ratios in eq. (3.37) as a function of x, one must first compute the matrix elements for the quasi-beam functions at all b^z, then take the Fourier transform. Because UV divergences in the bare quasi-beam function matrix elements are b^z-independent, they factor out of the Fourier integral. So, in principle we can skip renormalization and matching to the $\overline{\text{MS}}$ scheme when calculating TMD ratios, *if* there are no b^z-dependent finite operator mixings on the discretized lattice. However, in the presence of such mixings, lattice renormalization is necessary, as studied in refs. [43, 73]. Also, in numerical analyses it can be advantageous to consider the $\tilde{\eta} \to \infty$ limit separately for the numerator and denominator of eq. (3.37) separately. This can be accomplished by utilizing the naive quasi-soft function or quasi-beam function at $b^z = 0$ to cancel the large $\tilde{\eta}$-dependence.

3.2.4 Matching MHENS and continuum TMDs

We now consider the relation between the MHENS lattice TMD and Collins continuum TMD, focusing again on the quark case. In the literature, the MHENS scheme has primarily been used to study matrix elements evaluated at $P \cdot b = 0$ [27–32]. In this case, the equal-time-restricted Wilson line path in the MHENS beam function is the same as that of the quasi-beam function. This is easily seen by comparing the integral over x of the MHENS beam function in eq. (2.39), with the integral over x of the quasi-beam function in eq. (2.29), and noting that both give the same correlator $\Omega^{[\Gamma]}_{q/h}\left[\vec{b}_T, \tilde{P}, a, \tilde{\eta}\hat{z}, 0\right] = \tilde{\Phi}^{[\Gamma]}_{\text{unsubtr.}}\left[\vec{b}_T, \tilde{P}, a, \tilde{\eta}\hat{z}\right]$ times a factor of N_Γ/P^z. For the integral over x we define

$$\int \mathrm{d}x \; \tilde{f}^{[\Gamma]}_{q_i/h}(x, \vec{b}_T, \mu, \tilde{\zeta}, x\tilde{P}^z, \tilde{\eta}) = \tilde{f}^{[\Gamma]}_{q_i/h}(b^z = 0, \vec{b}_T, \mu, \tilde{P}^z, y_n - y_B, \tilde{\eta}) \tag{3.38}$$
$$= f^{[\Gamma]\text{MHENS}}_{q_i/h}(b^z = 0, \vec{b}_T, \mu, \tilde{P}^z, y_n - y_B, \tilde{\eta}).$$

The first quasi-TMD here has x-dependence in three of its arguments (two written explicitly and the other in $\tilde{\zeta}$), so it is convenient to write the x-independent result as a new function, whose distinction is tagged by the first $b^z = 0$ argument. The results on the right hand side correspond to the hadronic matrix element of the operator with $b^z = 0$. We adopt the same notation for the MHENS TMD, as shown. Given this correspondence, we can simply adopt the same terms used in defining the quasi-TMD in eq. (2.27) to define a renormalized and soft subtracted MHENS TMD for $\tilde{P} \cdot b = 0$, $b^0 = 0$, and $v = \hat{z}$, giving

$$f^{[\Gamma]\text{MHENS}}_{q_i/h}(b^z = 0, \vec{b}_T, \mu, \tilde{P}, y_n - y_B, \tilde{\eta}) \tag{3.39}$$
$$\equiv \lim_{a \to 0} Z'_{\text{uv}}(\mu, \tilde{\mu}) \, Z_{\text{uv}}(a, \tilde{\mu}, y_n - y_B) \, \frac{N_\Gamma}{P^z} \, \tilde{\Phi}^{[\Gamma]q_i/h}_{\text{unsubtr.}}(\vec{b}_T, \tilde{P}, a, \tilde{\eta}\hat{z}) \, \tilde{\Delta}^q_S(b_T, a, \tilde{\eta}, y_n, y_B).$$

The limit $\tilde{\eta} \to \infty$ of eq. (3.39) gives a finite result independent of $\tilde{\eta}$, since the Wilson line self-energy power law divergences cancel between $\tilde{\Phi}^{[\Gamma]}_{\text{unsubtr.}}$ and $\tilde{\Delta}^q_S$. With this definition for the MHENS TMD, our result in eq. (1.2) relating the quasi- and Collins TMDs also yields

a relationship between the MHENS and Collins TMDs:

$$\lim_{\tilde{\eta}\to\infty} \tilde{f}_{q_i/h}^{[\Gamma]\text{MHENS}}(b^z=0,\vec{b}_T,\mu,\tilde{P},y_n-y_B,\tilde{\eta}) = \int dx\, C_q(x\tilde{P}^z,\mu)\, f_{q_i/h}^{[\Gamma]}(x,\vec{b}_T,\mu,\zeta)$$

$$\times \left\{ 1 + \mathcal{O}\left[\frac{1}{(\tilde{P}^z b_T)^2}, \frac{\Lambda_{\text{QCD}}^2}{(\tilde{P}^z)^2} \right] \right\}. \quad (3.40)$$

Here, the MHENS TMD (or quasi-TMD) on the l.h.s. is calculated with states involving proton momentum $\tilde{P}$, while the Collins TMD on the r.h.s. utilizes states with proton momentum P. We have chosen to relate these two momenta by the rapidity relation $y_P = y_{\tilde{P}} + y_B$ that appeared in our proof of factorization. In the large $\tilde{P}^z$ limit, we have $\zeta = (2xP^z e^{-y_n})^2 = (2x\tilde{P}^z e^{y_B-y_n})^2 = \tilde{\zeta}$, which eliminates the $\ln(\tilde{\zeta}/\zeta)$-dependent term in eq. (1.2), which would otherwise appear in the integrand in eq. (3.40). Note that for large $\tilde{P}^z$ we also have $\hat{\zeta} \to \infty$, where $\hat{\zeta}$ was defined in eq. (2.43).

We now consider the implications of the factorization in eq. (3.40) for computing Collins TMD ratios. Taking ratios of MHENS TMDs with different choices of spin structures Γ, we see that the UV renormalization factors Z'_{uv} and Z_{uv} and soft factor $\tilde{\Delta}_S^q$ all drop out. Thus, ratios of MHENS beam functions give us information about the ratios of Collins-TMDs,

$$\lim_{\substack{a\to 0 \\ \tilde{\eta}\to\infty}} \frac{N_{\Gamma_1}\tilde{\Phi}_{\text{unsubtr.}}^{[\Gamma_1]q_i/h}(\vec{b}_T,\tilde{P},a,\tilde{\eta}\hat{z})}{N_{\Gamma_2}\tilde{\Phi}_{\text{unsubtr.}}^{[\Gamma_2]q_i/h}(\vec{b}_T,\tilde{P},a,\tilde{\eta}\hat{z})} = \frac{\int dx\, C_q(x\tilde{P}^z,\mu) f_{q_i/h}^{[\Gamma_1]}(x,\vec{b}_T,\mu,\zeta)}{\int dx\, C_q(x\tilde{P}^z,\mu) f_{q_i/h}^{[\Gamma_2]}(x,\vec{b}_T,\mu,\zeta)}, \quad (3.41)$$

albeit with an integration over the matching coefficient $C_q(x\tilde{P}^z,\mu)$. Here there is power law sensitivity to $\tilde{\eta}$ in the numerator and denominator of the l.h.s., but this sensitivity cancels in the ratio, as does the dependence on a (assuming that there is no mixing amongst spin structures for the lattice fermion discretization chosen [43, 73, 79, 80]). As explained in section 3.1.3, C_q arises precisely because of the different orders in which renormalization and the large rapidity limit are taken to be performed between the MHENS and Collins TMDs. Equation (3.41) reduces to the relation between MHENS beam functions and the moment of the Collins TMDs discussed in earlier literature [28–32] if one sets $C_q = 1 + \mathcal{O}(\alpha_s)$, i.e. works to tree level in the matching coefficient. Beyond tree-level, the convolution becomes nontrivial. Nevertheless, one can plug the TMDs from global analysis into eq. (3.41) to compare with the lattice ratio of the MHENS beam function. It is worth noting that the CS evolution for the ζ dependence is multiplicative and independent of x, and hence the ratio of Collins TMDs on the r.h.s. is independent of ζ as long as the same value of ζ is used in the numerator and denominator.

By constructing lattice TMD ratios with the same spin structures but different momenta $\tilde{P}^z$ in the numerator and denominator, one can extract the CS kernel $\gamma_\zeta(\mu,b_T)$ [35]. Once again one cannot avoid the need to include the matching coefficient whether working in longitudinal momentum or position space [37]. Thus a formula for obtaining γ_ζ that does not explicitly rely on a truncation of the α_s expansion always requires calculation of the full b^z dependence of lattice beam functions. When the series expansion in α_s is utilized, a broader range of extraction techniques are possible, see for example ref. [45].

Next we consider the use of the MHENS correlator for obtaining x-dependent information about Collins TMDs. There are two complications in this case relative to the use of

quasi-TMDs. The first is that the MHENS staple-shaped Wilson line path for the beam functions has non-trivial cusp angles $\gamma(v, b)$, which from eq. (2.6) is given by

$$\cosh[\gamma(v, b)] = \pm \frac{v \cdot b}{|v||b|}\,, \tag{3.42}$$

where the sign is determined by $\pm = \text{sign}(\tilde{\eta})$. For $b^z \neq 0$ we have $v \cdot b \neq 0$, and the UV renormalization factor $Z_{\text{uv}}^{\text{MHENS}}$ will depend on $\gamma(v, b)$ irrespective of whether or not we extrapolate towards infinitely long staples, $|\tilde{\eta}| \to \infty$. This complicates the analysis because the UV renormalization is now b^z dependent and hence will not cancel in ratios formed from correlators with the same x.

The second complication for x-dependent MHENS calculations is that the length of the Wilson line path becomes b^z-dependent, since using eq. (2.5) we have

$$L_{\text{staple}}^{\text{MHENS}} = 2|\tilde{\eta}v| + |b|\,. \tag{3.43}$$

This implies that if we do a Fourier transform in $b \cdot P$ to obtain x-dependent correlators, then the power law dependence on the staple length does not cancel for ratios taken at finite $\tilde{\eta}$, where the $|b|$ term can not be neglected.

To make these issues more transparent, we consider the generalization of the MHENS TMD definition in eq. (3.39) that is needed to include b^z-dependence. Working in an equal-time configuration with $b^0 = 0$ and $v^0 = 0$ that is suitable for lattice calculations, we expect that the definition would take the form

$$f_{q_i/h}^{[\Gamma]\text{MHENS}}(b, \mu, \tilde{P}, v, \tilde{v}) \equiv \lim_{\substack{a \to 0 \\ |\tilde{\eta}| \to \infty}} Z'_{\text{uv}}(\mu, \tilde{\mu})\, Z_{\text{uv}}^{\text{MHENS}}[a, \tilde{\mu}, v, \tilde{v}, \gamma(v, b), \dots] \tag{3.44}$$

$$\times \frac{N_\Gamma}{P^z}\, \tilde{\Phi}_{\text{unsubtr.}}^{[\Gamma]q_i/h}(b, \tilde{P}, a, \tilde{\eta}v)\, \tilde{\Delta}_S^{q\,\text{MHENS}}(b, a, \tilde{\eta}v, \tilde{\eta}\tilde{v})\,.$$

Although $Z_{\text{uv}}^{\text{MHENS}}$ depends on the cusp angle $\gamma(v, b)$ this is unlikely to be a fundamental road block, since this renormalization can be carried out perturbatively (for example, four-loop results for the related cusp-anomalous dimension are now available in $\overline{\text{MS}}$ [81]). It also seems likely that a non-perturbative method of carrying out the calculation of $Z_{\text{uv}}^{\text{MHENS}}$ on the lattice could also be formulated. A greater difficulty will be determining a suitable soft factor $\tilde{\Delta}_S^{q\,\text{MHENS}} = (S_{\text{MHENS}}^q)^{-1/2}$, which itself must satisfy three non-trivial constraints. In particular, it should be constructed from a soft function S_{MHENS}^q which is a vacuum matrix element of a closed Wilson loop that has a total length $2L_{\text{staple}}^{\text{MHENS}}$ with eq. (3.43). This ensures that the $|\tilde{\eta}| \to \infty$ limit for $f_{q_i/h}^{[\Gamma]\text{MHENS}}$ will exist. An additional constraint is that it should include dependence which compensates for the mismatch in the Lorentz invariants in the 12th and 13th rows of table 2. Finally, it must have the proper infrared dependence on b_T such that $\tilde{f}_{q_i/h}^{[\Gamma]\text{MHENS}}$ correctly reproduces the infrared structure of the Collins TMD. This last constraint is necessary for a factorization formula relating the MHENS TMD and Collins TMD to exist. The construction of a suitable $\tilde{\Delta}_S^{q\,\text{MHENS}}$ involves two steps: finding an operator definition for this quantity satisfying the above constraints, and then developing a method by which this factor can be computed with lattice QCD. The

argument $\tilde{v}$ that we have written for $\tilde{\Delta}_S^{q\,\text{MHENS}}$ in eq. (3.44) should be a suitably chosen space-like vector. The ellipses in $Z_{\text{uv}}^{\text{MHENS}}$ in eq. (3.44) denote any further arguments needed due to UV renormalization for the soft factor (like additional cusp angles).

Let us assume that a suitable $\tilde{\Delta}_S^{q\,\text{MHENS}}$ has been determined. In this case the factorization formula for the MHENS TMD to Collins TMD should take the form

$$
f_{q_i/h}^{[\Gamma]\text{MHENS}}(x, \vec{b}_T, \mu, \tilde{P}, v, \tilde{v}) \equiv \int \frac{\mathrm{d}(b \cdot \tilde{P})}{2\pi}\, e^{-\mathrm{i}x(\tilde{P}\cdot b)}\, f_{q_i/h}^{[\Gamma]\text{MHENS}}(b, \tilde{P}, \mu, v, \tilde{v})
$$
$$
= C_q^{\text{MHENS}}(xv \cdot \tilde{P}, \ldots, \mu)\, \exp\left[\frac{1}{2}\gamma_\zeta^q(\mu, b_T)\ln\frac{\tilde{\zeta}}{\zeta}\right]\, f_{q_i}^{[\Gamma]}(x, \vec{b}_T, \mu, \zeta)
$$
$$
\times \left\{1 + \mathcal{O}\left[\frac{1}{(xv \cdot \tilde{P}b_T)^2}, \frac{\Lambda_{\text{QCD}}^2}{(xv \cdot \tilde{P})^2}\right]\right\}, \tag{3.45}
$$

where based on results from the JMY scheme we expect $\tilde{\zeta} = 2(x\tilde{P} \cdot v)^2\sqrt{|v^2||\tilde{v}^2|}/(v^2\, v \cdot \tilde{v})$. Our notation anticipates the fact that the matching coefficient C_q^{MHENS} is likely to differ from the C_q in the quasi-TMD factorization. This is expected due to the fact that the UV behavior of $\tilde{\Delta}_S^{q\,\text{MHENS}}$ can differ from $\tilde{\Delta}_S^q$, and the fact that $Z_{\text{uv}}^{\text{MHENS}}$ differs from Z_{uv}.

Instead of directly trying to match the MHENS-TMD onto the Collins-TMD as in eq. (3.45), one can consider determining the x-dependence of ratios. For example, taking ratios with potentially different Dirac structures, flavors q_i and q_j, and hadrons h and h', but the same x and $\tilde{P}$ we have

$$
\frac{f_{q_i/h}^{[\Gamma_1]}(x, \vec{b}_T, \mu, \zeta)}{f_{q_j/h'}^{[\Gamma_2]}(x, \vec{b}_T, \mu, \zeta)} = \frac{f_{q_i/h}^{[\Gamma_1]\text{MHENS}}(x, \vec{b}_T, \mu, \tilde{P}, v, \tilde{v})}{f_{q_j/h'}^{[\Gamma_2]\text{MHENS}}(x, \vec{b}_T, \mu, \tilde{P}, v, \tilde{v})} \tag{3.46}
$$
$$
= \lim_{\substack{a \to 0 \\ |\tilde{\eta}| \to \infty}} \frac{\int \mathrm{d}(b \cdot \tilde{P})\, e^{-\mathrm{i}x(\tilde{P}\cdot b)}\, Z_{\text{uv}}^{\text{MHENS}}(a, \ldots)N_{\Gamma_1}\tilde{\Phi}_{\text{unsubtr.}}^{[\Gamma_1]q_i/h}(b, \tilde{P}, a, \tilde{\eta}\hat{z})\, \tilde{\Delta}_S^{q\,\text{MHENS}}(b, a, \tilde{\eta}v, \tilde{\eta}\tilde{v})}{\int \mathrm{d}(b \cdot \tilde{P})\, e^{-\mathrm{i}x(\tilde{P}\cdot b)}\, Z_{\text{uv}}^{\text{MHENS}}(a, \ldots)N_{\Gamma_2}\tilde{\Phi}_{\text{unsubtr.}}^{[\Gamma_2]q_j/h'}(b, \tilde{P}, a, \tilde{\eta}\hat{z})\, \tilde{\Delta}_S^{q\,\text{MHENS}}(b, a, \tilde{\eta}v, \tilde{\eta}\tilde{v})}.
$$

In taking ratios using eq. (3.45) the C_q^{MHENS} and CS kernel terms drop out, giving the first equality in eq. (3.46). Using eq. (3.44) then gives the second equality. For finite $\tilde{\eta}$ the soft factors $\tilde{\Delta}_S^{q\,\text{MHENS}}(b, a, \tilde{\eta}v, \tilde{\eta}\tilde{v})$ do not cancel out from the numerator and denominator, due to their dependence on the integration variable, namely the component of b that is parallel to $\tilde{P}$.[6] In addition the UV counterterms $Z_{\text{uv}}^{\text{MHENS}}(a, \ldots, \gamma(b, v), \ldots)$ depend on the integration variable through their dependence on the cusp angle $\gamma(b, v)$, and the dependence on these variables remains regardless of how large $\tilde{\eta}$ is.[7] Equation (3.46) can be contrasted with the ratios involving quasi-TMDs in the first line of eq. (3.37). The situation is simpler for the quasi-TMDs because of the simpler dependence of the UV counterterm and soft factor, which cancel out in the ratios at finite $\tilde{\eta}$.

---

[6]It is possible that one may be able to construct $\tilde{\Delta}_S^{q\,\text{MHENS}}$ such that the dependence on the component $b \cdot \tilde{P}/m_h$ is subleading as $|\tilde{\eta}| \to \infty$, just like it is in $L_{\text{staple}}^{\text{MHENS}}$, in which case these soft factors can be canceled out in the ratio in eq. (3.46) as $|\tilde{\eta}| \to \infty$.

[7]It is possible that one may be able to define the soft factor $\Delta_S^{q\,\text{MHENS}}$ so as to cancel the UV dependence on the cusp angles, and thus make $Z_{\text{uv}}^{\text{MHENS}}$ independent of $\gamma(b, v)$. However, this makes it more probable that $\Delta_S^{q\,\text{MHENS}}$ will not cancel between the numerator and denominator of eq. (3.46) as $|\tilde{\eta}| \to \infty$.

4 Conclusion

The central focus of this paper was to derive the factorization formula eq. (1.2) that relates the lattice-calculable quasi-TMD to physical TMD schemes through a simple perturbative matching coefficient. This formula is valid at all orders in α_s up to power corrections for any light quark flavor and for gluons.

We began our derivation by developing a generalized TMD notational framework applicable to both continuum and lattice TMDs, enabling us to unify various choices used in the literature and thus more easily unpack the relationships between various physical and lattice TMD schemes. Comparing the operator structures and Lorentz invariants appearing in each scheme, we observed a close relation between the Collins and quasi-TMDs. We then constructed a new continuum TMD scheme intermediate between the Collins and quasi-TMDs, which we called the large rapidity (LR) scheme. The LR and Collins schemes differ by the order of UV renormalization and the lightcone limits, so they are related by a perturbative matching in the spirit of LaMET. Meanwhile, using Lorentz invariance we showed that the quasi- and LR TMDs are equivalent. This enabled us to prove the full factorization relation between the Collins and quasi-TMDs. For any quark flavor q_i and for gluons g, the relations are

$$\tilde{f}_{q_i/h}(x, \vec{b}_T, \mu, \tilde{\zeta}, x\tilde{P}^z) = C_q(x\tilde{P}^z, \mu) \exp\left[\frac{1}{2}\gamma_\zeta^q(\mu, b_T) \ln \frac{\tilde{\zeta}}{\zeta}\right] f_{q_i/h}(x, \vec{b}_T, \mu, \zeta) + \dots, \quad (4.1)$$

$$\tilde{f}_{g/h}(x, \vec{b}_T, \mu, \tilde{\zeta}, x\tilde{P}^z) = C_g(x\tilde{P}^z, \mu) \exp\left[\frac{1}{2}\gamma_\zeta^g(\mu, b_T) \ln \frac{\tilde{\zeta}}{\zeta}\right] f_{g/h}(x, \vec{b}_T, \mu, \zeta) + \dots, \quad (4.2)$$

where the ellipses indicate power corrections. The quark matching coefficient C_q and CS kernel γ_ζ^q are both independent of the quark flavor.

The factorization formula has many implications. First, when matching quasi- and continuum TMDs, there is no mixing between quarks and gluons, nor is there flavor mixing. This means that lattice calculations of TMDs for various flavors and for gluons should be easier than anticipated. We confirmed the momentum renormalization-group evolution for the matching coefficient, and solved it to obtain a explicit result at NLL, confirming it agreed with earlier fixed-order results in the literature. Finally, our proof has implications for factorization formulas matching the Lorentz-invariant approach (MHENS scheme) to lattice TMDs. It implies that ratios of MHENS TMDs with $b = \vec{b}_T$ give direct access to information about the ratio of Collins TMDs integrated against the matching coefficient $C_q(x\tilde{P}^z, \mu)$ in the numerator and denominator. The treatment of factorization for x-dependent ratios of MHENS correlators is a bit more complicated, and we identified the additional ingredients as being from cusp anomalous dimensions in the lattice renormalization and the need for a different soft factor subtraction in the relation to the Collins TMD.

Our results are an important step in pushing forward the knowledge we can extract from the lattice about TMD observables, yet much remains to be done. We have derived a factorization formula at leading power to all orders in α_s. However, the perturbative quasi-to-Collins matching coefficient C_q is only known at one-loop, except for certain logarithmic terms constrained by its RGE, see section 3.2.2. Recently there has been renewed interest

in TMDs at subleading power, with for example a derivation of the necessary form of the factorization formula for polarized SIDIS at subleading power [82, 83]. Finding continuum-to-lattice factorization formulas for subleading power TMDs would be interesting.

As experiments come online that promise to push our knowledge of hadronic structure to new depths, the need for corresponding first-principles predictions becomes ever more clear. The challenges faced in calculating TMDs on the lattice give us a roadmap for efficiently deriving other key hadronic properties. Constructing a generic operator encompassing all possible physical and lattice scheme choices for a specific distribution is useful for understanding the space of possibilities. Comparing the quasi-to-Collins and MHENS-to-Collins factorizations, we see that we must walk a fine line between perturbative and numerical challenges when choosing a lattice observable. From the lattice standpoint, unless headway is made on the sign problem, matrix element correlators from which distributions are constructed must employ Wilson lines on equal-time paths. Wilson lines should have as few sides and cusps as possible to minimize difficulties with renormalization. From the start, it is also important to account for lattice renormalization, soft function subtractions, and finite Wilson line lengths. One must also be careful with different orders of limits and renormalization, which can often lead to additional perturbative matching kernels.

In the case of TMDs specifically, it is clear from the phase space of possible lattice correlators that there are additional freedoms in the definitions that could still be exploited. Quasi-TMDs and MHENS TMDs provide two examples of how things can differ due to these choices, and we have advocated for some of the benefits of the quasi-TMD approach. The calculation of MHENS TMDs has an excellent track record, and it will be important to continue to carry out calculations with various lattice TMDs, and confirm consistency amongst the results. Ultimately, this program has the potential to lead to precise determinations of the full functional dependence of the eight leading-power spin-dependent TMDs.

Acknowledgments

A Perturbative cross-checks

A.1 Matching unpolarized quark TMDs in different schemes at NLO

In this section, we perturbatively test our results from section 3 by first constructing the matching between the Collins and JMY TMDs at next-to-leading order (NLO), and then deriving the same matching between the Collins and LR TMDs. The latter immediately yields the matching between the quasi- and Collins TMDs.

A.1.1 Matching Collins and JMY TMDs

We first relate the Collins and JMY TMDs. Since the physical cross-section is scheme-independent, we have

$$
\frac{\mathrm{d}\sigma}{\mathrm{d}Q^2\mathrm{d}Y\mathrm{d}^2\vec{q}_T} \tag{A.1}
$$
$$
= \sigma_0 \sum_{i,j} H_{ij}(Q,\mu) \int \frac{\mathrm{d}^2\vec{b}_T}{(2\pi)^2} e^{i\vec{q}_T\cdot\vec{b}_T} f_{i/h_1}(x_1,\vec{b}_T,\mu,\zeta_1) f_{j/h_2}(x_2,\vec{b}_T,\mu,\zeta_2)
$$
$$
= \sigma_0 \sum_{i,j} H_{ij}(Q,\mu,\rho) \int \frac{\mathrm{d}^2\vec{b}_T}{(2\pi)^2} e^{i\vec{q}_T\cdot\vec{b}_T} f_{i/h_1}^{\mathrm{JMY}}(x_1,\vec{b}_T,\mu,x_1\zeta_v,\rho) f_{j/h_2}^{\mathrm{JMY}}(x_2,\vec{b}_T,\mu,x_2\zeta_{\tilde{v}},\rho)\,,
$$

where the first and second lines employ the Collins and JMY schemes as given in eqs. (2.15) and (2.21), respectively. We want to choose a frame where the TMDs appear symmetrically, such that there is no CS evolution from an asymmetric split of soft radiation. This can be ensured by choosing $\zeta_1 = \zeta_2$ and $x_1\zeta_v = x_2\zeta_{\tilde{v}}$, which using their definitions implies[8]

$$
\zeta_1 = \zeta_2 = Q^2\,, \qquad (x_1\zeta_v)^2 = (x_2\zeta_{\tilde{v}})^2 = \rho Q^2\,. \tag{A.2}
$$

The last equality fixing ρ results from the definition in eq. (2.23). Eq. (A.1) then implies

$$
f_{i/h}^{\mathrm{JMY}}(x_1,b_T,\mu,\sqrt{\rho}Q,\rho) = C_i^{\mathrm{JMY}}(Q,\mu,\rho) f_{i/h}(x_1,b_T,\mu,Q^2)\,, \tag{A.3}
$$

where C_i^{JMY} is a perturbative kernel which is defined as

$$
C_i^{\mathrm{JMY}}(Q,\mu,\rho) = \sqrt{\frac{H_{i\bar{i}}(Q,\mu)}{H_{i\bar{i}}(Q,\mu,\rho)}}\,. \tag{A.4}
$$

Here, we set $j = \bar{i}$ because this relation must hold for the simplest cases of flavor-diagonal Drell-Yan scattering. The hard function is independent of quark flavor, so the matching is also flavor-independent.[9] We can write an asymmetric form of eq. (A.3) using CS evolution,

$$
f_{i/h}^{\mathrm{JMY}}(x,b_T,\mu,\sqrt{\rho}Q,\rho) = C_i^{\mathrm{JMY}}(Q,\mu,\rho) \exp\left[\frac{1}{2}\gamma_\zeta^i(b_T,\mu)\ln\frac{Q^2}{\zeta}\right] f_{i/h}(x,b_T,\mu,\zeta)\,. \tag{A.5}
$$

---

[8]The one-loop expressions for eq. (A.1) only agree if one fixes $x_1\zeta_v = x_2\zeta_{\tilde{v}}$. This may simply be a result of using this particular frame when calculating the NLO ingredients in ref. [56]; the factorization theorem in ref. [56] does not make a definite statement on this. For more details, see appendix B.

[9]This is violated starting at three loops due to closed quark loops that couple to the vector current. In order for eq. (A.1) to be true, such contributions must precisely cancel in the ratio in eq. (A.4).

Here, C_i^{JMY} and γ_ζ^i differ for quarks and gluons, but do not depend on quark flavor. Appendix B verifies eq. (A.5) at one loop; here, we only show one-loop results for the hard function,

$$H_{q\bar{q}}(Q,\mu) = 1 + \frac{\alpha_s C_F}{2\pi}\left[-\ln^2\frac{Q^2}{\mu^2} + 3\ln\frac{Q^2}{\mu^2} + \frac{7}{6}\pi^2 - 8\right] + \mathcal{O}(\alpha_s^2)\,, \tag{A.6}$$

$$H_{q\bar{q}}(Q,\mu,\rho) = 1 + \frac{\alpha_s C_F}{2\pi}\left[-\ln^2\frac{Q^2}{\mu^2} + 3\ln\frac{Q^2}{\mu^2} + \ln^2\frac{\rho Q^2}{\mu^2} - 2\ln\frac{\rho Q^2}{\mu^2} + 2\pi^2 - 4\right] + \mathcal{O}(\alpha_s^2)\,,$$

see eqs. (B.2) and (B.12). We stress that the second line only holds in the frame defined by eq. (A.2). Inserting eq. (A.6) into eq. (A.4), we obtain the one-loop quark matching kernel

$$C_q^{\mathrm{JMY}}(Q,\mu,\rho) = 1 + \frac{\alpha_s C_F}{2\pi}\left(-\frac{1}{2}L_\rho^2 + L_\rho - \frac{5}{12}\pi^2 - 2\right) + \mathcal{O}(\alpha_s^2)\,, \tag{A.7}$$

where we abbreviate the logarithm as

$$L_\rho = \ln\frac{\rho Q^2}{\mu^2} = \ln\frac{(2x_1 P_1 \cdot v)^2}{v^2\mu^2}\,. \tag{A.8}$$

A.1.2 Matching Collins and LR/quasi TMDs

The LR and JMY TMDs differ only by the direction of their Wilson lines, so the LR-to-Collins and JMY-to-Collins matchings should be equivalent, up to accounting for the Wilson line change. First, we make the choice

$$v^\mu = n_B^\mu(y_B) = (e^{2y_B}, 1, 0_\perp)\,, \qquad \tilde{v}^\mu = n_A^\mu(y_n) = (1, e^{-2y_n}, 0_\perp)\,, \tag{A.9}$$

which are the *timelike* versions of the Wilson line directions defining the LR scheme; we will address the continuation to the spacelike case soon. Note that here, y_n is a parameter in the LR scheme, *not* in Collins scheme. Also note that $\tilde{v}$ does not obey the hierarchy $\tilde{v}^+ \gg \tilde{v}^-$ assumed in the JMY scheme. As long as we only consider the v-collinear TMD, this does not matter, as the hierarchy $v^- \gg v^+$ ensures the validity of the expressions for ζ_v and ρ as given in eq. (2.23),

$$(x_1\zeta_v)^2 = \frac{(2x_1 P_1 \cdot v)^2}{v^2} = (\sqrt{2}x_1 P_1^+ e^{-y_B})^2\,, \qquad \rho^2 = \frac{4(v \cdot \tilde{v})^2}{v^2\tilde{v}^2} = e^{2(y_n - y_B)}\,. \tag{A.10}$$

So far, y_B and y_n are not fixed, as the LR scheme is well defined as long as $-y_B \gg 1$. However, to use the results that can be perturbatively matched to the physical scheme in appendix A.1.1, we have to work in the symmetric frame as specified by eq. (A.2), namely $(x_1\zeta_v)^2 = \rho Q^2$. Thus, we find

$$\rho = e^{y_n - y_B} \overset{!}{=} \frac{(x_1\zeta_v)^2}{Q^2} = e^{2(Y - y_B)} \qquad \Rightarrow \qquad y_n = 2Y - y_B\,, \tag{A.11}$$

where the dependence on the final-state rapidity Y arises through $\sqrt{2}x_1 P_1^+ = Qe^Y$. Here we choose to treat y_B as the independent parameter, since it specifies the geometry of the Wilson line in the hadronic matrix element, while y_n only enters through the soft function

and thus is considered a derived quantity. With this special choice of y_n, we can make use of eq. (A.5) to obtain

$$f_{i/h}^{\mathrm{JMY}}(x, b_T, \mu, x_1\zeta_v, \rho) = C_i^{\mathrm{JMY}}(Q, \mu, \rho) f_{i/h}(x, b_T, \mu, Q^2), \qquad \rho = \frac{(x_1\zeta_v)^2}{Q^2}. \qquad (A.12)$$

To obtain the corresponding result for the LR scheme, we have to replace the timelike Wilson lines in eq. (A.9) by spacelike ones,

$$\begin{aligned}
v^\mu &= (e^{2y_B}, 1, 0_\perp) \to (-e^{2y_B}, 1, 0_\perp), \\
\tilde{v}^\mu &= (1, e^{-2y_n}, 0_\perp) \to (1, -e^{-2y_n}, 0_\perp).
\end{aligned} \qquad (A.13)$$

The Lorentz invariants in eq. (A.10) then change to

$$\zeta_v^2 = \frac{(2P_1 \cdot v)^2}{v^2} \to -\frac{(2P_1 \cdot v)^2}{|v^2|} = -|\zeta_v^2|, \qquad \rho = \frac{(x_1\zeta_v)^2}{Q^2} \to -|\rho|. \qquad (A.14)$$

Note that the sign change of ρ is not directly obvious from eq. (A.10), which only fixes ρ^2, but immediately follows from eq. (A.11). Applying these transformations to eq. (A.12), we obtain the matching between the LR and Collins scheme,

$$f_{i/h}^{\mathrm{LR}}(x, b_T, \mu, \zeta = Q^2, y_P - y_B) = C_i^{\mathrm{LR}}(Q, \mu, \rho) f_{i/h}(x, b_T, \mu, \zeta = Q^2), \qquad (A.15)$$

where $f_{i/h}^{\mathrm{LR}}$ arises from the appropriate analytic continuation of the JMY TMD at operator level. Due to the symmetry constraints both TMDs are evaluated at $\zeta = Q^2$, and the matching coefficient is given by

$$C_i^{\mathrm{LR}}(Q, \mu, \rho) = C_i^{\mathrm{JMY}}(Q, \mu, -\rho). \qquad (A.16)$$

Since C_i^{JMY} depends on ρ only through $L_\rho = \ln(\rho Q^2/\mu^2)$, we need to analytically continue ρ to $-\rho$ to make use of eq. (A.16),

$$L_\rho = \ln \frac{\rho Q^2}{\mu^2} \quad \to \quad L_{-\rho} = \ln \frac{-\rho Q^2}{\mu^2} = L_{|\rho|} \pm \mathrm{i}\pi. \qquad (A.17)$$

The sign of this phase induced by the spacelike $v^2 < 0$ cannot be easily reconstructed a *posteriori*, but is fixed by the i0 prescription in perturbation theory. Fortunately, we do not need to fix this sign for our purpose, as the hard function is the squared magnitude of a complex amplitude, so at NLO we deduce that the spacelike version of eq. (A.7) is

$$\begin{aligned}
C_q^{\mathrm{LR}}(Q, \mu, \rho) &= 1 + \frac{\alpha_s C_F}{2\pi} \Re \left(-\frac{1}{2}(L_{|\rho|} \pm \mathrm{i}\pi)^2 + (L_{|\rho|} \pm \mathrm{i}\pi) - \frac{5}{12}\pi^2 - 2 \right) + \mathcal{O}(\alpha_s^2) \\
&= 1 + \frac{\alpha_s C_F}{4\pi} \left(-L_{|\rho|}^2 + 2L_{|\rho|} + \frac{\pi^2}{6} - 4 \right) + \mathcal{O}(\alpha_s^2).
\end{aligned} \qquad (A.18)$$

Using eq. (A.11), the logarithm can be expressed as

$$L_{|\rho|} = \ln \frac{|\rho| Q^2}{\mu^2} = \ln \frac{(2x_1 P_1 \cdot v)^2}{|v^2|\mu^2}. \qquad (A.19)$$

To complete our derivation, we first replace Q^2 with ζ, corresponding to a simple relabelling, and employ that the hard coefficient only depends on the combination

$$\rho Q^2 = \frac{(2x_1 P_1 \cdot v)^2}{|v^2|} = e^{2(y_n - y_B)}\zeta = x^2 m_h^2 e^{2(y_P - y_B)} \approx \zeta_{\text{LR}}\,, \qquad (\text{A.20})$$

where the $\approx$ indicates equality for the large $-y_B$ limit. We can then rewrite eq. (A.12) as

$$f_{i/h}^{\text{LR}}(x, b_T, \mu, \zeta, y_P - y_B) = C_i(\zeta_{\text{LR}}, \mu) f_{i/h}(x, b_T, \mu, \zeta)\,, \qquad (\text{A.21})$$

where ζ_{LR} is given by eq. (3.24) and we have defined

$$C_i(\rho Q^2, \mu) = C_i^{\text{LR}}(Q, \mu, \rho)\,. \qquad (\text{A.22})$$

Eq. (A.21) reproduces eq. (3.26), with the one-loop conversion given by eq. (A.18). This provides a one-loop confirmation of one of the key parts of our all orders factorization analysis.

For the quasi-TMD, where $v = (0, 0, 0, 1)$ and $\zeta_{\text{LR}} = (2x\tilde{P}^z)^2$, eq. (A.18) exactly reproduces the matching coefficient for quasi-TMD obtained in refs. [35, 37]; see also refs. [34, 49] for an independent calculation.

A.2 NLO results for quark-gluon mixing

We next calculate quark-gluon mixing in TMDs and quasi-TMDs at $\mathcal{O}(\alpha_s)$. We work in coordinate space to obtain matrix elements as a function of the Lorentz invariants b^2 and $p \cdot b$, where p^μ is the on-shell momentum of the external parton ($p^2 = 0$). As expected from the factorization theorem, the TMD and quasi-TMD will turn out to be identical at fixed b^2 and $p \cdot b$, so there is no mixing.

A.2.1 Mixing of quarks into gluon distributions

We first study mixing of quarks into gluon distributions. At $\mathcal{O}(\alpha_s)$, we have two Feynman diagrams, shown in figure 5. These diagrams do not suffer from a rapidity divergence, so we can work without a rapidity regulator. For the quasi-TMD, we take $\tilde{\eta} \to \infty$.

In figure 5, the Feynman rule for the insertion of gluon field strength tensor in the gluon beam function in eq. (2.7) is
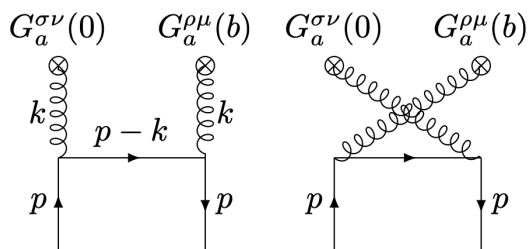
$$\overset{k}{\underset{\alpha,\, a'}{\text{lllllll}}}\!\!\otimes G_a^{\mu\nu}(b) = (-ik^\mu g^{\nu\alpha} + ik^\nu g^{\mu\alpha})\delta^{aa'}e^{-ik\cdot b}\,. \qquad (\text{A.23})$$

Therefore, the two diagrams have values

$$
\begin{aligned}
f_a^{\mu\rho\nu\sigma}(b, p) = \mu_0^{2\epsilon} \int \frac{\mathrm{d}^d k}{(2\pi)^d} \bar{u}(p)(ig\gamma_\alpha \tau^a)\frac{-i}{k^2}(ik^\rho g^{\mu\alpha} - ik^\mu g^{\rho\alpha})e^{ik\cdot b}\frac{i}{\not{p} - \not{k}} \\
\times (-ik^\sigma g^{\nu\beta} + ik^\nu g^{\sigma\beta})\frac{-i}{k^2}e^{ik\cdot 0}(ig\gamma_\beta \tau^a)u(p)\,, \qquad (\text{A.24})
\end{aligned}
$$

$$
\begin{aligned}
f_b^{\mu\rho\nu\sigma}(b, p) = \mu_0^{2\epsilon} \int \frac{\mathrm{d}^d k}{(2\pi)^d} \bar{u}(p)(ig\gamma_\alpha \tau^a)\frac{-i}{k^2}(ik^\sigma g^{\nu\alpha} - ik^\nu g^{\sigma\alpha})e^{ik\cdot 0}\frac{i}{\not{p} - \not{k}} \\
\times (-ik^\rho g^{\mu\beta} + ik^\mu g^{\rho\beta})\frac{-i}{k^2}e^{-ik\cdot b}(ig\gamma_\beta \tau^a)u(p)\,. \qquad (\text{A.25})
\end{aligned}
$$

Figure 5. Mixing of quark TMDs into gluon TMDs at lowest order, i.e. $\mathcal{O}(\alpha_s)$. The Lorentz indices correspond to the gluon TMD operator, while p is the momentum of the external on-shell quark.

Let us pull all coefficients out of the integrals:

$$f_a^{\mu\rho\,\nu\sigma}(b,p) = \frac{\alpha_s C_F}{4\pi}\mathrm{Tr}\left[\gamma_\alpha(\not{p}+\mathrm{i}\not{\partial})\gamma_\beta\frac{\not{p}}{2}\right](\partial^\rho g^{\mu\alpha}-\partial^\mu g^{\rho\alpha})(\partial^\sigma g^{\nu\beta}-\partial^\nu g^{\sigma\beta})\mathcal{I}_v(b^2,p\cdot b)\,,$$

$$f_b^{\mu\rho\,\nu\sigma}(b,p) = f_a^{\nu\sigma\,\mu\rho}(b,-p) = \left[f_a^{\nu\sigma\,\mu\rho}(b,p)\right]^*\,, \tag{A.26}$$

where as in ref. [40] we define the integral

$$\mathcal{I}_v(b^2,p\cdot b) = -4\mathrm{i}\mu_0^{2\epsilon}\int\frac{\mathrm{d}^d k}{(2\pi)^{d-2}}\frac{e^{\mathrm{i}k\cdot b}}{k^4(p-k)^2} = -\frac{(\pi\mu_0^2)^\epsilon}{4}\Gamma(-1-\epsilon)\frac{1+\mathrm{i}p\cdot b-e^{\mathrm{i}p\cdot b}}{(p\cdot b)^2}(-b^2)^{1+\epsilon}\,. \tag{A.27}$$

Let us examine the first derivative of $\mathcal{I}_v(b)$ for use in eq. (A.26),

$$\partial^\alpha\mathcal{I}_v(b^2,p\cdot b) = 2b^\alpha\frac{\partial\mathcal{I}_v}{\partial(b^2)} + p^\alpha\frac{\partial\mathcal{I}_v}{\partial(p\cdot b)}\,. \tag{A.28}$$

Eventually, we will need to specify the directions associated with free Lorentz indices (n_a, n_b, $\hat{n}_\perp$). Doing so early on streamlines our work with power counting. Examining all derivative terms that arise when we contract indices relevant at leading power, we have

$$n_a\cdot\partial\,\mathcal{I}_v(b^2,p\cdot b) = 2n_a\cdot b\frac{\partial\mathcal{I}_v}{\partial(b^2)}\,,$$

$$n_b\cdot\partial\,\mathcal{I}_v(b^2,p\cdot b) = n_b\cdot p\frac{\partial\mathcal{I}_v}{\partial(p\cdot b)}\,,$$

$$\partial_\perp^\alpha\mathcal{I}_v(b^2,p\cdot b) = 2b_\perp^\alpha\frac{\partial\mathcal{I}_v}{\partial(b^2)}\,. \tag{A.29}$$

Quasi-TMD factorization gives us $p\cdot b\sim 1$, $1/b_T^2\ll(n_b\cdot p)^2$, and $n_a\cdot b\ll|b_T|$. This leads to a power counting of

$$(n_b\cdot\partial,n_a\cdot\partial,\partial_\perp)\sim(1,\lambda^2,\lambda)\,n_b\cdot p\,, \tag{A.30}$$

where $\lambda\sim 1/(b_T\,n_b\cdot p)\ll 1$. This is the same power counting as for the momenta of particles created by n-collinear fields in SCET [84–87].

We now obtain leading-power results. We start with the TMDs, for which we must contract μ and ν with n_b^μ and n_b^ν, as well as take ρ,σ to be transverse Lorentz indices:

$$f_a^{\bar{n}\sigma_\perp\bar{n}\rho_\perp} = \frac{\alpha_s C_F}{4\pi}\mathrm{Tr}\left[\gamma_\alpha(\not{p}+\mathrm{i}\not{\partial})\gamma_\beta\frac{\not{p}}{2}\right]\left(n_b^\alpha\partial_\perp^\rho-g_\perp^{\rho\alpha}n_b\cdot\partial\right)\left(n_b^\beta\partial_\perp^\sigma-g_\perp^{\sigma\beta}n_b\cdot\partial\right)\mathcal{I}_v(b)\,,$$

$$f_b^{\bar{n}\sigma_\perp\bar{n}\rho_\perp} = \frac{\alpha_s C_F}{4\pi}\mathrm{Tr}\left[\gamma_\alpha(\not{p}-\mathrm{i}\not{\partial})\gamma_\beta\frac{\not{p}}{2}\right]\left(n_b^\alpha\partial_\perp^\sigma-g_\perp^{\sigma\alpha}n_b\cdot\partial\right)\left(n_b^\beta\partial_\perp^\rho-g_\perp^{\rho\beta}n_b\cdot\partial\right)\mathcal{I}_v(-b)\,. \tag{A.31}$$

The Dirac traces lead to the following tensor structures

$$g_{\alpha\beta}\, p \cdot \partial, \quad p_\alpha p_\beta, \quad p_\alpha \partial_\beta + p_\beta \partial_\alpha \,. \tag{A.32}$$

When we contract the indices α and β with the remaining parts of each Feynman diagram, both diagrams have a nonvanishing contribution at leading power of order

$$p \cdot \partial (n_b \cdot \partial)^2 g_\perp^{\rho\sigma} \sim (n_b \cdot p)^2 \partial_\perp^\rho \partial_\perp^\sigma \sim \mathcal{O}(\lambda^2 (n_b \cdot p)^4)\,. \tag{A.33}$$

To obtain the corresponding quasi-TMDs, we contract μ and ν with $\bar{n}_1^\mu$ and $\bar{n}_2^\nu$, and we take ρ, σ to be transverse Lorentz indices. Here we are free to pick each of $\bar{n}_1$ and $\bar{n}_2$ to be in the time direction or z-direction, ie. $\bar{n}_{1,2} = n_t$ or $-n_z$. This leads to

$$\tilde{f}_a^{\bar{n}_1 \sigma_\perp \bar{n}_2 \rho_\perp} = \frac{\alpha_s C_F}{4\pi} \mathrm{Tr}\left[\gamma_\alpha (\not{p} + i\not{\partial})\gamma_\beta \frac{\not{p}}{2}\right] (\bar{n}_1^\alpha \partial_\perp^\rho - g_\perp^{\rho\alpha} \bar{n}_1 \cdot \partial)\left(\bar{n}_2^\beta \partial_\perp^\sigma - g_\perp^{\sigma\beta}\bar{n}_2 \cdot \partial\right)\mathcal{I}_v(b)\,,$$

$$\tilde{f}_b^{\bar{n}_1 \sigma_\perp \bar{n}_2 \rho_\perp} = \frac{\alpha_s C_F}{4\pi} \mathrm{Tr}\left[\gamma_\alpha (\not{p} - i\not{\partial})\gamma_\beta \frac{\not{p}}{2}\right] (\bar{n}_2^\alpha \partial_\perp^\sigma - g_\perp^{\sigma\alpha} \bar{n}_2 \cdot \partial)\left(\bar{n}_1^\beta \partial_\perp^\rho - g_\perp^{\rho\beta}\bar{n}_1 \cdot \partial\right)\mathcal{I}_v(-b)\,. \tag{A.34}$$

Because $n_t = (n_a + n_b)/\sqrt{2}$ and $n_z = (n_a - n_b)/\sqrt{2}$, the contributions from $n_a/\sqrt{2}$ either vanish due to $n_a \cdot p = 0$ or are power suppressed by $\mathcal{O}(\lambda^2)$ after contracting with the Dirac trace. Therefore, the leading power contribution to the quasi-TMD can be reduced to

$$\tilde{f}_a^{\bar{n}_1 \sigma_\perp \bar{n}_2 \rho_\perp} = \frac{1}{2}\frac{\alpha_s C_F}{4\pi}\mathrm{Tr}\left[\gamma_\alpha (\not{p} + i\not{\partial})\gamma_\beta \frac{\not{p}}{2}\right] (n_b^\alpha \partial_\perp^\rho - g_\perp^{\rho\alpha} n_b \cdot \partial)\left(n_b^\beta \partial_\perp^\sigma - g_\perp^{\sigma\beta}n_b \cdot \partial\right)\mathcal{I}_v(b)\,,$$

$$\tilde{f}_b^{\bar{n}_1 \sigma_\perp \bar{n}_2 \rho_\perp} = \frac{1}{2}\frac{\alpha_s C_F}{4\pi}\mathrm{Tr}\left[\gamma_\alpha (\not{p} - i\not{\partial})\gamma_\beta \frac{\not{p}}{2}\right] (n_b^\alpha \partial_\perp^\sigma - g_\perp^{\sigma\alpha} n_b \cdot \partial)\left(n_b^\beta \partial_\perp^\rho - g_\perp^{\rho\beta}n_b \cdot \partial\right)\mathcal{I}_v(-b)\,, \tag{A.35}$$

which is the same as the Collins TMD in eq. (A.31) except for the overall factor of $1/2$. After taking into account the Fourier transform in the definition of the quasi-TMDs in eq. (2.29), this $1/2$ factor is cancelled by the change of the integration measure, so the results are equal between quasi- and Collins TMDs in this channel.
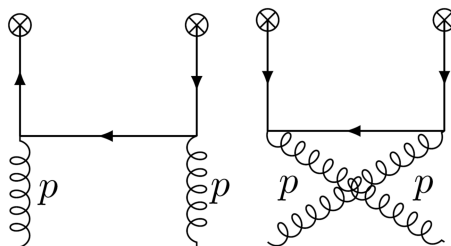
A.2.2 Mixing of gluons into quark distributions

Next, we consider the mixing of gluons into quark distributions. This process first receives corrections at $\mathcal{O}(\alpha_s)$, as shown in figure 6. The sum of these diagrams yields

$$f_{c+d}^{\rho\sigma} = ig^2 T_F \delta^{ab} \int \frac{d^d k}{(2\pi)^d} \mathrm{Tr}\left[\Gamma \frac{1}{\not{k}}\gamma_\perp^\rho \frac{1}{\not{p} - \not{k}}\gamma_\perp^\sigma \frac{1}{\not{k}}\right]\left[e^{-ik\cdot b} + e^{ik\cdot b}\right]\,, \tag{A.36}$$

where ρ and σ are transverse Lorentz indices because they contract with on-shell gluon polarization vectors. f_{c+d} reduces to a form expressible in terms of derivatives of $\mathcal{I}_v(b)$:

$$f_{c+d}^{\rho\sigma} = \frac{\alpha_s T_F \delta^{ab}}{4\pi}\left\{\mathrm{Tr}\left[\Gamma \not{\partial}\gamma_\perp^\rho (\not{p} + i\not{\partial})\gamma_\perp^\sigma \not{\partial}\right]\mathcal{I}_v(b) + \mathrm{Tr}\left[\Gamma \not{\partial}\gamma_\perp^\rho (\not{p} - i\not{\partial})\gamma_\perp^\sigma \not{\partial}\right]\mathcal{I}_v(-b)\right\}\,. \tag{A.37}$$

Figure 6. Mixing of gluon TMDs into quark TMDs at lowest order, $\mathcal{O}(\alpha_s)$. The quark fields of the TMD operator are denoted by $\otimes$.

To obtain the TMD, we take $\Gamma = \not{n}_b$. The trace in eq. (A.37) has leading-power contributions

$$\mathrm{Tr}\left[\not{n}_b \not{\partial} \gamma_\perp^\mu (\not{\partial} \pm i\not{p}) \gamma_\perp^\nu \not{\partial}\right] \sim \{g_\perp^{\mu\nu} n_b \cdot p \partial^2, g_\perp^{\mu\nu} n_b \cdot \partial \partial^2, n_b \cdot p \partial_\perp^\mu \partial_\perp^\nu, n_b \cdot \partial \partial_\perp^\mu \partial_\perp^\nu\} \sim \mathcal{O}(\lambda^2 (n_b \cdot p)^3). \tag{A.38}$$

To obtain the quasi-TMD, we choose $\Gamma = \not{n}_t$ or $\not{n}_z$, where $n_t = (n_a + n_b)/\sqrt{2}$ and $n_z = (n_a - n_b)/\sqrt{2}$. The contribution from $n_a/\sqrt{2}$ is once again suppressed by $\mathcal{O}(\lambda^2)$. Therefore, after Fourier transform we find that mixing graphs in figure 6 have identical values for the TMD and quasi-TMD at the same $p \cdot b$ and b^2.

B   One-loop comparison of JMY and Collins TMDs

Next, we validate the compatibility of the Collins and JMY schemes defined in section 2.2.1 and section 2.2.2, respectively. Let us write eq. (2.15) for each of these schemes:

$$\frac{\mathrm{d}\sigma}{\mathrm{d}Q^2 \mathrm{d}Y \mathrm{d}^2\vec{q}_T} = \sigma_0 \sum_{i,j} H_{ij}(Q,\mu) \int \frac{\mathrm{d}^2\vec{b}_T}{(2\pi)^2} e^{i\vec{q}_T \cdot \vec{b}_T} f_{i/h_1}(x_1, \vec{b}_T, \mu, \zeta_1) f_{j/h_2}(x_2, \vec{b}_T, \mu, \zeta_2) \tag{B.1}$$

$$= \sigma_0 \sum_{i,j} H_{ij}(Q,\mu,\rho) \int \frac{\mathrm{d}^2\vec{b}_T}{(2\pi)^2} e^{i\vec{q}_T \cdot \vec{b}_T} f_{i/h_1}(x_1, \vec{b}_T, \mu, x_1\zeta_v, \rho) f_{j/h_2}(x_2, \vec{b}_T, \mu, x_2\zeta_{\tilde{v}}, \rho).$$

Since perturbative results in the JMY scheme are only known for quark TMDs matched onto quark PDFs, we accordingly restrict our study to the Drell-Yan process. We first collect perturbative results in both schemes and then compare them to one other.

B.1   NLO results in the Collins scheme

The Drell-Yan hard function can be obtained from the corresponding vector form factor, which is known to three loops [88–96]. At one loop, we have

$$H_{q\bar{q}}(Q,\mu) = 1 + \frac{\alpha_s C_F}{2\pi} H_{q\bar{q}}^{(1)}(Q,\mu) + \mathcal{O}(\alpha_s^2),$$

$$H_{q\bar{q}}^{(1)}(Q,\mu) = -\ln^2 \frac{Q^2}{\mu^2} + 3\ln \frac{Q^2}{\mu^2} + \frac{7}{6}\pi^2 - 8. \tag{B.2}$$

The TMD is matched onto collinear PDFs as

$$f_{i/h}(x, \vec{b}_T, \mu, \zeta) = \sum_j \int_x^1 \frac{\mathrm{d}y}{y} C_{ij}(y, \vec{b}_T, \mu, \zeta) f_{j/h}\left(\frac{x}{y}, \mu\right) + \mathcal{O}(b_T \Lambda_{\mathrm{QCD}}), \tag{B.3}$$

The matching kernel C_{ij} is also known at three loops [97–106], and we expand it as

$$C_{ij}(x, b_T, \mu, \zeta) = \delta_{ij}\delta(1-x) + \frac{\alpha_s C_F}{2\pi} C_{ij}^{(1)}(x, b_T, \mu, \zeta) + \mathcal{O}(\alpha_s^2). \qquad \text{(B.4)}$$

At one loop, the quark-to-quark kernel reads

$$C_{qq}^{(1)}(x, b_T, \mu, \zeta) = -L_b P_{qq}(x) + (1-x) + \delta(1-x)\left[-\frac{1}{2}L_b^2 + L_b\left(\frac{3}{2} + \ln\frac{\mu^2}{\zeta}\right) - \frac{\pi^2}{12}\right], \qquad \text{(B.5)}$$

where we use the standard expressions

$$P_{qq}(x) = \left[\frac{1+x^2}{1-x}\right]_+, \qquad L_b = \ln\frac{b_T^2\mu^2}{b_0^2} \qquad \text{(B.6)}$$

for the quark-quark splitting kernel and the standard logarithm, respectively.

B.2 NLO results in the JMY scheme

Ref. [56] calculates the JMY hard function and TMD at NLO using a version of $\overline{\text{MS}}$ in which one absorbs the factor $S_\epsilon^{\text{JMY}} = (4\pi)^\epsilon/\Gamma(1-\epsilon)$ in the subtraction, as opposed to the standard scheme with $S_\epsilon^{\overline{\text{MS}}} = (4\pi e^{-\gamma_E})^\epsilon$. These schemes only begin to differ at $\mathcal{O}(\epsilon^2)$, so there is no impact on one-loop calculations, which have a single pole in ϵ. (It does affect on-lightcone calculations, for which the bare hard function and TMD have double poles.) Ref. [56] examined SIDIS, whereas we consider Drell-Yan; thus we must analytically continue from $q^2 = -Q^2 < 0$ (SIDIS) to $q^2 = Q^2 > 0$ (Drell-Yan).

In this section, we abbreviate

$$L_v = \ln\frac{(x_1\zeta_v)^2}{\mu^2}, \qquad L_{\tilde{v}} = \ln\frac{(x_2\zeta_{\tilde{v}})^2}{\mu^2}. \qquad \text{(B.7)}$$

Using eq. (2.23) and noting that $\zeta_v^2\zeta_{\tilde{v}}^2 = E_{\text{cm}}^4\rho^2$, where $E_{\text{cm}}^2 = (P_1 + P_2)^2$, we have

$$L_v + L_{\tilde{v}} = 2\ln\frac{Q^2}{\mu^2} + \ln\rho^2, \qquad \text{(B.8)}$$

where $Q^2 = x_1 x_2 E_{\text{cm}}^2$ is the invariant mass of the produced color-singlet final state.

We expand the hard function in the JMY scheme similar to eq. (B.2) as

$$H_{q\bar{q}}(Q, \mu, \rho) = 1 + \frac{\alpha_s C_F}{2\pi} H_{q\bar{q}}^{(1)}(Q, \mu, \rho) + \mathcal{O}(\alpha_s^2). \qquad \text{(B.9)}$$

The NLO result in SIDIS kinematics is given by [56]

$$\begin{aligned}
H_{q\bar{q}}^{\text{SIDIS}(1)}(Q, \mu, \rho) &= (1 + \ln\rho^2)\ln\frac{Q^2}{\mu^2} - \ln\rho^2 + \frac{1}{4}\ln^2\rho^2 + \pi^2 - 4 \\
&= -\ln^2\frac{Q^2}{\mu^2} + 3\ln\frac{Q^2}{\mu^2} + \frac{1}{4}(L_v + L_{\tilde{v}})^2 - (L_v + L_{\tilde{v}}) + \pi^2 - 4, \quad \text{(B.10)}
\end{aligned}$$

where in the second line we used eq. (B.8). To recover the corresponding result for Drell-Yan, we need to analytically continue $Q^2 \to -Q^2$, which is achieved by

$$\ln^2 \frac{Q^2}{\mu^2} = \Re\left[\ln^2 \frac{-q^2 - \mathrm{i}0}{\mu^2}\right]_{q^2=-Q^2} \quad \to \quad \Re\left[\ln^2 \frac{-q^2 - \mathrm{i}0}{\mu^2}\right]_{q^2=+Q^2} = \ln^2 \frac{Q^2}{\mu^2} - \pi^2. \quad \text{(B.11)}$$

The single logarithm of Q^2 is unaffected, as are logarithms of the fixed parameters v^2 and $\tilde{v}^2$. Applying this to eq. (B.10), we obtain the Drell-Yan hard function in the JMY scheme,

$$H_{q\bar{q}}^{(1)}(Q, \mu, \rho) = -\ln^2 \frac{Q^2}{\mu^2} + 3\ln \frac{Q^2}{\mu^2} + \frac{1}{4}(L_v + L_{\tilde{v}})^2 - (L_v + L_{\tilde{v}}) + 2\pi^2 - 4. \quad \text{(B.12)}$$

In ref. [56] the TMD was originally defined as $q_i = B_i/S$, which is distinguished from the definition $f_i = B_i/\sqrt{S}$ in eq. (2.24). Both q_i and f_i can be matched onto collinear PDFs similar to eq. (B.3),

$$q_{i/h}(x, \vec{b}_T, \mu, x\zeta_v, \rho) = \sum_j \int_x^1 \frac{\mathrm{d}y}{y} \tilde{C}_{ij}\left(\frac{x}{y}, \vec{b}_T, \mu, x\zeta_v, \rho\right) f_{j/h}(y, \mu) + \mathcal{O}(b_T \Lambda_{\text{QCD}}),$$

$$f_{i/h}(x, \vec{b}_T, \mu, x\zeta_v, \rho) = \sum_j \int_x^1 \frac{\mathrm{d}y}{y} C_{ij}\left(\frac{x}{y}, \vec{b}_T, \mu, x\zeta_v, \rho\right) f_{j/h}(y, \mu) + \mathcal{O}(b_T \Lambda_{\text{QCD}}), \quad \text{(B.13)}$$

where $\tilde{C}_{ij}$ and C_{ij} are the corresponding matching kernels. We expand both in the same fashion as eq. (B.4), and the one-loop result of $\tilde{C}_{ij}$ can be read off from ref. [56] as

$$\tilde{C}_{qq}^{(1)}(x, b_T, \mu, x\zeta_v, \rho) = -L_b P_{qq}(x) + (1 - x) \quad \text{(B.14)}$$
$$+ \delta(1 - x)\left[-\frac{1}{2}(L_b + L_v)^2 + L_b\left(\frac{1}{2} + \ln \rho^2\right) + L_v - 2 - \frac{\pi^2}{2}\right].$$

To obtain the result for $C_{ij}^{(1)}$, we first need the one-loop result for the soft function [56]

$$S(b_T, \mu, \rho) = 1 + \frac{\alpha_s C_F}{2\pi} S^{(1)}(b_T, \mu, \rho) + \mathcal{O}(\alpha_s^2), \quad S^{(1)}(b_T, \mu, \rho) = (2 - \ln \rho^2) L_b. \quad \text{(B.15)}$$

Using the relation between q_i and f_i, we then obtain

$$C_{qq}^{(1)}(x, b_T, \mu, x\zeta_v, \rho) = \tilde{C}_{qq}^{(1)}(x, b_T, \mu, x\zeta_v, \rho) + \frac{1}{2} S^{(1)}(b_T, \mu, \rho)$$
$$= -L_b P_{qq}(x) + (1 - x) \quad \text{(B.16)}$$
$$+ \delta(1 - x)\left[-\frac{1}{2}(L_b + L_v)^2 + L_b\left(\frac{3}{2} + \frac{1}{2}\ln \rho^2\right) + L_v - 2 - \frac{\pi^2}{2}\right].$$

B.3 Comparison at NLO

Using eqs. (B.3) and (B.13), at the perturbative level we recast eq. (B.1) as

$$1 \overset{!}{=} \frac{H_{ij}(Q, \mu) C_{ii'}(y_1, \vec{b}_T, \mu, \zeta_1) C_{jj'}(y_2, \vec{b}_T, \mu, \zeta_2)}{H_{ij}(Q, \mu, \rho) C_{ii'}(y_1, \vec{b}_T, \mu, x_1 \zeta_v, \rho) C_{jj'}(y_2, \vec{b}_T, \mu, x_2 \zeta_{\tilde{v}}, \rho)}, \quad \text{(B.17)}$$

where i, j are flavors of the underlying Born processes; i', j' are flavors summed over in eqs. (B.3) and (B.13); and $y_{1,2}$ are the corresponding convolution variables. We restrict our attention to the qq channel, using eqs. (B.2) and (B.5) for the numerator and eqs. (B.12) and (B.16) for the denominator:

$$1 \overset{!}{=} 1 + \frac{\alpha_s C_F}{2\pi} \left[L_b \ln \frac{Q^4}{\zeta_1 \zeta_2} + \frac{1}{4} (L_v - L_{\tilde{v}})^2 \right] + \mathcal{O}(\alpha_s^2). \tag{B.18}$$

Equality of schemes enforces the conditions

$$\zeta_1 \zeta_2 = Q^4 \qquad \text{and} \qquad L_v = L_{\tilde{v}}. \tag{B.19}$$

The first constraint on the CS scale is trivially obeyed by eq. (2.16), while the latter is a nontrivial restriction of JMY Wilson line paths. This implies that the one-loop results given in ref. [56] are only valid in the reference frame where eq. (B.19) is fulfilled. It may be possible to get a more generic result for the hard function without requiring $L_v = L_{\tilde{v}}$.

From eq. (B.7), we see that eq. (B.19) is equivalent to $x_1 \zeta_v = x_2 \zeta_{\tilde{v}}$, which implies that

$$\frac{v^+ \tilde{v}^+}{v^- \tilde{v}^-} = \left(\frac{x_1 P_1^+}{x_2 P_2^-} \right)^2 = e^{4Y}, \qquad \rho = \frac{\zeta_v \zeta_{\tilde{v}}}{E_{\text{cm}}^2} = \frac{(x_1 \zeta_v)^2}{Q^2} = \frac{(x_2 \zeta_{\tilde{v}})^2}{Q^2}, \tag{B.20}$$

where $E_{\text{cm}}^2 = (P_1 + P_2)^2 = 2P_1^+ P_2^-$, and $Q^2 = x_1 x_2 E_{\text{cm}}^2$ and Y are the invariant mass and rapidity of the final state, respectively.

It is also instructive to compare ratios of hard functions and TMDs in the two schemes. For the hard function, from eqs. (B.12) and (B.2) we obtain

$$\sqrt{\frac{H_{\text{DY}}(Q, \mu, \rho)}{H_{\text{DY}}(Q, \mu)}} = 1 + \frac{\alpha_s C_F}{2\pi} \left[\frac{1}{8} (L_v + L_{\tilde{v}})^2 - \frac{1}{2} (L_v + L_{\tilde{v}}) + \frac{5}{12} \pi^2 + 2 \right] + \mathcal{O}(\alpha_s^2)$$

$$\overset{(\text{B.19})}{=} 1 + \frac{\alpha_s C_F}{2\pi} \left[\frac{1}{2} L_v^2 - L_v + \frac{5}{12} \pi^2 + 2 \right] + \mathcal{O}(\alpha_s^2). \tag{B.21}$$

In the second step, we used $L_v = L_{\tilde{v}}$ as required by eq. (B.19). For the TMDs, comparing eqs. (B.16) and (B.5) yields

$$\frac{C_{qq}(x_1, b_T, \mu, x_1 \zeta_v, \rho)}{C_{qq}(x_1, b_T, \mu, \zeta_1)} = 1 + \frac{\alpha_s C_F}{2\pi} \left[L_b \ln \frac{\rho \zeta_1}{x_1^2 \zeta_v^2} - \left(\frac{1}{2} L_v^2 - L_v + \frac{5}{12} \pi^2 + 2 \right) \right] + \mathcal{O}(\alpha_s^2). \tag{B.22}$$

Note that the b_T-independent terms are exactly the negative of those in eq. (B.21). The leftover b_T dependence implies that eq. (B.22) is nonperturbative when $b_T \gtrsim \Lambda_{\text{QCD}}^{-1}$. However, since it is directly proportional to ζ_1 and ζ_v, it can be eliminated for a certain choice of the evolution parameters. Demanding that the L_b term vanishes to have a perturbative relation, we obtain

$$1 \overset{!}{=} \frac{\rho \zeta_1}{x_1^2 \zeta_v^2} = e^{-2y_n} \sqrt{\frac{v^+ \tilde{v}^+}{v^- \tilde{v}^-}}. \tag{B.23}$$

Here, we used $\zeta_1 = 2(x_1 P_1^+)^2 e^{-2y_n}$. In conclusion, we find that a perturbative matching requires the specific combination

$$\frac{v^+ \tilde{v}^+}{v^- \tilde{v}^-} = e^{4y_n} \,. \tag{B.24}$$

The corresponding requirement for the conjugate TMD is the same as eq. (B.24). The appearance of y_n in this condition is not surprising, as $y_n \neq 0$ implies that soft radiation is not split uniformly between the two TMDs in the Collins scheme, and the same asymmetry must be reflected in the JMY scheme to obtain a perturbative relation.

Note that eqs. (B.20) and (B.24) only agree if $y_n = Y$. For this specific choice, we have that $x_1 \zeta_v = x_2 \zeta_{\tilde{v}}$ *and* $\zeta_1 = \zeta_2 = Q^2$, i.e. the evolution variables appear symmetrically in both the Collins and JMY scheme. This symmetric choice was already enforced in appendix A.1.1 on more general grounds.

We are interested in the matching relation between a single JMY and Collins TMD PDF, for which we now limit ourselves to the case of the n-collinear PDF. In this case, we have to use eq. (B.24) to fix the value of ρ in the JMY TMD as

$$\rho_v^2 \equiv \left. \frac{v^-}{v^+} \frac{\tilde{v}^+}{\tilde{v}^-} \right|_{(B.24)} = \left[\frac{v^-}{v^+} e^{2y_n} \right]^2 = \frac{(x_1^2 \zeta_v^2)^2}{\zeta_1^2} \,. \tag{B.25}$$

At this particular value, we have the relation

$$f_{q_i/h}(x, b_T, \mu, x\zeta_v, \rho_v) = C_q^{\mathrm{JMY}}(Q, \mu, \rho_v) \, f_{q_i/h}(x, b_T, \mu, \zeta_1) \,, \tag{B.26}$$

where (at least to one loop) the matching kernel is identical to the ratios of hard functions,

$$\begin{aligned}
C_q^{\mathrm{JMY}}(Q, \mu, \rho_v) &= \left. \sqrt{\frac{H_{q\bar{q}}(Q, \mu)}{H_{q\bar{q}}(Q, \mu, \rho_v)}} \right|_{L_v = L_{\tilde{v}}} \\
&= 1 + \frac{\alpha_s C_F}{2\pi} \left(-\frac{1}{2} L_v^2 + L_v - 2 - \frac{5}{12}\pi^2 \right) + \mathcal{O}(\alpha_s^2) \,.
\end{aligned} \tag{B.27}$$

The logarithm on the right-hand side is given by

$$L_v = \ln \frac{(2xP_1 \cdot v)^2 / v^2}{\mu^2} = \ln \frac{\rho_v Q^2}{\mu^2} \,. \tag{B.28}$$

To obtain the final relation between the JMY and Collins TMDs at generic ρ and ζ, we can use the ζ evolution to obtain

$$f_i(x, b_T, \mu, x\zeta_v, \rho) = C_i^{\mathrm{JMY}}(Q, \mu, \rho) \exp\left[\frac{1}{2} \gamma_\zeta^i(\mu, b_T) \ln \frac{(x\zeta_v)^2 / \rho}{\zeta} \right] f_i(x, b_T, \mu, \zeta) \,. \tag{B.29}$$

To obtain this result we have replaced ζ_1 using eq. (B.25), which allows us to express the result using a generic value of ρ. The scheme conversion relation in eq. (B.29) can be compared to the factorization formula relating the quasi-TMD and Collins TMD in eq. (3.27), which has a very similar form.

C Wilson line self-energy at one loop

A key consideration for lattice TMDs is the cancellation of Wilson line self-energies. Here, we examine the self-energy of the Wilson staple in eq. (2.4). Using the auxiliary field formalism, the renormalization of an open, piecewise-smooth Wilson loop reads [107]

$$W^{\rm ren}[\gamma] = Z_z^{-1} e^{-\delta m_z \ell} \left[\prod_i Z_{\bar{z}z}^{-1}(\gamma_i) \right] W^{\rm bare}[\gamma] \,, \tag{C.1}$$

where Z_z and $Z_{\bar{z}z}$ are counterterms for the linear and quadratic operators of the auxiliary z field, δm_z is the mass counterterm, ℓ is the length of the Wilson loop, and the product runs over all cusps γ_i arising on the Wilson line path γ. The cusp angles are given by

$$\cosh \gamma_i = \frac{p_i \cdot q_i}{\sqrt{p_i^2 q_i^2}} \,, \tag{C.2}$$

where p_i and q_i are the unit vectors at the cusp. In the Euclidean case, one has

$$\gamma_i = {\rm i}\delta_i \,, \qquad \cos \delta_i = \frac{\vec{p}_i \cdot \vec{q}_i}{|\vec{p}_i||\vec{q}_i|} \,. \tag{C.3}$$

At one loop in the $\overline{\rm MS}$ scheme and in Feynman gauge, the counterterms are [107]

$$Z_z = 1 + \frac{\alpha_s C_F}{2\pi} \frac{1}{\epsilon} + \mathcal{O}(\alpha_s^2) \,,$$

$$Z_{\bar{z}z}(\gamma = {\rm i}\delta) = 1 + \frac{\alpha_s C_F}{2\pi} \frac{1}{\epsilon} (1 - \delta \cot \delta) + \mathcal{O}(\alpha_s^2) \,. \tag{C.4}$$

Here, we take $\delta \in [0, \pi)$; straight angles $\delta = \pi$ are mapped back onto $\delta = 0$, where $Z_{\bar{z}z} = 1$. For two-loop results, see ref. [108]. δm vanishes in dimensional regularization with the $\overline{\rm MS}$ scheme, but is important to take into account on the lattice.

We now restrict our discussion to purely Euclidean paths, with vanishing time component. The Wilson loop in eq. (2.4) has total length and cusp angles

$$\ell_\sqsupset = \left| \eta \vec{v} - \frac{\vec{\delta}}{2} \right| + \left| \vec{b} - \vec{\delta} \right| + \left| \eta \vec{v} + \frac{\vec{\delta}}{2} \right|$$

$$\cos \delta_1 = \frac{(\eta \vec{v} - \frac{\vec{\delta}}{2}) \cdot (\vec{\delta} - \vec{b})}{|\eta \vec{v} - \frac{\vec{\delta}}{2}||\vec{\delta} - \vec{b}|} \,, \quad \cos \delta_2 = -\frac{(\eta \vec{v} + \frac{\vec{\delta}}{2}) \cdot (\vec{\delta} - \vec{b})}{|\eta \vec{v} + \frac{\vec{\delta}}{2}||\vec{\delta} - \vec{b}|} \,, \tag{C.5}$$

with the appropriate mapping into $[0, \pi)$. By construction, $\delta_1 + \delta_2 = \pi$, as seen in figure 2. At one loop in the $\overline{\rm MS}$ scheme, it follows that the self-energy is

$$Z_\sqsupset = 1 + \frac{\alpha_s C_F}{2\pi} \frac{1}{\epsilon} \left[3 - \delta_1 \cot \delta_1 - \delta_2 \cot \delta_2 \right] + \mathcal{O}(\alpha_s^2) \,. \tag{C.6}$$

Quasi-beam function. Using $\vec{\delta} = (0, 0, b^z)$ and $\tilde{\eta} \vec{v} = (0, 0, \tilde{\eta})$ from eq. (2.30), we have

$$\ell_\sqsupset = 2\tilde{\eta} + b_T \,, \quad \delta_1 = \delta_2 = \frac{\pi}{2} \,, \qquad Z_\sqsupset = 1 + \frac{\alpha_s C_F}{2\pi} \frac{3}{\epsilon} + \mathcal{O}(\alpha_s^2) \,. \tag{C.7}$$

This UV divergence agrees with the result of the one-loop calculation in ref. [36]. Furthermore, we see that $Z_\sqsupset$ is independent of any kinematic variables, as the staple was constructed to involve only perpendicular angles. The mass divergence $\delta m_z \ell_\sqsupset$ is independent of b^z due to our choice of having the staple sides have lengths $\eta \pm b^z/2$, such that b^z dependence cancels in the sum.

MHENS scheme. The MHENS scheme in eq. (2.39) has arbitrary $\vec{v}$ and $\vec{\delta} = 0$, so

$$\ell_\perp = 2\eta|\vec{v}| + \sqrt{b_T^2 + (b^z)^2}\,, \qquad \cos\delta_{1,2} = \mp\frac{\vec{v}\cdot\vec{b}}{|\vec{v}||\vec{b}|}\,. \tag{C.8}$$

For illustration, we make the simplification $\vec{v}_T = 0$, which gives

$$\ell_\perp = 2\eta|v^z| + \sqrt{b_T^2 + (b^z)^2}\,, \qquad \delta_1 = \pi - \delta_2 = \tan^{-1}\frac{b_T}{|b^z|}\,,$$

$$Z_\sqsupset = 1 + \frac{\alpha_s C_F}{2\pi}\frac{1}{\epsilon}\left[3 - 2\frac{|b^z|}{b_T}\left(\tan^{-1}\frac{b_T}{|b^z|} - \frac{\pi}{2}\right)\right] + \mathcal{O}(\alpha_s^2)\,. \tag{C.9}$$

We see here b^z-dependence of the Wilson line self-energy, which must be removed by a b^z-dependent counterterm.

References

[1] A. Buckley et al., *LHAPDF6: parton density access in the LHC precision era*, *Eur. Phys. J. C* **75** (2015) 132 [arXiv:1412.7420] [INSPIRE].

[2] L.A. Harland-Lang, A.D. Martin, P. Motylinski and R.S. Thorne, *Parton distributions in the LHC era: MMHT 2014 PDFs*, *Eur. Phys. J. C* **75** (2015) 204 [arXiv:1412.3989] [INSPIRE].

[3] S. Dulat et al., *New parton distribution functions from a global analysis of quantum chromodynamics*, *Phys. Rev. D* **93** (2016) 033006 [arXiv:1506.07443] [INSPIRE].

[4] S. Alekhin, J. Blümlein, S. Moch and R. Placakyte, *Parton distribution functions, α_s, and heavy-quark masses for LHC Run II*, *Phys. Rev. D* **96** (2017) 014011 [arXiv:1701.05838] [INSPIRE].

[5] NNPDF collaboration, *Parton distributions from high-precision collider data*, *Eur. Phys. J. C* **77** (2017) 663 [arXiv:1706.00428] [INSPIRE].

[6] T.-J. Hou et al., *Progress in the CTEQ-TEA NNLO global QCD analysis*, arXiv:1908.11394 [INSPIRE].

[7] S. Bailey, T. Cridge, L.A. Harland-Lang, A.D. Martin and R.S. Thorne, *Parton distributions from LHC, HERA, Tevatron and fixed target data: MSHT20 PDFs*, *Eur. Phys. J. C* **81** (2021) 341 [arXiv:2012.04684] [INSPIRE].

[8] R.D. Ball et al., *The Path to Proton Structure at One-Percent Accuracy*, arXiv:2109.02653 [INSPIRE].

[9] A.S. Kronfeld and D.M. Photiadis, *Phenomenology on the Lattice: Composite Operators in Lattice Gauge Theory*, *Phys. Rev. D* **31** (1985) 2939 [INSPIRE].

[10] G. Martinelli and C.T. Sachrajda, *A Lattice Calculation of the Second Moment of the Pion's Distribution Amplitude*, *Phys. Lett. B* **190** (1987) 151 [INSPIRE].

[11] C. Best et al., *Pion and rho structure functions from lattice QCD*, *Phys. Rev. D* **56** (1997) 2743 [hep-lat/9703014] [INSPIRE].

[12] X. Ji, *Parton Physics on a Euclidean Lattice*, *Phys. Rev. Lett.* **110** (2013) 262002 [arXiv:1305.1539] [INSPIRE].

[13] X. Ji, *Parton Physics from Large-Momentum Effective Field Theory*, *Sci. China Phys. Mech. Astron.* **57** (2014) 1407 [arXiv:1404.6680] [INSPIRE].

[14] X. Ji, Y.-S. Liu, Y. Liu, J.-H. Zhang and Y. Zhao, *Large-momentum effective theory*, *Rev. Mod. Phys.* **93** (2021) 035005 [arXiv:2004.03543] [INSPIRE].

[15] K.-F. Liu and S.-J. Dong, *Origin of difference between $\bar{d}$ and $\bar{u}$ partons in the nucleon*, *Phys. Rev. Lett.* **72** (1994) 1790 [hep-ph/9306299] [INSPIRE].

[16] Z. Davoudi and M.J. Savage, *Restoration of Rotational Symmetry in the Continuum Limit of Lattice Field Theories*, *Phys. Rev. D* **86** (2012) 054505 [arXiv:1204.4146] [INSPIRE].

[17] W. Detmold and C.J.D. Lin, *Deep-inelastic scattering and the operator product expansion in lattice QCD*, *Phys. Rev. D* **73** (2006) 014501 [hep-lat/0507007] [INSPIRE].

[18] A.J. Chambers et al., *Nucleon Structure Functions from Operator Product Expansion on the Lattice*, *Phys. Rev. Lett.* **118** (2017) 242001 [arXiv:1703.01153] [INSPIRE].

[19] V. Braun and D. Müller, *Exclusive processes in position space and the pion distribution amplitude*, *Eur. Phys. J. C* **55** (2008) 349 [arXiv:0709.1348] [INSPIRE].

[20] A.V. Radyushkin, *Quasi-parton distribution functions, momentum distributions, and pseudo-parton distribution functions*, *Phys. Rev. D* **96** (2017) 034025 [arXiv:1705.01488] [INSPIRE].

[21] K. Orginos, A. Radyushkin, J. Karpie and S. Zafeiropoulos, *Lattice QCD exploration of parton pseudo-distribution functions*, *Phys. Rev. D* **96** (2017) 094503 [arXiv:1706.05373] [INSPIRE].

[22] Y.-Q. Ma and J.-W. Qiu, *Exploring Partonic Structure of Hadrons Using ab initio Lattice QCD Calculations*, *Phys. Rev. Lett.* **120** (2018) 022003 [arXiv:1709.03018] [INSPIRE].

[23] I. Scimemi and A. Vladimirov, *Non-perturbative structure of semi-inclusive deep-inelastic and Drell-Yan scattering at small transverse momentum*, *JHEP* **06** (2020) 137 [arXiv:1912.06532] [INSPIRE].

[24] A. Bacchetta et al., *Transverse-momentum-dependent parton distributions up to N^3LL from Drell-Yan data*, *JHEP* **07** (2020) 117 [arXiv:1912.07550] [INSPIRE].

[25] A. Accardi et al., *Electron Ion Collider: The Next QCD Frontier*: Understanding the glue that binds us all, *Eur. Phys. J. A* **52** (2016) 268 [arXiv:1212.1701] [INSPIRE].

[26] R. Abdul Khalek et al., *Science Requirements and Detector Concepts for the Electron-Ion Collider: EIC Yellow Report*, arXiv:2103.05419 [INSPIRE].

[27] P. Hagler, B.U. Musch, J.W. Negele and A. Schafer, *Intrinsic quark transverse momentum in the nucleon from lattice QCD*, *EPL* **88** (2009) 61001 [arXiv:0908.1283] [INSPIRE].

[28] B.U. Musch, P. Hagler, J.W. Negele and A. Schafer, *Exploring quark transverse momentum distributions with lattice QCD*, *Phys. Rev. D* **83** (2011) 094507 [arXiv:1011.1213] [INSPIRE].

[29] B.U. Musch, P. Hagler, M. Engelhardt, J.W. Negele and A. Schafer, *Sivers and Boer-Mulders observables from lattice QCD*, *Phys. Rev. D* **85** (2012) 094510 [arXiv:1111.4249] [INSPIRE].

[30] M. Engelhardt, P. Hägler, B. Musch, J. Negele and A. Schäfer, *Lattice QCD study of the Boer-Mulders effect in a pion*, *Phys. Rev. D* **93** (2016) 054501 [arXiv:1506.07826] [INSPIRE].

[31] B. Yoon et al., *Lattice QCD calculations of nucleon transverse momentum-dependent parton distributions using clover and domain wall fermions*, in *33rd International Symposium on Lattice Field Theory*, Kobe, Japan, 14–18 July 2015 [`arXiv:1601.05717`] [INSPIRE].

[32] B. Yoon et al., *Nucleon Transverse Momentum-dependent Parton Distributions in Lattice QCD: Renormalization Patterns and Discretization Effects*, *Phys. Rev. D* **96** (2017) 094508 [`arXiv:1706.03406`] [INSPIRE].

[33] X. Ji, P. Sun, X. Xiong and F. Yuan, *Soft factor subtraction and transverse momentum dependent parton distributions on the lattice*, *Phys. Rev. D* **91** (2015) 074009 [`arXiv:1405.7640`] [INSPIRE].

[34] X. Ji, L.-C. Jin, F. Yuan, J.-H. Zhang and Y. Zhao, *Transverse momentum dependent parton quasidistributions*, *Phys. Rev. D* **99** (2019) 114006 [`arXiv:1801.05930`] [INSPIRE].

[35] M.A. Ebert, I.W. Stewart and Y. Zhao, *Determining the Nonperturbative Collins-Soper Kernel From Lattice QCD*, *Phys. Rev. D* **99** (2019) 034505 [`arXiv:1811.00026`] [INSPIRE].

[36] M.A. Ebert, I.W. Stewart and Y. Zhao, *Towards Quasi-Transverse Momentum Dependent PDFs Computable on the Lattice*, *JHEP* **09** (2019) 037 [`arXiv:1901.03685`] [INSPIRE].

[37] M.A. Ebert, I.W. Stewart and Y. Zhao, *Renormalization and Matching for the Collins-Soper Kernel from Lattice QCD*, *JHEP* **03** (2020) 099 [`arXiv:1910.08569`] [INSPIRE].

[38] X. Ji, Y. Liu and Y.-S. Liu, *TMD soft function from large-momentum effective theory*, *Nucl. Phys. B* **955** (2020) 115054 [`arXiv:1910.11415`] [INSPIRE].

[39] X. Ji, Y. Liu and Y.-S. Liu, *Transverse-momentum-dependent parton distribution functions from large-momentum effective theory*, *Phys. Lett. B* **811** (2020) 135946 [`arXiv:1911.03840`] [INSPIRE].

[40] M.A. Ebert, S.T. Schindler, I.W. Stewart and Y. Zhao, *One-loop Matching for Spin-Dependent Quasi-TMDs*, *JHEP* **09** (2020) 099 [`arXiv:2004.14831`] [INSPIRE].

[41] X. Ji, Y. Liu, A. Schäfer and F. Yuan, *Single Transverse-Spin Asymmetry and Sivers Function in Large Momentum Effective Theory*, *Phys. Rev. D* **103** (2021) 074005 [`arXiv:2011.13397`] [INSPIRE].

[42] X. Ji and Y. Liu, *Computing light-front wave functions without light-front quantization: A large-momentum effective theory approach*, *Phys. Rev. D* **105** (2022) 076014 [`arXiv:2106.05310`] [INSPIRE].

[43] P. Shanahan, M.L. Wagman and Y. Zhao, *Nonperturbative renormalization of staple-shaped Wilson line operators in lattice QCD*, *Phys. Rev. D* **101** (2020) 074505 [`arXiv:1911.00800`] [INSPIRE].

[44] P. Shanahan, M. Wagman and Y. Zhao, *Collins-Soper kernel for TMD evolution from lattice QCD*, *Phys. Rev. D* **102** (2020) 014511 [`arXiv:2003.06063`] [INSPIRE].

[45] M. Schlemmer, A. Vladimirov, C. Zimmermann, M. Engelhardt and A. Schäfer, *Determination of the Collins-Soper Kernel from Lattice QCD*, *JHEP* **08** (2021) 004 [`arXiv:2103.16991`] [INSPIRE].

[46] LATTICE PARTON collaboration, *Lattice QCD Calculations of Transverse-Momentum-Dependent Soft Function through Large-Momentum Effective Theory*, *Phys. Rev. Lett.* **125** (2020) 192001 [`arXiv:2005.14572`] [INSPIRE].

[47] Y. Li et al., *Lattice QCD Study of Transverse-Momentum Dependent Soft Function*, *Phys. Rev. Lett.* **128** (2022) 062002 [`arXiv:2106.13027`] [INSPIRE].

[48] P. Shanahan, M. Wagman and Y. Zhao, *Lattice QCD calculation of the Collins-Soper kernel from quasi-TMDPDFs*, *Phys. Rev. D* **104** (2021) 114502 [arXiv:2107.11930] [INSPIRE].

[49] A.A. Vladimirov and A. Schäfer, *Transverse momentum dependent factorization for lattice observables*, *Phys. Rev. D* **101** (2020) 074517 [arXiv:2002.07527] [INSPIRE].

[50] J.C. Collins and D.E. Soper, *Back-To-Back Jets in QCD*, *Nucl. Phys. B* **193** (1981) 381 [*Erratum ibid.* **213** (1983) 545] [INSPIRE].

[51] J.C. Collins and D.E. Soper, *Back-To-Back Jets: Fourier Transform from B to K-Transverse*, *Nucl. Phys. B* **197** (1982) 446 [INSPIRE].

[52] J.C. Collins, D.E. Soper and G.F. Sterman, *Transverse Momentum Distribution in Drell-Yan Pair and W and Z Boson Production*, *Nucl. Phys. B* **250** (1985) 199 [INSPIRE].

[53] J. Collins, *Foundations of perturbative QCD*, Cambridge University Press, Cambridge, U.K. [*Camb. Monogr. Part. Phys. Nucl. Phys. Cosmol.* **32** (2011) 1] [INSPIRE].

[54] J.-H. Zhang, X. Ji, A. Schäfer, W. Wang and S. Zhao, *Accessing Gluon Parton Distributions in Large Momentum Effective Theory*, *Phys. Rev. Lett.* **122** (2019) 142001 [arXiv:1808.10824] [INSPIRE].

[55] M. Beneke and T. Feldmann, *Factorization of heavy to light form-factors in soft collinear effective theory*, *Nucl. Phys. B* **685** (2004) 249 [hep-ph/0311335] [INSPIRE].

[56] X.-d. Ji, J.-p. Ma and F. Yuan, *QCD factorization for semi-inclusive deep-inelastic scattering at low transverse momentum*, *Phys. Rev. D* **71** (2005) 034005 [hep-ph/0404183] [INSPIRE].

[57] J.-y. Chiu, F. Golf, R. Kelley and A.V. Manohar, *Electroweak Sudakov corrections using effective field theory*, *Phys. Rev. Lett.* **100** (2008) 021802 [arXiv:0709.2377] [INSPIRE].

[58] T. Becher and G. Bell, *Analytic Regularization in Soft-Collinear Effective Theory*, *Phys. Lett. B* **713** (2012) 41 [arXiv:1112.3907] [INSPIRE].

[59] J.-y. Chiu, A. Jain, D. Neill and I.Z. Rothstein, *The Rapidity Renormalization Group*, *Phys. Rev. Lett.* **108** (2012) 151601 [arXiv:1104.0881] [INSPIRE].

[60] J.-Y. Chiu, A. Jain, D. Neill and I.Z. Rothstein, *A Formalism for the Systematic Treatment of Rapidity Logarithms in Quantum Field Theory*, *JHEP* **05** (2012) 084 [arXiv:1202.0814] [INSPIRE].

[61] J.-y. Chiu, A. Fuhrer, A.H. Hoang, R. Kelley and A.V. Manohar, *Soft-Collinear Factorization and Zero-Bin Subtractions*, *Phys. Rev. D* **79** (2009) 053007 [arXiv:0901.1332] [INSPIRE].

[62] M.G. Echevarria, A. Idilbi and I. Scimemi, *Factorization Theorem For Drell-Yan At Low q_T And Transverse Momentum Distributions On-The-Light-Cone*, *JHEP* **07** (2012) 002 [arXiv:1111.4996] [INSPIRE].

[63] Y. Li, D. Neill and H.X. Zhu, *An exponential regulator for rapidity divergences*, *Nucl. Phys. B* **960** (2020) 115193 [arXiv:1604.00392] [INSPIRE].

[64] M.A. Ebert, I. Moult, I.W. Stewart, F.J. Tackmann, G. Vita and H.X. Zhu, *Subleading power rapidity divergences and power corrections for q_T*, *JHEP* **04** (2019) 123 [arXiv:1812.08189] [INSPIRE].

[65] T. Becher and M. Neubert, *Drell-Yan Production at Small q_T, Transverse Parton Distributions and the Collinear Anomaly*, *Eur. Phys. J. C* **71** (2011) 1665 [arXiv:1007.4005] [INSPIRE].

[66] J. Collins and T.C. Rogers, *Connecting Different TMD Factorization Formalisms in QCD*, *Phys. Rev. D* **96** (2017) 054011 [arXiv:1705.07167] [INSPIRE].

[67] D. Gutiérrez-Reyes, I. Scimemi and A.A. Vladimirov, *Twist-2 matching of transverse momentum dependent distributions*, *Phys. Lett. B* **769** (2017) 84 [arXiv:1702.06558] [INSPIRE].

[68] P.J. Mulders and J. Rodrigues, *Transverse momentum dependence in gluon distribution and fragmentation functions*, *Phys. Rev. D* **63** (2001) 094021 [hep-ph/0009343] [INSPIRE].

[69] M.G. Echevarria, T. Kasemets, P.J. Mulders and C. Pisano, *QCD evolution of (un)polarized gluon TMDPDFs and the Higgs q_T-distribution*, *JHEP* **07** (2015) 158 [*Erratum ibid.* **05** (2017) 073] [arXiv:1502.05354] [INSPIRE].

[70] X.-d. Ji and F. Yuan, *Parton distributions in light cone gauge: Where are the final state interactions?*, *Phys. Lett. B* **543** (2002) 66 [hep-ph/0206057] [INSPIRE].

[71] X. Ji, J.-H. Zhang and Y. Zhao, *Renormalization in Large Momentum Effective Theory of Parton Physics*, *Phys. Rev. Lett.* **120** (2018) 112001 [arXiv:1706.08962] [INSPIRE].

[72] J. Green, K. Jansen and F. Steffens, *Nonperturbative Renormalization of Nonlocal Quark Bilinears for Parton Quasidistribution Functions on the Lattice Using an Auxiliary Field*, *Phys. Rev. Lett.* **121** (2018) 022004 [arXiv:1707.07152] [INSPIRE].

[73] J.R. Green, K. Jansen and F. Steffens, *Improvement, generalization, and scheme conversion of Wilson-line operators on the lattice in the auxiliary field approach*, *Phys. Rev. D* **101** (2020) 074509 [arXiv:2002.09408] [INSPIRE].

[74] J.G.M. Gatheral, *Exponentiation of Eikonal Cross-sections in Nonabelian Gauge Theories*, *Phys. Lett. B* **133** (1983) 90 [INSPIRE].

[75] J. Frenkel and J.C. Taylor, *Nonabelian eikonal exponentiation*, *Nucl. Phys. B* **246** (1984) 231 [INSPIRE].

[76] X. Ji and Y. Liu, in preparation.

[77] I.W. Stewart, F.J. Tackmann and W.J. Waalewijn, *The Quark Beam Function at NNLL*, *JHEP* **09** (2010) 005 [arXiv:1002.2213] [INSPIRE].

[78] M.A. Ebert, *Analytic results for Sudakov form factors in QCD*, *JHEP* **02** (2022) 136 [arXiv:2110.11360] [INSPIRE].

[79] M. Constantinou, H. Panagopoulos and G. Spanoudes, *One-loop renormalization of staple-shaped operators in continuum and lattice regularizations*, *Phys. Rev. D* **99** (2019) 074508 [arXiv:1901.03862] [INSPIRE].

[80] Y. Ji, J.-H. Zhang, S. Zhao and R. Zhu, *Renormalization and mixing of staple-shaped Wilson line operators on the lattice revisited*, *Phys. Rev. D* **104** (2021) 094510 [arXiv:2104.13345] [INSPIRE].

[81] J.M. Henn, G.P. Korchemsky and B. Mistlberger, *The full four-loop cusp anomalous dimension in $\mathcal{N} = 4$ super Yang-Mills and QCD*, *JHEP* **04** (2020) 018 [arXiv:1911.10174] [INSPIRE].

[82] A. Vladimirov, V. Moos and I. Scimemi, *Transverse momentum dependent operator expansion at next-to-leading power*, *JHEP* **01** (2022) 110 [arXiv:2109.09771] [INSPIRE].

[83] M.A. Ebert, A. Gao and I.W. Stewart, *Factorization for Azimuthal Asymmetries in SIDIS at Next-to-Leading Power*, arXiv:2112.07680 [INSPIRE].

[84] C.W. Bauer, S. Fleming and M.E. Luke, *Summing Sudakov logarithms in $B \to X_s \gamma$ in effective field theory*, *Phys. Rev. D* **63** (2000) 014006 [hep-ph/0005275] [INSPIRE].

[85] C.W. Bauer and I.W. Stewart, *Invariant operators in collinear effective theory*, *Phys. Lett. B* **516** (2001) 134 [hep-ph/0107001] [INSPIRE].

[86] C.W. Bauer, S. Fleming, D. Pirjol and I.W. Stewart, *An Effective field theory for collinear and soft gluons: Heavy to light decays*, *Phys. Rev. D* **63** (2001) 114020 [hep-ph/0011336] [INSPIRE].

[87] C.W. Bauer, D. Pirjol and I.W. Stewart, *Soft collinear factorization in effective field theory*, *Phys. Rev. D* **65** (2002) 054022 [hep-ph/0109045] [INSPIRE].

[88] G. Kramer and B. Lampe, *Two Jet Cross-Section in e^+e^- Annihilation*, *Z. Phys. C* **34** (1987) 497 [*Erratum ibid.* **42** (1989) 504] [INSPIRE].

[89] T. Matsuura and W.L. van Neerven, *Second Order Logarithmic Corrections to the Drell-Yan Cross-section*, *Z. Phys. C* **38** (1988) 623 [INSPIRE].

[90] T. Matsuura, S.C. van der Marck and W.L. van Neerven, *The Calculation of the Second Order Soft and Virtual Contributions to the Drell-Yan Cross-Section*, *Nucl. Phys. B* **319** (1989) 570 [INSPIRE].

[91] T. Gehrmann, T. Huber and D. Maître, *Two-loop quark and gluon form-factors in dimensional regularisation*, *Phys. Lett. B* **622** (2005) 295 [hep-ph/0507061] [INSPIRE].

[92] S. Moch, J.A.M. Vermaseren and A. Vogt, *Three-loop results for quark and gluon form-factors*, *Phys. Lett. B* **625** (2005) 245 [hep-ph/0508055] [INSPIRE].

[93] S. Moch, J.A.M. Vermaseren and A. Vogt, *The Quark form-factor at higher orders*, *JHEP* **08** (2005) 049 [hep-ph/0507039] [INSPIRE].

[94] P.A. Baikov, K.G. Chetyrkin, A.V. Smirnov, V.A. Smirnov and M. Steinhauser, *Quark and gluon form factors to three loops*, *Phys. Rev. Lett.* **102** (2009) 212002 [arXiv:0902.3519] [INSPIRE].

[95] R.N. Lee, A.V. Smirnov and V.A. Smirnov, *Analytic Results for Massless Three-Loop Form Factors*, *JHEP* **04** (2010) 020 [arXiv:1001.2887] [INSPIRE].

[96] T. Gehrmann, E.W.N. Glover, T. Huber, N. Ikizlerli and C. Studerus, *Calculation of the quark and gluon form factors to three loops in QCD*, *JHEP* **06** (2010) 094 [arXiv:1004.3653] [INSPIRE].

[97] S. Catani, L. Cieri, D. de Florian, G. Ferrera and M. Grazzini, *Vector boson production at hadron colliders: hard-collinear coefficients at the NNLO*, *Eur. Phys. J. C* **72** (2012) 2195 [arXiv:1209.0158] [INSPIRE].

[98] T. Gehrmann, T. Lubbert and L.L. Yang, *Transverse parton distribution functions at next-to-next-to-leading order: the quark-to-quark case*, *Phys. Rev. Lett.* **109** (2012) 242003 [arXiv:1209.0682] [INSPIRE].

[99] T. Gehrmann, T. Luebbert and L.L. Yang, *Calculation of the transverse parton distribution functions at next-to-next-to-leading order*, *JHEP* **06** (2014) 155 [arXiv:1403.6451] [INSPIRE].

[100] Y. Li and H.X. Zhu, *Bootstrapping Rapidity Anomalous Dimensions for Transverse-Momentum Resummation*, *Phys. Rev. Lett.* **118** (2017) 022004 [arXiv:1604.01404] [INSPIRE].

[101] M.G. Echevarria, I. Scimemi and A. Vladimirov, *Unpolarized Transverse Momentum Dependent Parton Distribution and Fragmentation Functions at next-to-next-to-leading order*, *JHEP* **09** (2016) 004 [arXiv:1604.07869] [INSPIRE].

[102] T. Lübbert, J. Oredsson and M. Stahlhofen, *Rapidity renormalized TMD soft and beam functions at two loops*, *JHEP* **03** (2016) 168 [arXiv:1602.01829] [INSPIRE].

[103] M.-X. Luo, X. Wang, X. Xu, L.L. Yang, T.-Z. Yang and H.X. Zhu, *Transverse Parton Distribution and Fragmentation Functions at NNLO: the Quark Case*, *JHEP* **10** (2019) 083 [arXiv:1908.03831] [INSPIRE].

[104] M.-x. Luo, T.-Z. Yang, H.X. Zhu and Y.J. Zhu, *Quark Transverse Parton Distribution at the Next-to-Next-to-Next-to-Leading Order*, *Phys. Rev. Lett.* **124** (2020) 092001 [arXiv:1912.05778] [INSPIRE].

[105] M.A. Ebert, B. Mistlberger and G. Vita, *Transverse momentum dependent PDFs at N^3LO*, *JHEP* **09** (2020) 146 [arXiv:2006.05329] [INSPIRE].

[106] M.-x. Luo, T.-Z. Yang, H.X. Zhu and Y.J. Zhu, *Unpolarized quark and gluon TMD PDFs and FFs at N^3LO*, *JHEP* **06** (2021) 115 [arXiv:2012.03256] [INSPIRE].

[107] H. Dorn, *Renormalization of Path Ordered Phase Factors and Related Hadron Operators in Gauge Field Theories*, *Fortsch. Phys.* **34** (1986) 11 [INSPIRE].

[108] G.P. Korchemsky and A.V. Radyushkin, *Renormalization of the Wilson Loops Beyond the Leading Order*, *Nucl. Phys. B* **283** (1987) 342 [INSPIRE].